MARCELLE FERREIRA SILVA

ROLE OF MITOCHONDRIAL CALCIUM TRANSPORT AND REDOX METABOLISM ON DARK-INDUCED SENESCENCE AND ALUMINUM STRESS TOLERANCE

Thesis presented to the Universidade Federal de Viçosa, as part of the requirements of the Plant Physiology Graduate Program to obtain the degree of *Doctor Scientiae.*

Advisor: Wagner L. Araújo

VIÇOSA - MINAS GERAIS
2024

Ficha catalográfica elaborada pela Biblioteca Central da Universidade Federal de Viçosa - Campus Viçosa

T
S586r
2024

Silva, Marcelle Ferreira, 1994-
Role of mitochondrial calcium transport and redox metabolism on dark-induced senescence and aluminum stress tolerance / Marcelle Ferreira Silva. – Viçosa, MG, 2024.
1 tese eletrônica (106 f.): il. (algumas color.).

Orientador: Wagner Luiz Araújo.
Tese (doutorado) - Universidade Federal de Viçosa, Departamento de Biologia Vegetal, 2024.
Referências bibliográficas: f. 41-48.
DOI: https://doi.org/10.47328/ufvbbt.2024.429
Modo de acesso: World Wide Web.

1. Plantas - Efeito do alumínio. 2. Plantas - Efeito da luz. 3. Células - Envelhecimento. 4. Estresse oxidativo. 5. Cálcio - Metabolismo. 6. Mitocôndria - Metabolismo. I. Araújo, Wagner Luiz, 1980-. II. Universidade Federal de Viçosa. Departamento de Biologia Vegetal. Programa de Pós-Graduação em Fisiologia Vegetal. III. Título.

CDD 22. ed. 632.1

Bibliotecário(a) responsável: Euzébio Luiz Pinto CRB-6/3317

MARCELLE FERREIRA SILVA

ROLE OF MITOCHONDRIAL CALCIUM TRANSPORT AND REDOX METABOLISM ON DARK-INDUCED SENESCENCE AND ALUMINUM STRESS TOLERANCE

Thesis presented to the Universidade Federal de Viçosa, as part of the requirements of the Plant Physiology Graduate Program to obtain the degree of *Doctor Scientiae.*

APPROVED: April 30th, 2024.

Assent:

Documento assinado digitalmente
gov.br
MARCELLE FERREIRA SILVA
Data: 30/07/2024 09:05:05-0300
Verifique em https://validar.iti.gov.br

Marcelle Ferreira Silva

Author

Documento assinado digitalmente
gov.br
WAGNER LUIZ ARAUJO
Data: 30/07/2024 09:35:47-0300
Verifique em https://validar.iti.gov.br

Wagner L. Araújo

Adviser

ACKNOWLEDGEMENTS

First, I would like to thank the support of my family; in special, my parents Clara and Enio, and my sister Luísa for always inspiring me to be fearless.

To all my teachers and Professors that contribute to my academic and personal development through the years, in special my adviser Prof. Wagner, for trusting my work and for the guidance over this path. Also, Prof. Adriano and Prof. Markus for overseeing this work while in progress. And to all others that contribute to my scientific thinking.

To all financing agencies and educational institutions that directly or indirectly contributed to making this study possible. This study was financed in part by the Coordenação de Aperfeiçoamento de Pessoal de Nível Superior – Brasil (CAPES) – Finance Code 001 and Fundação de Amparo à Pesquisa do Estado de Minas Gerais (FAPEMIG). To the Conselho Nacional de Desenvolvimento Científico e Tecnológico (CNPq), for granting the scholarship. To the Coordenação de Aperfeiçoamento de Pessoal de Nível Superior (CAPES), for granting the scholarship to the interuniversity exchange doctorate with the Münster University, Germany.

To all my friends who hold my back in this process. To my workmates who also became friends, for making my days at UCP and Plant Energy Biology Lab funnier, and to all UCP and Plant Energy Biology members for the support with the experiments and work.

To everyone who directly or indirectly collaborated with the accomplishment of this work, my sincere acknowledgments and appreciation.

Thank you.

ABSTRACT

FERREIRA-SILVA, Marcelle, D.Sc., Universidade Federal de Viçosa, April, 2024. **Role of Mitochondrial Calcium Transport and Redox Metabolism on Dark-Induced Senescence and Aluminum Stress Tolerance.** Adviser: Wagner L. Araújo.

Stress can be caused by a broad range of conditions and different cellular responses can significantly alter plant metabolism to cope with such conditions. Aluminum (Al) toxicity is a critical factor limiting plant growth in acidic soils. Al is a highly redox reactive element, and its main symptom is root growth inhibition. Dark is another common stress that affects plants; in this scenario, dark-induced senescence is a highly regulated process that requires massive transcriptional and metabolic reprogramming to break down and remobilize valuable resources. For both stresses aforementioned, mitochondrial metabolism is crucial to support cellular processes; accordingly, in Al toxicity it is involved in providing organic acids (OA) to complex Al, whereas in dark conditions it is intimately related to carbon and nitrogen remobilization. In this context, two main processes, related to mitochondria, underpin important cellular responses to these different abiotic stress conditions namely (i) redox system and (ii) calcium (Ca^{2+}) transients. Evidence suggests that thioredoxin (TRX) system are responsible for mitigating oxidative damage through the control of reactive oxygen species (ROS), thus making it important to sustain plant development following abiotic stress. Moreover, Ca^{2+} signaling is directly involved in responses to environmental cues. Here we attempted to understand how the *Arabidopsis*' mitochondrial TRX system participates in the mitigation of the Al toxicity and how mitochondrial Ca^{2+} transporters modulate the dark-induced senescence responses. Surprisingly, our findings revealed the major importance of the GR redox system status in Al mitigation compared to the TRX system. Our results further demonstrated a clear difference in chlorophyll degradation pathway under dark conditions for the mutants lacking the mitochondrial Ca^{2+} transporter. We further asked whether this phenomenon was related to the matrix enzyme glutamate dehydrogenase (GDH2) and its regulation by Ca^{2+}; nevertheless, a clear connection between the mitochondrial Ca^{2+} transporter and matrix Ca levels and the chlorophyll degradation was not unequivocally apparent. Collectively, our results indicate that mitochondrial metabolism plays an important role in coping with abiotic stress conditions and perturbations in this organelle lead to differential metabolic response under stress conditions.

Keywords: Glutamate dehydrogenase; Glutathione; Thioredoxin.

RESUMO

FERREIRA-SILVA, Marcelle, D.Sc., Universidade Federal de Viçosa, abril de 2024. **Papel dos Transportadores de Cálcio e do Metabolismo Redox Mitocondriais na Senescência Induzida pelo Escuro e na Tolerância ao Estresse por Alumínio.** Orientador: Wagner L. Araújo.

Uma ampla gama de condições pode causar estresses em plantas, que podem alterar significativamente o metabolismo vegetal. A toxicidade causada pelo alumínio (Al) é um fator crítico que limita o crescimento das plantas em solos ácidos, levando a inibição do crescimento radicular. O escuro é outro estresse que afeta as plantas, neste cenário a senescência induzida pelo escuro é um processo que requer uma reprogramação transcricional e metabólica para quebrar e remobilizar recursos. Para ambos os estresses mencionados, o metabolismo mitocondrial é crucial, enquanto para o Al está envolvido no fornecimento de ácidos orgânicos (AO) para complexar o Al, para condições de escuro está relacionado à remobilização de carbono e nitrogênio. Neste contexto, dois processos principais, relacionados com as mitocôndrias, sustentam respostas importantes a estas diferentes condições, (i) sistema redox e (ii) transientes de cálcio (Ca^{2+}). Evidências sugerem que o sistema tioredoxina (TRX) é responsável por mitigar o dano oxidativo através do controle de espécies reativas de oxigênio (ROS). Além disso, a sinalização de Ca^{2+} está diretamente envolvida nas respostas aos sinais ambientais. Aqui tentamos entender como o sistema TRX participa na mitigação da toxicidade do Al e como os transportadores mitocondriais de Ca^{2+} modulam as respostas da senescência induzida pelo escuro em *Arabidopsis*. Diferente do que era esperado, nossos resultados mostraram uma grande importância do status do sistema redox GR na mitigação de Al em comparação ao sistema TRX. Observamos uma clara diferença na via de degradação da clorofila em condições de escuro para os mutantes sem o transportador mitocondrial de Ca^{2+}. Tentamos elucidar se este fenómeno estava relacionado com a enzima de remobilização da matriz mitocondrial glutamato desidrogenase 2 (GDH2) e a sua regulação pelo cálcio, no entanto, não foi possível postular uma ligação clara entre o transportador mitocondrial de Ca^{2+} e os níveis de Ca na matriz e a degradação da clorofila. Coletivamente, nossos dados nos levaram a concluir que o metabolismo mitocondrial desempenha um papel essencial no enfrentamento de condições de estresse abiótico e perturbações em tal organela levam a diferentes fenótipos em condições de estresse.

Palavras-chave: Glutamato desidrogenase; Glutationa, Tioredoxina

SUMMARY

GENERAL INTRODUCTION **8**
Mitochondrial metabolism e regulation **8**
Thioredoxins **10**
Calcium signaling **12**
Dark-induced senescence **15**
Aluminum stress **17**
Reactive Oxygen Species - ROS **19**
***In vivo* biosensors** **21**
CHAPTERS OVERVIEW **23**
Chapter 1: Deciphering the significance of the thioredoxin system in aluminum stress response **24**
Chapter 2: Deciphering the significance of the mitochondrial calcium uniport to leaf senescence **24**
REFERENCES **25**
CHAPTER 1: Deciphering the significance of the thioredoxin system in aluminum stress response **40**
ABSTRACT **40**
INTRODUCTION **41**
MATERIAL AND METHODS **44**
Plant materials **44**
Experimental conditions and root growth assays **46**
Histochemical Al localization assay **46**
Histochemical ROS assays **47**
***In vivo* sensor measurement of physiological dynamics** **47**
Data and statistical analyses **48**
RESULTS **48**
Lack of a functional mitochondrial TRX reductase system leads to a greater Al tolerance **48**
Alterations in histochemical ROS staining in *A. thaliana* under Al stress **51**
Glutathione synthesis impairment strongly affect Al mitigation process **53**
H_2O_2 and pH rapidly changes in response to Al stress **55**
DISCUSSION **57**
CONCLUSIONS **60**
SUPPLEMENTAL DATA **62**

REFERENCES **63**

CHAPTER 2: Deciphering the significance of the mitochondrial calcium uniport during leaf senescence **71**

ABSTRACT **71**

INTRODUCTION **72**

MATERIAL AND METHODS **75**

Plant materials **75**

Experimental conditions and chlorophyll quantification **76**

Phylogenetic analysis of *GDH2* **77**

Molecular cloning of GDH2 ..... **80**

Protein expression and purification **81**

Enzymatic GDH2 assay **81**

RNA extraction and RT–qPCR analysis **81**

***In vivo* sensor measurement of Ca^{2+} dynamics** **82**

Data and statistical analyses **83**

RESULTS **83**

Change in chlorophyll degradation can be related to the absence of *mcu* Ca^{2+} transporter **83**

***Arabidopsis thaliana* GDH2 seems not to be regulated by calcium** **86**

Cellular calcium levels decrease in single-darkened leaves **89**

***mcu123* modifies chlorophyll degradation pattern but does not delay the senescence** **91**

DISCUSSION **92**

CONCLUSIONS **97**

SUPPLEMENTAL DATA **98**

REFERENCES **100**

FUTURE PERSPECTIVES **106**

GENERAL INTRODUCTION

Mitochondrial metabolism e regulation

Mitochondria originated from an endosymbiotic event of a once free-living *alphaproteobacteria*, therefore mitochondria present their own distinct genetic material (MAEDA & FERNIE, 2021). However, from the original genetic material, only a small part remains within the mitochondria, while the majority was transferred to the nucleus (MAEDA & FERNIE, 2021). Therefore, its cellular functions depend on proteins encoded by the nucleus, synthesized in the cytosol, and later imported to mitochondria (MURCHA et al., 2014). Thus, it is crucial to have proper communication between mitochondria and the nucleus to coordinate cellular functions (MURCHA et al., 2014). It is important to notice that the genome size of plant mitochondria is variable (SMITH & KEELING, 2015), but most of it retains the genes to encode the main set of enzymes related to oxidative phosphorylation (OXPHOS) (LIBERATORE et al., 2016). The interaction between nuclear and mitochondrial genomes is still an "ongoing integration process", that could explain the variation in genome size among the organelle (KOZIK et al., 2019).

Plant mitochondria can present different shapes, from spherical to tubular shape (MØLLER et al., 2021), and it is usually aggregate in cellular areas that need a direct supply of ATP, being able to change this location throughout the cell cycle (LOGAN, 2006). Actin and microtubules participate in the movements of plant mitochondria (Van GESTEL et al., 2002). ATP production is needed for cellular maintenance and growth (JACOBY et al., 2012). Briefly, it is an energy-conserving process that oxidates high-energy organic acids intermediates, releasing CO_2 and reducing O_2 to H_2O to fuel the OXPHOS that will generate the electrochemical pump to synthesize ATP (JACOBY et al., 2012). This process can be framed in a sequential set of biochemical processes, (i) tricarboxylic acid cycle (TCA), (ii) OXPHOS mitochondrial electron transport chain (mETC), (iii) non-phosphorylating bypasses of the mETC (MILLAR et al., 2011).

First, the TCA cycle will reduce $NAD(P)^+$ and FAD^+ to NAD(P)H and $FADH_2$, through the oxidative decarboxylation of organic acids (MCDONALD & VANLERBERGHE, 2006). This process involves nine enzymes and is the major carbon metabolism machinery of mitochondria (MILLAR et al., 2011). Beginning with the pyruvate dehydrogenase complex (PDC) that will form acetyl-CoA, from the pyruvate, which can enter the mitochondria from the cytosol or be formed in the matrix through the malic enzyme (ME) (LUETHY et al., 1995).

Afterward, the citrate synthase (CS) will produce citrate and release CoA cofactor using acetyl-CoA and dicarboxylate oxaloacetate (La COGNATA et al. 1996). Citrate is then converted to isocitrate via aconitase (ACO), and later formed 2-oxoglutarate (2OG) by isocitrate dehydrogenase (IDH) (ZHANG & FERNIE, 2018). 2OG is converted to succinyl CoA by 2-Oxoglutarate dehydrogenase (OGDC), and succinyl CoA ligase will generate succinate (JACOBY et al., 2012). Later the succinate dehydrogenase (SDH or Complex II - a connection between TCA cycle and mETC) will transform the succinate into fumarate; fumarate is converted into malate through fumarase (FUM). In the end, malate dehydrogenase (MDH) will generate oxaloacetate completing the cycle (ZHANG & FERNIE, 2023). These intermediate metabolites and enzymes are not related only to the TCA cycle, and they can be also involved in other physiological processes (SWEETLOVE et al., 2010; ZHANG & FERNIE, 2023). As an example, mutants in FUM and SDH showed changes in stomatal aperture leading to impairment and improvement of photosynthetic rate, respectively (NUNES-NESI et al., 2007; ARAUJO et al., 2011).

Second, the NAD(P)H and $FADH_2$ generated in the TCA cycle are used to reduce O_2 in water while increasing the electrochemical potential by the mETC (MILLAR et al., 2011). The mETC is formed by four complexes (I – VI) that are connected by the interaction with ubiquinone (UQ) and cytochrome c (JACOBY et al., 2012). Complex I will oxidase NADH and reduce the UQ; Complex II is the succinate dehydrogenase and as mentioned before, also part of TCA cycle; Complex III will oxidase UQ and reduce cytochrome c; Complex IV will re-oxidase the cytochrome c (JACOBY et al., 2012). ATP synthase (sometimes referred to as Complex V) is the last step in the oxidative phosphorylation, it uses the electrochemical gradient as a force to pump the ADP and phosphorylate it (MILLAR et al., 2011).

Finally, the non-phosphorylating proteins, the alternative NADH dehydrogenases, alternative oxidase (AOX), and uncoupling proteins (UCPs) operate as bypasses of the mETC (BARRETO et al., 2022). The NADH dehydrogenases are present not only in the mitochondria (CARRIE et al., 2008) and they work without the translocation of protons (RASMUSSON et al., 2004). NADH dehydrogenases are also insensitive to rotenone (a Complex I inhibitor) (MØLLER et al., 2021). The AOX is cyanide-insensitive and works as a branch of the mETC, where the UQ reduces O_2 to water without proton translocation (BARRETO et al., 2022). It is related to redox homeostasis, since it is induced by oxidative stress (VAN AKEN et al., 2009), is crucial in tissues of thermogenic plants (ZHU et al., 2011), and keeps reactive oxygen species

(ROS) low in abiotic stress, as hypoxia (BARRETO et al., 2022). The UCPs are a carrier protein that transports H^+ back across the inner membrane, this way it dissipates the electrical potential generated before (VERCESI et al., 2006). Their regulation and activation are also strongly related to ROS (CONSIDINE et al., 2003).

It is important to note that even though energy production is the main function attributed to mitochondria, it is also related to other cellular processes, such as nitrogen metabolism, oxidative stress responses, and in photosynthetic tissues is indispensable for chloroplast role (JACOBY et al., 2012). Mitochondria is a key player in metabolism regulation, intracellular signaling, and programmed cell death (PCD), even changing shape before PCD (LOGAN, 2006; BRAS et al., 2005). Mitochondria metabolism is dynamically tuned to supply the amount of energy demanded by the cell, in direct response to different tissue types or environmental cues, moreover, it can alter their morphology and respiration capacity to do it. (MILLAR et al., 2011). Mitochondrial metabolism is tightly connected with cellular status, disturbances in mitochondrial enzymes can alter whole-plant redox balance affecting stress responses (TOMAZ et al., 2010). One example of a link between mitochondria and cellular metabolic status is, in abiotic stress situations, if the TCA cycle flux is affected, mitochondria can provide 2OG as a precursor for N-containing metabolites (SWEETLOVE et al., 2010). In addition, in stress environments is an increase in ROS, that usually is associated with a change in the redox status of mitochondrial ascorbate and glutathione to a more oxidized state (FOYER & NOCTOR, 2011). Stress, abiotic and biotic, can impact productively worldwide (LIBERATORE et al., 2016), if metabolic pathways are disrupted, mitochondria recognize the energy-deficiency signals and re-establish metabolic balance (HUNER et al., 1998). Additionally, upon non-optimal conditions, the respiration flux can change, which will lead to a general cellular response, such as organellar and nuclear gene expression (LIBERATORE et al., 2016).

Thioredoxins

Thioredoxins (TRX) can be found in different organisms from bacteria and fungi to more complex ones such as animals, and plants, acting in all as a redox regulator (GEIGENBERGER et al., 2017). They are small proteins with an active disulfide bridge with two redox-active cysteines (Cys) separated by a pair of amino acids (CxxC) (SCHÜRMANN & JACQUOT, 2000). This structure, the redox center of TRXs, can interact with the disulfide

bridges of target proteins allowing the TRXs to regulate their functions through an efficient protein disulfide oxidoreductase (MEYER et al., 2009). It is important to notice that even though similar in these characteristics they fulfill specific and different functions, which is possible due to singular structural complementarity between the TRX and their specific target (SCHÜRMANN & JACQUOT, 2000). In plants, TRXs belongs to a large family gene, Arabidopsis presents 20 different isoforms, being TRXs *f*, *m*, *x*, *y*, and *z* chloroplastic; *o* mitochondrial and nuclear, *h* distributed between cytosol, endoplasmatic reticulum and mitochondria (GEIGENBERGER et al., 2017; DELORME-HINOUX et al., 2016). Depending on the intracellular localization of the TRXs, it can be reduced by different systems, using NADPH or reduced ferredoxin (Fdx) as electron donors (SERRATO et al., 2004).

In non-photosynthetic tissues and extraplastidial compartments the TRXs are reduced by NADPH-dependent reductase (NTR) types A and B (LALOI et al., 2001). Both can be found in cytosol and mitochondria, NTRA mainly in the cytosol and NTRB in the mitochondria (REICHHELD et al., 2005), but A can also be present in the nucleus (GEIGENBERGER et al., 2017) and both share redundant functions (CHA et al., 2014). In the cytosol, the main source for NADPH is the oxidative pentose phosphate pathway (OPPP), while in the mitochondria it is the NADH kinases (GEIGENBERGER et al., 2017). The TRXs *h*, which are controlled by NTRs, can regulate different processes in the plant including stress response (ZHANG et al., 2011), intercellular communication (MENG et al., 2010), seed germination (HÄGGLUND et al., 2016), redox regulation photorespiratory metabolism (FONSECA-PEREIRA et al., 2020) and specifically in the mitochondria, *in vitro* assays, showed that the Trx*h*2 can regulate the AOX (GELHAYE et al., 2004). Also, in the mitochondria the NTRs controlled the Trx*o1* and Trx*o2* that were shown to regulate the activity of TCA cycle enzymes *in vivo* (succinate dehydrogenase and mitochondrial fumarase) (DALOSO et al., 2015) and *in vitro* citrate synthase (SCHMIDTMANN et al., 2014).

In chloroplasts the TRXs are reduced via two different systems, the ferredoxin thioredoxin reductase (FTR) or NTR type C (SCHÜRMANN & BUCHANAN, 2008; SPÍNOLA et al., 2008). The electrons for FTR come from ferredoxin reduced by photosystem I, therefore it is a light-dependent system (BUCHANAN, 2016). FTR regulates the Trx*f* and *m* with equal efficiency (HIRASAWA et al.1999). Trx*f* was shown to be responsible for controlling the Calvin-Benson-Bassham cycle enzyme fructose-1,6-bisphosphatase (FBPase) (YOSHIDA et al., 2015), rubisco activase (NARANJO et al., 2016) and starch synthase (THORMÄHLEN et al., 2013). While TRX *m* was shown to regulate the function of also

FBPase, ATP synthase, sedoheptulose-1,7-bisphosphatase (SBPase), malate transport (OKEGAWA & MOTOHASHI, 2015), and alternative electron transport chain (COURTEILLE et al., 2013). The other plastidial TRX (*x*, *y,* and *z*) were found to act as reducing substrates related to the antioxidant defense systems (YOSHIDA et al., 2015). The NTRC uses NADPH as a redox donor and its functions are strongly related to lower light intensities and fluctuations (NIKKANEN et al., 2016). Since NADPH can come from different metabolic reactions, as OPPP, NTRC can work in the dark (GEIGENBERGER et al., 2017) and be related to other regulations inside the chloroplast in addition to photosynthesis, like starch synthesis (MICHALSKA et al., 2009), antioxidant system (YOSHIDA & HISABORI, 2016). This demonstrates that both plastidial TRX systems are independent and important for light acclimation and plant development (YOSHIDA & HISABORI, 2016). Accordingly, at low light intensities, an overexpression of NTRC could enhance photosynthesis (NIKKANEN et al., 2016).

Due to their fundamental importance, mutants in TRX systems are affected, and *ftrb ntrc* double mutants have severe disruptions in photosynthesis, being lethal in photoautotrophic conditions (YOSHIDA & HISABORI, 2016). While the *ntra ntrb* double mutant, and *ntrabc* triple mutant are viable, however, they were characterized by reduced growth (REICHHELD et al., 2007; SOUZA et al., 2023). Interestingly, single mutants usually do not show a drastic phenotype under standard conditions, revealing some redundancy among the systems (MEYER et al., 2009; MATA-PÉREZ& SPOEL, 2019). Trxs are a complex network that controls various metabolic pathways, helps to cope with fluctuating environments, and integrates cellular communication, and plants have the most versatile Trx system among other organisms (GEIGENBERGER et al., 2017).

Calcium signaling

Calcium is essential to plant nutrition, considered a macronutrient (WHITE & BROADLEY, 2003). As a divalent cation (Ca^{2+}), it is required for intracellular messages (calcium signaling), in the cell wall and membranes it presents a structural role, and in the vacuole, it can also act as a counter-cation for inorganic and organic anions (MARSCHNER, 1995). Ca concentrations in shoots depend on Ca availability in the environment and can vary according to the requirements of the plant species (WHITE, 2001). Root cation exchange capacity (CEC) will determine the cation uptake into the symplast and cation transport through

the apoplast (RAY & GEORGE, 2010). After acquired from the soil solution it is translocated via the xylem and cannot be remobilized from older tissues through the phloem, therefore in Ca-deficiency situations, all symptoms occur in new organs (YANG & JIE, 2005). Within the leaf, depending on the plant species, Ca can accumulate in trichomes, mesophyll, or epidermal cells that are close to the stomata (KARLEY et al., 2000). It is important to notice that for nutritional and structure roles, Ca^{2+} supply comes via constitutive ion channels, and Ca^{2+} influx channels (DEMIDCHIK & MAATHUIS, 2007).

Ca is a ubiquitous cellular messenger to all eukaryote cells (BERRIDGE et al., 2000). Various biological processes are related to temporally and spatially defined modifications in Ca^{2+} concentration in the cytoplasm ($[Ca^{2+}]_{cyt}$) or specific organelles (KUDLA et al., 2010). These signals are essential for transducing stimuli (internal or external) into cellular responses (DEMIDCHIK et al., 2018). Such responses can be physiological, metabolic, or gene expression (EDEL et al., 2017). The $[Ca^{2+}]_{cyt}$ is kept at 50–150 nM level, with amazing accuracy, once (i) the Ca is attracted to the negative electric potential of the plasma membrane (PM); (i) organelles like endoplasmic reticulum (ER) and vacuole have (0.1–10 mM). For that, to maintain the $[Ca^{2+}]_{cyt}$ low cells need to work against the electrochemical gradient, Ca^{2+} transport across membranes is complex, and the transport systems, including Ca^{2+}-permeable ion channels Ca^{2+}-ATPases and Ca^{2+}/H^{+} exchangers that work consuming energy, from ATP or an ATP-dependent H^{+} gradient (DEMIDCHIK et al., 2018). *Arabidopsis thaliana* presents five Ca^{2+}-permeable channel families: glutamate receptors (GLRs); cyclic nucleotide-gated channels (CNGCs); reduced hyperosmolality-induced $[Ca^{2+}]_{cyt}$ increase (OSCAs); mechanosensitive channels (MCAs) and two-pore channels (TPCs) (KUDLA et al., 2018). In addition to the low $[Ca^{2+}]_{cyt}$, to be effective, the Ca^{2+} signal also needs to be stimulus-specific, which will lead to an exclusive Ca^{2+} 'signature', with specific frequency, amplitude, and location pattern (DODD et al., 2010). Thus, very tight regulation of Ca^{2+} transport is vital, and combined action of the influx and efflux activity leads to the Ca^{2+} signatures (KUDLA et al., 2018).

Also, the decoding processes of this Ca net are important, for the Ca^{2+} sensing proteins are essential (HASHIMOTO & KUDLA, 2011). The EF-hand Ca^{2+}-binding motifs are the most common calcium-binding motif found in proteins (LEWIT-BENTLEY & RÉTY, 2000). In *Arabidopsis thaliana* 250 proteins carry at least one predicted EF-hand motif (DAY et al., 2002), that reflects the importance of Ca sensing (KUDLA et al., 2018). Calmodulin (CaM), has four EF-hand motifs and it is one typical Ca^{2+} sensor protein, present in all eukaryotic cells

(EDEL & KUDLA, 2015). CaM is responsible for regulating enzyme activity (PEROCHON et al., 2011) and gene expression (GALON et al., 2010). Carrying from one to six EF-hands the CaM-like proteins (CMLs) (ZHU et al., 2015) are involved in different cellular responses, from developmental processes (DOBNEY et al., 2009) to stress responses (MAGNAN et al., 2008). Calcineurin B-like proteins (CBL) contain four EF-hands and have a complex interaction with CBL interacting protein kinases (CIPKs) regulating metabolic reactions through target phosphorylation sites (BATISTIC et al., 2010). Ca^{2+}-dependent protein kinases (CDPKs or CPKs) regulate proteins through kinase (WERNIMONT et al., 2010), it contains four EF-hands and a calmodulin-like domain (CLD) (LIESE, 2013).

One organelle closely related to the cellular Ca^{2+} network is the chloroplast, it can modulate cytosolic Ca^{2+} transients and is central in retrograde signaling (KUDLA et al., 2018). Chloroplasts have an autonomous Ca^{2+} signature (STAEL et al., 2012), and during the light/dark its uptakes and release, respectively Ca^{2+} from/to the cytosol (LORO et al., 2016). Moreover, chloroplasts have the chloroplast Ca^{2+} sensor protein (CAS) that contributes to cellular Ca^{2+} homeostasis and signaling (HOCHMAL et al., 2015). Guo et al. (2016), described that the CAS can generate cytosolic and stromal Ca^{2+} transient and also participates in the modulation of mitogen-activated protein kinase (MAPK) signaling. MAPK is strongly related to stress responses (TAJ et al., 2010). Ca in the chloroplast is also related to a structural component of photosystem II (PSII) (UMENA et al., 2011), facilitating K^+ transport into the stroma (CARRARETTO et al., 2013), and the regulation of metabolic enzymes (HOCHMAL et al., 2015).

Along with chloroplasts, mitochondria are another organelle that contributes to plant Ca^{2+} signaling (RIZZUTO et al., 2012). The outer membrane is not selective to Ca^{2+}, therefore cytosol and the mitochondrial intermembrane space share similar [Ca^{2+}] (KUDLA et al., 2018). It is important to notice that many studies in that area were conducted in the animal field, where it was discovered that mitochondria influence cytosolic Ca^{2+} signals (WAGNER et al., 2016). Phylogenetic analyses showed similarities in mitochondrial Ca^{2+} machinery between mammals and plants (WAGNER et al., 2016). As an example, the matrix influx channel specialized Ca^{2+} uniporter complexes (MCUC) have been first identified in animals, but present a homolog in plants, the pore-forming MCU (mitochondrial Ca^{2+} uniporter) (TEARDO et al., 2017). It has recently been demonstrated that MCU proteins mediate mitochondrial Ca^{2+} transport in plants and that this mechanism is the main route for a rapid influx of Ca^{2+} into the matrix (RUBERTI et al., 2022). Such channels are regulated by the mitochondrial Ca^{2+} uptake protein 1 (MICU1),

which has EF-hand domains that function as a [Ca^{2+}] sensor in the mitochondrial matrix and restrict Ca^{2+} influx, preventing saturation (WAGNER et al., 2015; KUDLA et al., 2018) and modulating Ca responses within this organelle (WAGNER et al., 2015).

Dark-induced senescence

Senescence can occur as part of plant development or it can be induced by stress, prematurely (BUCHANAN-WOLLASTON et al., 2002). It is easily percept by the dramatic color changes in the leaves, common in fall of temperate regions of the globe, and in annual plants such as grain crops (BHALERAO et al., 2003). However, foliar senescence may also be a consequence of stress conditions, such as pathogens, extreme temperatures (SMART, 1994), and altered light conditions (WEAVER & AMASINO, 2001). In both scenarios, it is a highly regulated process requiring massive transcriptional and metabolic reprogramming to break down and remobilize valuable resources (MAILLARD et al., 2015). Leaves are a complex organ that supports plants' growth by harnessing light energy through photosynthesis (KRIEGER-LISZKAY et al., 2019). Therefore, under stressful conditions that lead a leaf to be not photosynthetically productive, it will senescence to make its resources available to other organs (LIEBSCH & KEECH, 2016). Accordingly, light plays an essential role in senescence regulation, and the dark-induced senescence as a consequence of light deprivation leads to rapid leaf senescence, particularly if only a part of the plant is shadowed or darkened (KEECH et al., 2010).

Leaf senescence allows the remobilization of valuable resources, for example, nitrogen, phosphorus, and carbon skeletons to grow or reserve organs and it is a highly regulated ordered process (KEECH et al., 2007). It involves the degradation of chlorophyll and proteins (BROUWER et al, 2012). It is important to notice that when chlorophyll is degraded and the yellowing of the leaf can be seen, most of the senescence process, implying the protein and RNA degradation, loss in photosynthetic activity; and nutrient remobilization, has already occurred (BUCHANAN-WOLLASTON et al., 2002). In dark-induced senescence, the main regulator of this process are phytochromes (phy) – red/far-red light (R/FR) receptors of plants, that mediate the light signaling (SAKURABA et al., 2014). The phy can interchange between their active Pfr form when absorbing R to the inactive form Pr if absorbing FR (BROUWER et al., 2012). Accordingly, the mutants overexpressing phyB and phyA showed a delay in dark-induced senescence and leaf yellowing in response (SAKURABA et al., 2014; ROUSSEAUX

et al., 1997). These active Pfr are associated with PHYTOCHROME-INTERACTING FACTORS (PIFs) that are related to several light responses (LIEBSCH & KEECH, 2016). PIFs are transcription factors that act as negative regulators of light signaling and positive regulators of light deprivation-related responses (LEIVAR & QUAIL, 2011). PIFs are induced in prolonged darkness and *pif* mutants showed a reduction in typical transcriptome changes associated with senescence, including genes of ethylene and abscisic acid (ABA) signaling, chlorophyll degradation, and photosynthesis, an attenuation of reactive oxygen species (ROS), and (SONG et al., 2014). Moreover, PIFs can affect other senescence regulators directly or indirectly, like WRKY transcription factor WRKY22 and NAC transcription factor NAP (ANAC029), both related to the dark-induced senescence signal transduction pathway (ZHOU et al., 2011; GUO & GAN, 2006). It is important to notice that this PIF regulated mechanisms work in a Feed-forward loops (FFLs) of gene regulation that occur when one component regulates the second, and only the two together then regulate a downstream third component (LIEBSCH & KEECH, 2016).

Another interesting point is the regulation of dark-induced senesce through carbon starvation, key transcription factors are induced in the low-energy response, such as bZIPs (DIETRICH et al., 2011). Mutant overexpression bZIPs showed an accelerated dark-induced senesce (MAIR et al., 2015). Prolonged darkness induces starvation in the plant, however, intriguingly if the darkness is imposed in the whole plant the senescence effect is delayed, even with the strong carbon starvation, which indicates that other factors also play a role (KEECH et al., 2007).

During dark-induced senescence mitochondria are reported to be intact until the latter stages of the leaf senescence (RIO et al., 2003). It is believed that mitochondria are the main responsible for the supply of carbon skeletons from the TCA cycle and, therefore, facilitating the relocation of nitrogen and other nutrients, and ATP production (KEECH et al., 2007). In fall senescence leaves of poplar, it was shown that mitochondria play an important role in energy conversion and carbon metabolism (KESKITALO et al., 2005). Corroborating, the genes related to photosynthesis are quickly decreased, while the respiration and mitochondrial electron transport chain genes are maintained or even upregulated during foliar senescence (ANDERSSON et al., 2004). Specific for dark-induced senescence, Keech et al., (2007) demonstrated that depending on the type of the dark, mitochondria behave differently. When the whole plant is in the dark, the mitochondrial activity is low, on the opposite, if only one leaf

is covered, high mitochondrial activity is observed, which could be related to an efficient remobilization of nutrients (KEECH et al., 2007).

Aluminum stress

Most potentially arable land worldwide is located in acid soils (SINGH et al., 2017). This characteristic is strongly influenced by the source material during soil formation (WONG et al., 2008). Acidic soils are those with a pH equal to or less than 5.5, reaching a pH < 3.0 in extreme cases (BOJÓRQUEZ-QUINTAL et al., 2017). It is important to notice that not only usual farming practices, such as the application of ammonium-based fertilizers but also industrial pollution unceasingly increase the acidification of soils (CHAUHAN et al., 2021; KOCHIAN et al., 2015). Soil acidity is in itself a limiting factor in nutritional terms for plants (GUPTA et al., 2013), once it disturbs the availability of important nutritional minerals, such as phosphorus (P) and calcium (Ca) (Von UEXKÜLL & MUTERT, 1995).

In tropical and subtropical regions, soil acidity is an important constraint that hinders the increase of food production (GUPTA et al., 2013), given that aluminum (Al) is the most abundant metallic element in Earth's crust (SINGH et al., 2017), the toxicity triggered by Al is considered the main factor limiting world agricultural production in acidic soils (KOCHIAN et al., 2015). Even being a non-toxic metal if present in the pH range 6.0 to 8.0, existing mostly in aluminum silicate (Al_2SiO_5), aluminum sulfate ($Al_2(SO_4)_3$), and aluminum phosphate ($AlPO_4$) in soil solution (SADE et al., 2016; YAN et al., 2022), with pH < 5.0 the formation of toxic species of Al occurs, when solubilized in the forms of aluminum hydroxide ($Al(OH)_2^+$, $Al(OH)^{2+}$) aluminum cation (Al^{3+}) (LIU et al., 2022; DELHAIZE & RYAN, 1995). Of these, the latter has a greater capacity to interfere with the growth and root development of several plants (MA, 2007; KOCHIAN et al., 2015).

Even at micromolar concentrations (KOCHIAN et al., 2004) and within 30 min to 2 h of exposure, Al^{3+} may promote rhizotoxic effects in higher plants, being the inhibition of root elongation the initial and main symptom of Al toxicity (KOCHIAN et al., 2002). Accordingly, the root distal transition zone (DTZ), a region with a high rate of cell division, is considered the most susceptible to Al (KOPITTKE et al., 2015). The inhibition of root elongation in response to Al is a consequence of alterations in both division and cellular elongation (KOCHIAN et al., 2002). Al interacts with the large number of negative charges in cell wall pectins, which increases the rigidity of the cell wall and interferes with cell division, leading to atrophy of root

hairs (YAN et al., 2022). Furthermore, it can depolymerize the microtubules distorting the cytoskeletal actin network (PANDA et al., 2008), additionally, it disrupts the polar auxin transport (ZHANG et al., 2020). All those factors culminate in root growth inhibition. The abundance of Al also results in changes in physiological cellular functions, like the depolarization of membranes, which can affect a series of physiological mechanisms (OFOE et al., 2022), interfering with voltage-gated, like the Ca^{2+} permeable channels (JONES et al., 1998), that will decrease in the cytoplasmic concentration of free Ca^{2+}, which can lead to an interruption of signaling cascades related to Ca^{2+}. Furthermore, it increases the rigidity of the double helix, leading to a reduction in DNA replication (EEKHOUT et al., 2017; SIQUEIRA et al., 2022). Al can form a link with oxygen donor compounds, like carboxylate (-COOH) groups, that will cause lipid peroxidation and disturbing membrane structure (REN et al., 2022). In effect, Al leads to a disturbance of the surface charge of the plasma membrane, leading to ATP depletion (YAMAMOTO et al., 2002). Being a highly reactive element, Al can induce oxidative stress, rapidly forming reactive oxygen species (ROS) that can lead to cell death (CHAUHANA et al., 2021). Consistently, in the presence of Al, the content of superoxide radicals and hydrogen peroxide are significantly increased in isolated mitochondria (PANDA et al., 2008).

Through evolution, plants have developed strategies capable of preventing or mitigating Al toxicity effects. These include: (i) mechanisms of tolerance – that are based on sequestration and internal detoxification of Al, and (ii) exclusion mechanisms – that prevent the entrance of toxic Al species into the root apex (RYAN et al., 2007; KOCHIAN et al., 2015). Both mechanisms involve different transporters and the formation of Al complexes with organic acid (OA), more specifically malate, citrate, and, in some species, oxalate (NUNES-NESI et al., 2014). The transporters ABC (ATP-BINDING CASSETTE) are strongly associated with the internal mechanisms of tolerance since it was reported to be one Al influx channel that increases the Al tolerance for rice (*Oryza sativa*) (HUANG et al., 2009), wild soybean (*Glycine soja*) (WEN et al., 2021) and barley (*Hordeum vulgare* L.) (LIU et al., 2021). For rice, as well as ABC the Al influx channel NRAMP (NATURAL RESISTENCE-ASSOCIATED MACROPHAGE PROTEIN), was reported (OsNRAT1) (LI et al., 2014). Another possible pathway for Al influx is aquaporins, first discovered for Al-accumulator hydrangea (*Hydrangea macrophylla*) that translocate the Al and accumulates it in sepal tissue (NEGISHI et al., 2012). In *Arabidopsis thaliana* the aquaporin NIP1;2 was reported to help translocate the Al-malate complex from root to shoot (WANG et al., 2017). Once inside the root, the plants need to

detoxify the Al^{3+} in their cytosol (SINGH et al., 2017), a process that is tightly associated with the complexation of organic acids (KOCHIAN et al., 2015). In addition, Al stress-responsive antioxidative defense mechanisms are upregulated to scavenge the Al oxidative damage (MA et al., 2012). Multiple species were reported to have an upregulation of antioxidative enzymes in response to Al-ROS production, rice (RIBEIRO et al., 2012), wheat (*Triticum aestivum*) (LIU et al., 2018), maize (*Zea mays*) (GIANNAKOULA et al., 2010), tobacco (*Nicotiana tabacum*) (DING et al., 2003).

For the exclusion mechanism, the family of transporters MATE (MULTIDRUG AND TOXIC COMPOUND EXTRUSION) have been shown to contribute to Al tolerance, performing an OA: H^+ antiport that governs the transport exudation of citrate (KOCHIAN et al., 2015). MATE was found in maize (MARON et al., 2010), sorghum (*Sorghum bicolor*) (MAGALHAES et al., 2007), barley (FURUKAWA et al., 2007), *Arabidopsis* (LIU et al., 2009), beans (*Vigna umbellata*) (YANG et al., 2007) and rice (OsFRD1) (YOKOSHO et al., 2011). Even though MATE is present, in species such as wheat and *Arabidopsis* the main OA exuded by the roots and used to chelate Al in the rhizosphere for both is malate. This process of transporting the malate out of the cell involves a transporter belonging to the multigenic family of ion channels ALMT (AL-ACTIVATED MALATE TRANSPORTER) (SASAKI et al., 2004; KOBAYASHI et al., 2007). In *Arabidopsis* Ca^{2+} regulates transcription factor CALMODULIN-BINDING TRANSCRIPTION ACTIVATOR2 (CAMTA) that binds to the ALMT1 transporter promoter contributing to the positive regulation of ALMT1 expression (TOKIZAWA et al., 2015) and SENSITIVE TO PROTON RHIZOTOXICITY (STOP1) also induces the genes ALMT1 (SAWAKI et al., 2009), while the WRKY46 is a repressor of the ALMT1 (DING et al., 2013).

Reactive Oxygen Species - ROS

The baseline of reactive oxygen species (ROS) levels, that characterize cellular homeostasis, depend on the environmental conditions, circadian clock, plant development stage, and physiological conditions (MITTLER et al., 2022). ROS are molecules that contain oxygen (O_2), however in those the O_2 presents a higher chemical activity (WASZCZAK, et al. 2018). The group of free radicals in ROS can damage the cells and cellular components, yet it can also work as a metabolic signal (WILLEMS et al., 2016). Such ROS signals can transmit

specific information that will later regulate growth, development, and stress response (SCHWARZLÄNDER & FINKEMEIER, 2013).

During cellular processes that involve the presence of O_2 in energy or electron transfer, the formation of ROS is inevitable (WASZCZAK, et al. 2018). The most common ROS forms are H_2O_2 (hydrogen peroxide), O_2^- (superoxide), and OH (hydroxyl radical) (ALIYARI RAD et al., 2022), being the H_2O_2 the most stable one (MATTILA et al., 2015). All subcellular compartments can generate all types of ROS, except the apoplast (FOYER & NOCTOR, 2016). In the cellular compartments, the ROS levels are kept low (NOCTOR et al., 2016) even with the ROS production inherent to the metabolism process. ROS scavenger machinery, enzymatic or nonenzymatic, exists to control and avoid the potential cellular damage that ROS production can cause to the cells (WASZCZAK et al., 2018). Another function of the antioxidant machinery is the maintenance of redox homeostasis, which is important to alleviate the excessive ROS, allowing it to serve as a signaling molecule (WILLEMS et al., 2016). Accordingly, the increase in ROS concentration is transitory, if a high production of ROS occurs the redox balance is disturbed in a more oxidized state and that can trigger downstream responses (MITTLER et al., 2022; BURKE et al., 2020). These responses can rearrange the transcriptome, and gene expression, to increase detoxification, and antioxidant defense system to alleviate cellular damage (WILLEMS et al., 2016). Therefore, protecting against tensions leads to an increase in ROS that can impact the oxidation of cellular materials and ultimately lead to cell death (ALIYARI RAD et al., 2022).

The mitochondrial redox balance can act as a parameter of environmental cues (WASZCZAK et al., 2018). Being the main source of energy production, the mitochondrion is also the main site for ROS production (SWEETMAN et al., 2020). The synthesis of ATP in the mitochondria is one example of ROS production during cellular metabolism (HUANG et al., 2016), although, this ROS production can be elevated in any cellular compartment during stress conditions (MITTLER et al., 2022).

The mitochondrial electron transport chain (mETC) is deeply associated with mitochondria-generated ROS (mtROS) (HUANG et al., 2016). Impairments in respiration lead to an increase in mETC that can provoke electron transfer to O_2 (WASZCZAK et al., 2018). Consequently, the O_2^- generated in the matrix is dismutated to H_2O_2 through MnSOD, or spontaneously, and afterwards, it can be scavenged by matrix antioxidant enzymes (SCHWARZLÄNDER & FINKEMEIER, 2013). Plant mitochondria matrix also has a

significant number of proteins regulated by redox-active thiols that can be affected by local H_2O_2 levels and mediate an *in situ* mitochondrial response (SCHWARZLÄNDER & FINKEMEIER, 2013). Moreover, these mtROS have been suggested to work as signaling for stress defense in plants (HUANG et al., 2016), information that can go from mitochondria to the nucleus, retrograded signaling (RTG), being the H_2O_2 the most promising molecule candidate for that (MATTILA et al., 2015).

Plants have some strategies to avoid over-ROS production in the mitochondria (HUANG et al., 2016). The overexpression of *UNCOUPLING PROTEIN1* (*UCP*) in tobacco enhanced its resistance to various abiotic stresses by reducing ROS generation and inducing the antioxidant system (BARRETO et al., 2014). The electron flow can also avoid complexes III and IV and be redirected in an alternative pathway by the alternative oxidases (AOXs) (GIRAUD et al., 2016). *AOX* genes are upregulated in stress conditions that cause disturbance to mETC; accordingly, it is essential in stress conditions that induce mitochondrial redox bursts (WASZCZAK et al., 2018).

The cellular role of ROS is defined by their interaction with other metabolites and their removal by the ROS-scavenging machinery (WASZCZAK et al., 2018). Previously considered only a harmful by-product of aerobic metabolism, it is now elucidated as also a major regulatory molecule, with a role in signaling cellular perturbation and environmental stimuli (MITTLER et al., 2022).

In vivo biosensors

Understanding how signaling molecules, metabolites, and resource information are temporally and spatially distributed in plants is crucial to elucidating how they cope with environmental changes and coordinating many cellular responses to environmental cues (WALIA et al., 2018). Thus, it is important to measure the levels of key molecular components and monitor their physiological dynamics, however technically it is a challenge (SCHWARZLÄNDER & FINKEMEIER, 2013). Some methodologies are invasive, and it is possible that the extraction method itself changes some metabolite features or does not allow subcellular localization specificity (OKUMOTO et al., 2012). Even though, much about plant physiology was discovered with analyses of isolated organelles and whole tissue extraction (SADOINE et al., 2021).

To overcome these challenges, genetically encoded fluorescent biosensor approaches have developed and can measure metabolites levels with more accuracy and with minimally invasive assays (WALIA et al., 2018). After the discovery of the green fluorescent protein (SHIMOMURA, JOHNSON & SAIGA 1962) it was possible the development of *in vivo* tools to monitor metabolic dynamics, not only in the plant field but also in the mammalian field (ZHOU et al., 2015; WALIA et al., 2018).

A biosensor is defined as a molecule, device, or organism that monitors a specific molecule of interest and emits a signal in a biological context (SADANANDOM & NAPIER, 2010). Additionally, to be considered an *in vivo* biosensor the probe must (i) have a high specificity to the molecule that it will sensor; (ii) allow a quantitative readout of biological concentrations in time; (iii) have a higher signal than the noise readout signal; and (iv) be nontoxic for the biological process that it will be monitor (OKUMOTO et al., 2012). All those features allow an equilibrium with the surrounding environment to monitor physiological changes (SCHWARZLÄNDER & FINKEMEIER, 2013). Moreover, those probes can be genetically targeted to specific subcellular compartments (HUANG et al., 2016).

Those genetically encoded fluorescent biosensors are formed by a sensor portion combined with a fluorescent protein (FP); the signal of the FP is detected by fluorescence microscopy or fluorimetry (ROSENWASSER et al., 2010). The biosensors can also be divided into two categories indirect or direct (WALIA et al., 2018). The indirect ones need additional cellular components to report, usually used for monitoring transcription, degradation, and translocation (USLU & GROSSMANN, 2016). They are typically irreversible and can only be reported in a cellular environment (USLU & GROSSMANN, 2016). In contrast, direct biosensors can also report *in vitro*, the first one was developed to monitor cellular calcium levels (MIYAWAKI et al., 1997).

Based on their FPs and sensory portion properties, the sensors can also be categorized as intrinsic biosensors, when the FP itself senses the target molecule; or extrinsic biosensors, when a sensory module (polypeptide or nucleotide sequence) is fused with the FP (OKUMOTO et al., 2012). Additionally, another categorization is based on the number of FPs and type of fluorescent readout (WALIA et al., 2018). Biosensors single-FPs intensiometric present only FP with one excitation (Ex) and one emission (Em), nevertheless, single-FPs can be radiometric and present two wavelengths of Ex that will report different molecules (HANSON et al., 2004). Moreover, a single-FP radiometric can also exhibit two Em to different target molecules

(HANSON et al., 2002). The double-FPs can form a Förster Resonance Energy Transfer (FRET) when the rearrangement of the binding domain enables energy transfer in response to the analyte (USLU & GROSSMANN, 2016).

A large variety of biosensors that can also be genetically encoded to the mitochondria have been used to cover the central metabolic parameters of this organelle (SCHWARZLÄNDER & FINKEMEIER, 2013). Those include usually the FRET-based biosensors with a cyan FP (CFP) and yellow FP (YFP), to monitor Ca^{2+} levels (YC 3.6) (KREBS et al., 2011); A circularly permutated fluorescent proteins (cpYFP) to monitor pH changes (SCHWARZLÄNDER et al., 2014); the green fluorescent protein redox-sensitive (GRX1-roGFP2) probe that has cysteine residues and monitor GSH/GSSG ratio (MEYER et al., 2007) and pH-insensitive roGFP2-Orp1, to monitor H_2O_2 (GUTSCHER et al., 2009).

CHAPTERS OVERVIEW

This thesis is largely focused on understanding how and to which extent the mitochondria metabolism acts in abiotic stress responses. Since mitochondria metabolism plays an essential role in plant growth, development, and communication with other organelles, elucidating how it works in mitigating environmental stress is extremely important for future genetic engineering that will allow crop improvement. The main goal of this study was to elucidate how the mitochondrial (i) redox system interferes with Al stress responses and (ii) Ca^{2+} transporters adjust chlorophyll degradation. To achieve this, several different, yet complementary, experimental approaches were undertaken using *Arabidopsis thaliana* mutants and thus the thesis is organized into two independent chapters.

The first chapter brings together the characterization of mitochondrial redox apparatus in response to Al stress. For that, mutants of the TRX and GSH systems were used. The second chapter is focused on comprehending the relation between chlorophyll degradation and the lack of the mitochondrial Ca^{2+} transporter MCU. Each of these chapters presents its introduction, discussion, and details of the methodologies. At the end of the thesis is a brief conclusion of the whole work as well as an outlook of future perspectives.

Overall, the results presented here suggest that mitochondria play an important yet unrecognized role in Al and dark stress responses. The mitochondrial ROS response is tightly connected to the Al tolerance, and our results indicate that the GSH system is most likely one

of the important players regulating mitochondrial ROS during Al stress. Our results also demonstrated an expected tight connection between the mitochondrial matrix Ca^{2+} concentrations and chlorophyll degradation pathway; however, more importantly, it seemingly does not occur through the regulation of the GDH2.

Chapter 1: Deciphering the significance of the thioredoxin system in aluminum stress response

Toxicity triggered by Al is a critical factor that limits agricultural production in acidic soils (pH < 5.0). Being a highly reactive element, Al can alter the energetic state, disturbing redox homeostasis, and its main symptom is root growth inhibition. Plants display mechanisms to prevent or mitigate the effects of this toxicity. All known strategies involve the presence of organic acids (OA), that come from mitochondrial processes to complex Al. In this context, mitochondrial metabolism is crucial to support cellular processes in mitigating the effect of Al. Here we attempted to demonstrate the existence of a correlation between better mitochondrial redox homeostasis and Al tolerance. We characterized the tolerance to Al by measuring their root development in the stress and using genetically encoded biosensors we could monitor the alterations in the GSH/GSSG ratio, H_2O_2, and pH in response to Al in multiple organs of mutants for mitochondrial redox system (NADPH-TRX reductase A and B double mutant, *ntra/b* and GLUTATHIONE REDUCTASE 1, *gr1-1*). The main results obtained here indicate that mitochondria are a target for Al stress and the redox status is strongly and rapidly imbalanced. Also, it is possible to infer that the glutathione antioxidant system is most likely the main route for ROS scavenging in response to Al stress.

Chapter 2: Deciphering the significance of the mitochondrial calcium uniport to leaf senescence

Leaf senescence is a consequence of natural aging but can also be a result of stress response. Usually, it is an active and complex process mainly regulated by light. During this process many metabolic adjustments occur, beginning with a decrease in photosynthesis and leading ultimately to cell death. Chlorosis is one visible symptom that appears in darkened leaves and can be directly related to chlorophyll degradation. Here we attempted to understand the phenotype of a delayed chlorophyll degradation during dark-induced senescence showed by a mitochondrial Ca^{2+} transporter mutant (*mcu123*). One possible pathway for the degraded

chlorophyll molecules is the remobilization of resources, which can be strongly correlated with mitochondria through glutamate dehydrogenase 2 (GDH2), which connects nitrogen and carbon metabolism. Therefore, we tested the activation of GDH2 by calcium *in vitro,* and using a sensor we could monitor the Ca^{2+} levels in mitochondria and cytosol during senescence. Our data could not corroborate the correlation between the GDH2 regulation by calcium and the delay in the chlorophyll degradation, leading us to a new novel of future ideas of mitochondria and chloroplast crosstalk in dark stress response.

REFERENCES

ALIYARI RAD, S.; DEHGHANIAN, Z.; ASGARI LAJAYER, B.; NOBAHARAN, K.; ASTATKIE, T. Mitochondrial Respiration and Energy Production Under Some Abiotic Stresses. **Journal of Plant Growth Regulation**, v. 41, p. 3285–3299, 2021.

ANDERSSON, A.; KESKITALO, J.; SJÖDIN, A.; BHALERAO, R.; STERKY, F.; WISSEL, K.; TANDRE, K.; ASPEBORG, H.; MOYLE, R.; OHMIYA, Y.; BHALERAO, R. A transcriptional timetable of autumn senescence. **Genome Biology**, v. 5, pp.1-13, 2004.

ARAUJO, W.L.; NUNES-NESI, A.; OSORIO, S.; USADEL, B.; FUENTES, D.; NAGY, R.; BALBO, I.; LEHMANN, M.; STUDART-WITKOWSKI, C.; TOHGE, T.; MARTINOIA, E. Antisense inhibition of the iron-sulphur subunit of succinate dehydrogenase enhances photosynthesis and growth in tomato via an organic acid–mediated effect on stomatal aperture. **The Plant Cell**, v. 23, n. 2, p.600-627, 2011.

BARRETO, P.; KOLTUN, A.; NONATO, J.; YASSITEPE, J.; MAIA, I.D.G.; ARRUDA, P. Metabolism and signaling of plant mitochondria in adaptation to environmental stresses. **International Journal of Molecular Sciences**, v. 23, n. 19, p.11176, 2022.

BARRETO, P.; OKURA, VK.; NESHICH, IAP.; MAIA, IDEG.; ARRUDA, P. Overexpression of *UCP1* in tobacco induces mitochondrial biogenesis and amplifies a broad stress response. **BMC Plant Biol**, v. 14, n. 144, 2014.

BATISTIC, O.; WAADT, R.; STEINHORST, L.; HELD, K.; KUDLA, J. CBL-mediated targeting of CIPKs facilitates the decoding of calcium signals emanating from distinct cellular stores. **The Plant Journal**, v. 61, p. 211–222, 2010.

BERRIDGE, M.J.; BOOTMAN, M.D.; RODERICK, H.L. Calcium signalling: dynamics, homeostasis and remodelling. **Nature Reviews Molecular Cell Biology**, v. 4, n. 7, p.517-529, 2003.

BHALERAO, R.; KESKITALO, J.; STERKY, F.; ERLANDSSON, R.; BJORKBACKA, H.; BIRVE, S.J.; KARLSSON, J.; GARDESTROM, P.; GUSTAFSSON, P.; LUNDEBERG, J.; JANSSON, S. Gene expression in autumn leaves. **Plant Physiology**, v. 131, n. 2, p.430-442, 2003.

BOJÓRQUEZ-QUINTAL, E.; ESCALANTE-MAGAÑA, C.; ECHEVARRÍA-MACHADO, I.; MARTÍNEZ-ESTÉVEZ, M. Aluminum, a Friend or Foe of Higher Plants in Acid Soils. **Frontiers in Plant Science**, v. 8, p. 1767, 2017.

BROUWER, B.; ZIOLKOWSKA, A.; BAGARD, M.; KEECH, O.; GARDESTRÖM, P. The impact of light intensity on shade-induced leaf senescence. **Plant, Cell & Environment**, v. 35, n. 6, p.1084-1098, 2012.

BUCHANAN, B.B. The path to thioredoxin and redox regulation in chloroplasts. **Annual Review of Plant Biology**, v. 67, p. 1-24, 2016.

BUCHANAN-WOLLASTON, V.; EARL, S.; HARRISON, E.; MATHAS, E.; NAVABPOUR, S.; PAGE, T.; PINK, D. The molecular analysis of leaf senescence a genomics approach. **Plant Biotechnology Journal**, v. 1, n. 1, p.3-22, 2003.

BURKE, R.; SCHWARZE, J.; SHERWOOD, OL.; JNAID, Y.; MCCABE, PF.; KACPRZYK, J. Stressed to death: The role of transcription factors in plant programmed cell death induced by abiotic and biotic stimuli. **Frontiers in Plant Science**, v.11, n. 1235, 2020.

CARRARETTO, L.; FORMENTIN, E.; TEARDO, E.; CHECCHETTO, V.; TOMIZIOLI, M.; MOROSINOTTO, T.; GIACOMETTI, GM.; FINAZZI, G.; SZABÓ, I. A thylakoid-located two-pore K^+ channel controls photosynthetic light utilization in plants. **Science**, v. 342, p. 114–118, 2013.

CARRIE, C.; MURCHA, M.W.; KUEHN, K.; DUNCAN, O.; BARTHET, M.; SMITH, P.M.; EUBEL, H.; MEYER, E.; DAY, D.A.; MILLAR, A.H.; WHELAN, J. Type II NAD(P)H dehydrogenases are targeted to mitochondria and chloroplasts or peroxisomes in *Arabidopsis thaliana*. **FEBS letters**, v. 582, n. 20, p.3073-3079, 2008.

CHA, J.Y.; KIM, J.Y.; JUNG, I.J.; KIM, M.R.; MELENCION, A.; ALAM, S.S.; YUN, D.J.; LEE, S.Y.; KIM, M.G.; KIM, W.Y. NADPH-dependent thioredoxin reductase A (NTRA) confers elevated tolerance to oxidative stress and drought. **Plant Physiology and Biochemistry**, v. 80, p. 184-191, 2014.

CHAUHAN, A.D.K.; YADAV, V.; VACULÍK, M.; GASSMANN, W.; PIKE, S.; ARIF, N.; SINGH, S.P.; RUPESH, D.; SAHI, S.; TRIPATHI, D.K. Aluminum toxicity and aluminum stress-induced physiological tolerance responses in higher plants. **Critical Reviews in Biotechnology**, v. 41, p. 715-730, 2021.

CONSIDINE, M.J.; GOODMAN, M.; ECHTAY, K.S.; LALOI, M.; WHELAN, J.; BRAND, M.D.; SWEETLOVE, L.J. Superoxide stimulates a proton leak in potato mitochondria that is related to the activity of uncoupling protein. **Journal of Biological Chemistry**, v. 278, n. 25, p.22298-22302, 2003.

COURTEILLE, A.; VESA, S.; SANZ-BARRIO, R.; CAZALÉ, A.C.; BECUWE-LINKA, N.; FARRAN, I.; HAVAUX, M.; REY, P.; RUMEAU, D. Thioredoxin *m4* controls photosynthetic alternative electron pathways in *Arabidopsis*. **Plant Physiology**, v. 161, n. 1, p. 508-520, 2013.

DALOSO, D.M.; MÜLLER, K.; OBATA, T.; FLORIAN, A.; TOHGE, T.; BOTTCHER, A.; RIONDET, C.; BARIAT, L.; CARRARI, F.; NUNES-NESI, A.; BUCHANAN, B.B.

Thioredoxin, a master regulator of the tricarboxylic acid cycle in plant mitochondria. **Proceedings of the National Academy of Sciences**, v. 112, n. 11, p. E1392-E1400, 2015.

DAY, I.S.; REDDY, V.S.; SHAD ALI, G.; REDDY, A.S.N. Analysis of EF-hand-containing proteins in *Arabidopsis*. **Genome biology**, v. 3, p.1-24, 2002.

DELORME-HINOUX, V.; BANGASH, S.A.; MEYER, A.J.; REICHHELD, J.P. Nuclear thiol redox systems in plants. **Plant Science**, v. 243, p. 84-95, 2016.

DEMIDCHIK, V.; MAATHUIS, F.J. Physiological roles of nonselective cation channels in plants: from salt stress to signalling and development. **New Phytologist**, v. 175, n. 3, p.387-404. 2007.

DEMIDCHIK, V.; SHABALA, S.; ISAYENKOV, S.; CUIN, T.A.; POTTOSIN, I. Calcium transport across plant membranes: mechanisms and functions. **New Phytologist**, v. 220, n. 1, p.49-69, 2018.

DEVI, S.R.; YAMAMOTO, Y.; MATSUMOTO, H. An intracellular mechanism of aluminum tolerance associated with high antioxidant status in cultured tobacco cells. **Journal of Inorganic Biochemistry**, v. 97, n. 1, p. 59-68, 2003.

DIETRICH, K.; WELTMEIER, F.; EHLERT, A.; WEISTE, C.; STAHL, M.; HARTER, K.; DRÖGE-LASER, W. Heterodimers of the *Arabidopsis* transcription factors *bZIP1* and *bZIP53* reprogram amino acid metabolism during low energy stress. **The Plant Cell**, v. 23, p. 381–395, 2011.

DING, Z.J.; YAN, J.Y.; XU, X.Y.; LI, G.X. AND ZHENG, S.J. *WRKY 46* functions as a transcriptional repressor of *ALMT 1*, regulating aluminum-induced malate secretion in *Arabidopsis*. **The Plant Journal**, v. 76, n. 5, p. 825-835, 2013.

DOBNEY, S.; CHIASSON, D.; LAM, P.; SMITH, SP.; SNEDDEN, WA. The calmodulin-related calcium sensor CML42 plays a role in trichome branching. **Journal of Biological Chemistry**, v. 284, n. 31, p. 647–31 657, 2009.

DODD, A.N.; KUDLA, J.; SANDERS, D. The language of calcium signaling. **Annual Review of Plant Biology**, v. 61, p.593-620, 2010.

DOURMAP, C.; ROQUE, S.; MORIN, A.; CAUBRIÈRE, D.; KERDILES, M.; BÉGUIN, K.; PERDOUX, R.; REYNOUD, N.; BOURDET, L.; AUDEBERT, P.A.; MOULLEC, J.L. Stress signalling dynamics of the mitochondrial electron transport chain and oxidative phosphorylation system in higher plants. **Annals of Botany**, v. 125, n. 5, p.721-736, 2020.

EDEL, K.H.; KUDLA, J. Increasing complexity and versatility: how the calcium signaling toolkit was shaped during plant land colonization. **Cell Calcium**, v. 57, n. 3, p.231-246, 2015.

EDEL, K.H.; MARCHADIER, E.; BROWNLEE, C.; KUDLA, J.; HETHERINGTON, A.M. The evolution of calcium-based signalling in plants. **Current Biology**, v. 27, n. 13, p.R667-R679, 2017.

EEKHOUT, T.; LARSEN, P.; DE VEYLDER, L. Modification of DNA checkpoints to confer aluminum tolerance. **Trends in Plant Science**, v. 22, n. 2, p. 102-105, 2017.

FONSECA-PEREIRA, P.; SOUZA, P.V.; HOU, L.Y.; SCHWAB, S.; GEIGENBERGER, P.; NUNES-NESI, A.; TIMM, S.; FERNIE, A.R.; THORMÄHLEN, I.; ARAÚJO, W.L.;

DALOSO, D.M. Thioredoxin *h2* contributes to the redox regulation of mitochondrial photorespiratory metabolism. **Plant, Cell & Environment**, v. 43, n. 1, p. 188-208, 2020.

FOYER, C.H.; NOCTOR, G. Stress-triggered redox signalling: What's in pROSpect? **Plant, Cell & Environment.** v. 39, n. 9, p. 51–64, 2016.

FURUKAWA, J.; YAMAJI, N.; WANG, H.; MITANI, N.; MURATA, Y.; SATO, K.; KATSUHARA, M.; TAKEDA, K.; MA, J.F. An aluminum-activated citrate transporter in barley. **Plant and Cell Physiology**, v. 48, n. 8, p. 1081-1091, 2007.

GALON, Y.; FINKLER, A.; FROMM, H. Calcium-regulated transcription in plants. **Molecular Plant**, v. 3, n. 4, p.653-669, 2010.

GEIGENBERGER, P.; THORMÄHLEN, I.; DALOSO, D.M.; FERNIE, A.R. The unprecedented versatility of the plant thioredoxin system. **Trends in Plant Science**, v. 22, n. 3, p. 249-262, 2017.

GELHAYE, E.; ROUHIER, N.; GÉRARD, J.; JOLIVET, Y.; GUALBERTO, J.; NAVROT, N.; OHLSSON, P.I.; WINGSLE, G.; HIRASAWA, M.; KNAFF, D.B.; WANG, H. A specific form of thioredoxin *h* occurs in plant mitochondria and regulates the alternative oxidase. **Proceedings of the National Academy of Sciences**, v. 101, n. 40, p. 14545-14550, 2004.

GIANNAKOULA, A.; MOUSTAKAS, M.; SYROS, T.; YUPSANIS, T. Aluminum stress induces up-regulation of an efficient antioxidant system in the Al-tolerant maize line but not in the Al-sensitive line. **Environmental and Experimental Botany**, v. 67, n. 3, p. 487-494, 2010.

GIRAUD, E.; HO, LHM.; CLIFTON, R.; CARROLL, A.; ESTAVILLO, G.; TAN, Y.F.; HOWELL, K.A.; IVANOVA, A.; POGSON, B.J.; MILLAR, A.H.; WHELAN, J. The absence of ALTERNATIVE OXIDASE1a in *Arabidopsis* results in acute sensitivity to combined light and drought stress. **Plant Physiology,** v. 147, p. 595–610, 2008.

GUO, H.; FENG, P.; CHI, W.; SUN, X.; XU, X.; LI, Y.; REN, D.; LU, C.; DAVID ROCHAIX, J.; LEISTER, D.; ZHANG, L. Plastid-nucleus communication involves calcium-modulated MAPK signalling. **Nature Communications**, v. 7, p. 12173, 2016.

GUO, Y.; GAN, S. AtNAP, a NAC family transcription factor, has an important role in leaf senescence. **The Plant Journal**, v. 46, n. 4, p.601-612, 2006.

GUPTA, N.; GAURAV, S.S.; KUMAR, A. Molecular Basis of Aluminium Toxicity in Plants: A Review. **American Journal of Plant Sciences**, v.4, p.21–37, 2013.

GUTSCHER, M.; SOBOTTA, M. C.; WABNITZ, G.H.; BALLIKAYA, S.; MEYER, A.J.; SAMSTAG, Y.; DICK, T. P. Proximity-based protein thiol oxidation by H_2O_2-scavenging peroxidases. **Journal of Biological Chemistry**, v. 284, p. 31532–31540, 2009.

HÄGGLUND, P.; FINNIE, C.; YANO, H.; SHAHPIRI, A.; BUCHANAN, B.B.; HENRIKSEN, A.; SVENSSON, B. Seed thioredoxin *h*. **BBA-Proteins and Proteomics**, v. 1864, n. 8, p.974-982, 2016.

HANSON, G.T.; AGGELER, R.; OGLESBEE, D.; CANNON, M.; CAPALDI, R. A.; TSIEN, R.Y.; REMINGTON, S.J. Investigating mitochondrial redox potential with redox-sensitive green fluorescent protein indicators. **Journal of Biological Chemistry**, v. 279, p.13044–13053, 2004.

HANSON, G. T.; MCANANEY, T. B.; PARK, E. S.; RENDELL, M.E.; YARBROUGH, D. K.; CHU, S.; XI, L.; BOXER, S.G.; MONTROSE, M.H.; REMINGTON, S.J. Green fluorescent protein variants as ratiometric dual emission pH sensors structural characterization and preliminary application, **Biochemistry**, v. 41, n. 52, p. 15477–15488, 2002.

HASHIMOTO, K.; KUDLA, J. Calcium decoding mechanisms in plants. **Biochimie**, v. 93, n. 12, p.2054-2059, 2011.

HIRASAWA, M.; SCHÜRMANN, P.; JACQUOT, J.P.; MANIERI, W.; JACQUOT, P.; KERYER, E.; HARTMAN, F.C.; KNAFF, D.B. Oxidation-reduction properties of chloroplast thioredoxins, ferredoxin: thioredoxin reductase, and thioredoxin f-regulated enzymes. **Biochemistry**, v. 38, n. 16, p. 5200-5205, 1999.

HOCHMAL, A.K.; SCHULZE, S.; TROMPELT, K.; HIPPLER, M. Calcium-dependent regulation of photosynthesis. **Biochimica et Biophysica Acta (BBA) – Bioenergetics**, v. 1847, p. 993–1003, 2015.

HUANG, C.F.; YAMAJI, N.; MITANI, N.; YANO, M.; NAGAMURA, Y.; MA, J.F. A bacterial-type ABC transporter is involved in aluminum tolerance in rice. **Plant Cell**, v. 21, n. 2, p. 655-667, 2009.

HUANG, S.; AKEN, O.; SCHWARZLÄNDER, BELT, K.A.; MILLAR, H. The Roles of Mitochondrial Reactive Oxygen Species in Cellular Signaling and Stress Response in Plants, **Plant Physiology**, v. 171, n. 3, p. 1551–1559, 2016.

HUNER, N.P.; ÖQUIST, G.; SARHAN, F. Energy balance and acclimation to light and cold. **Trends in Plant Science,** v. 3, n. 6, p.224-230, 1998.

JACOBY, R.P.; LI, L.; HUANG, S.; PONG LEE, C.; MILLAR, A.H.; TAYLOR, N.L. Mitochondrial composition, function and stress response in plants F. **Journal of Integrative Plant Biology**, v. 54, n. 11, p.887-906, 2012.

JONES, D. L.; KOCHIAN, L.V.; GILROY, S. Aluminum Induces a Decrease in Cytosolic Calcium Concentration in BY-2 Tobacco Cell Cultures. **Plant Physiology,** v. 116, p. 81–9, 1998.

KARLEY, A.J.; LEIGH, R.A.; SANDERS, D. Differential ion accumulation and ion fluxes in the mesophyll and epidermis of barley. **Plant Physiology**, v. 122, n. 3, p.835-844, 2000.

KEECH, O.; PESQUET, E.; AHAD, A.; ASKNE, A.; NORDVALL, D.A.G.; VODNALA, S.M.; TUOMINEN, H.; HURRY, V.; DIZENGREMEL, P.; GARDESTRÖM, P. The different fates of mitochondria and chloroplasts during dark-induced senescence in *Arabidopsis* leaves. **Plant, Cell & Environment**, v. 30, n. 12, p.1523-1534, 2007.

KEECH, O.; PESQUET, E.; GUTIERREZ, L.; AHAD, A.; BELLINI, C.; SMITH, S.M.; GARDESTRÖM, P. Leaf senescence is accompanied by an early disruption of the microtubule network in *Arabidopsis*. **Plant Physiology**, v. 154, n. 4, p.1710-1720, 2010.

KESKITALO, J.; BERGQUIST, G.; GARDESTRÖM, P.; JANSSON S. A cellular timetable of autumn senescence. **Plant Physiology**, v. 139, p.1635–1648, 2005.

KOBAYASHI, Y.; HOEKENGA, A.; ITOH, H.; NAKASHIMA, M.; SAITO, S.; SHAFF, J.E.; MARON, L.; PIÑEROS M.; KOCHIAN, L.; KOYAMA, H. Characterization of *AtALMT1*

Expression in Aluminum-Inducible Malate Release and Its Role for Rhizotoxic Stress Tolerance in *Arabidopsis*. **Plant Physiology** 145: 843–852, 2007.

KOCHIAN, L.V.; PENCE, N.S.; LETHAM, D.L.; PINEROS, M.A.; MAGALHAES, J.V.; HOEKENGA, O.A.; GARVIN, D.F. Mechanisms of metal resistance in plants: aluminum and heavy metals. **Progress in Plant Nutrition: Plenary Lectures of the XIV International Plant Nutrition Colloquium**, v. 247, p.109–119, 2002.

KOCHIAN, L. V.; HOEKENGA, O. A.; PIÑEROS, M. A. How Do Crop Plants Tolerate Acid Soils? Mechanisms of Aluminum Tolerance and Phosphorous Efficiency. **Annual Review of Plant Biology**, v. 55, p. 459–493, 2004.

KOCHIAN, L. V.; PIÑEROS, M. A.; LIU, J.; MAGALHAES, J. V. Plant Adaptation to Acid Soils: The Molecular Basis for Crop Aluminum Resistance. **Annual Review of Plant Biology**, v. 11, n. 66, p.1–28, 2015.

KOPITTKE, P.M.; MOORE, K.L.; LOMBI, E.; GIANONCELLI, A., FERGUSON, B.J., BLAMEY, F.P.C., MENZIES, N.W., NICHOLSON, T.M., MCKENNA, B.A., WANG, P. AND GRESSHOFF, P.M. Identification of the primary lesion of toxic aluminum in plant roots. **Plant Physiology**, v. 167, n. 4, pp.1402-1411. 2015.

KOZIK, A.; ROWAN, B.A.; LAVELLE, D.; BERKE, L.; SCHRANZ, M.E.; MICHELMORE, R.W.; CHRISTENSEN, A.C. The alternative reality of plant mitochondrial DNA: One ring does not rule them all. **PLOS GENETICS**, v. 15, n. 8, p.e1008373, 2019.

KREBS, M.; HELD, K.; BINDER, A.; HASHIMOTO, K.; HERDER, G.; PARNISKE, M.; KUDLA, J.; SCHUMACHER, K. FRET-based genetically encoded sensors allow high-resolution live cell imaging of Ca^{2+} dynamics, **The Plant Journal**, v. 69, n. 1, p. 181 – 192, 2012.

KRIEGER-LISZKAY, A.; KRUPINSKA, K.; SHIMAKAWA, G. The impact of photosynthesis on initiation of leaf senescence. **Physiologia Plantarum**, v. 166, n. 1, p.148-164, 2019.

KUDLA, J.; BATISTIČ, O.; HASHIMOTO, K. Calcium signals: the lead currency of plant information processing. **The Plant Cell**, v. 22, n. 3, p.541-563, 2010.

KUDLA, J.; BECKER, D.; GRILL, E.; HEDRICH, R.; HIPPLER, M.; KUMMER, U.; PARNISKE, M.; ROMEIS, T.; SCHUMACHER, K. Advances and current challenges in calcium signaling. **New Phytologist**, v. 218, n. 2, p. 414-431, 2018.

LA COGNATA, U.; LANDSCHÜTZE, V.; WILLMITZER, L.; MÜLLER-RÖBER, B. Structure and expression of mitochondrial citrate synthases from higher plants. **Plant and Cell Physiology**, v. 37, n. 7, p.1022-1029, 1996.

LALOI, C.; RAYAPURAM, N.; CHARTIER, Y.; GRIENENBERGER, J.M.; BONNARD, G.; MEYER, Y. Identification and characterization of a mitochondrial thioredoxin system in plants. **Proceedings of the National Academy of Sciences**, v. 98, n. 24, p.14144-14149, 2001.

LEIVAR, P.; QUAIL, PH. PIFs: pivotal components in a cellular signaling hub. **Trends in Plant Science**, v. 16, p.19–28, 2011.

LEWIT-BENTLEY, A.; RÉTY, S. EF-hand calcium-binding proteins. **Current Opinion in Structural Biology**, v. 10, n. 6, p.637-643, 2000.

LI, J.Y.; LIU, J.; DONG, D.; JIA, X.; MCCOUCH, S.R.; KOCHIAN, L.V. Natural variation underlies alterations in Nramp aluminum transporter (*NRAT1*) expression and function that play a key role in rice aluminum tolerance. **Proceedings of the National Academy of Sciences**, v. 111, n. 17, p. 6503-6508, 2014.

LIBERATORE, K.L.; DUKOWIC-SCHULZE, S.; MILLER, M.E.; CHEN, C.; KIANIAN, S.F. The role of mitochondria in plant development and stress tolerance. **Free Radical Biology and Medicine**, v. 100, p.238-256, 2016.

LIEBSCH, D.; KEECH, O. Dark-induced leaf senescence: new insights into a complex light-dependent regulatory pathway. **New Phytologist**, v. 212, n. 3, p.563-570, 2016.

LIESE, A.; ROMEIS, T. Biochemical regulation of *in vivo* function of plant calcium-dependent protein kinases (CDPK). **Biochimica et Biophysica Acta (BBA)-Molecular Cell Research**, v. 1833, p. 1582–1589, 2013.

LIU, H.; ZHU, R.; SHU, K.; LV, W.; WANG, S.; WANG, C. Aluminum stress signaling, response, and adaptive mechanisms in plants. **Plant Signaling & Behavior**, v. 17, n. 1, p. 2057060, 2022.

LIU, J.; MAGALHAES, J.V.; SHAFF, J.; KOCHIAN, L.V. Aluminum-activated citrate and malate transporters from the *MATE* and *ALMT* families function independently to confer *Arabidopsis* aluminum tolerance. **The Plant Journal**, v. 57, n. 3, p. 389-399, 2009.

LIU, W.; FENG, X.; CAO, F.; WU, D.; ZHANG, G.; VINCZE, E.; WANG, Y.; CHEN, Z.H.; WU, F. An ATP binding cassette transporter HvABCB25 confers aluminum detoxification in wild barley. **Journal of Hazardous Materials**, v. 401, p. 123371, 2021.

LIU, W.; XU, F.; LV, T.; ZHOU, W.; CHEN, Y.; JIN, C.; LU, L.; LIN, X. Spatial responses of antioxidative system to aluminum stress in roots of wheat (*Triticum aestivum* L.) plants. **Science of the Total Environment**, v. 627, p. 462-469, 2018.

LOGAN, D.C. The mitochondrial compartment. **Journal of Experimental Botany**, v. 57, n. 6, p.1225-1243, 2006.

LORO, G.; WAGNER, S.; DOCCULA, FG.; BEHERA, S.; WEINL, S.; KUDLA, J.; SCHWARZLÄNDER, M.; COSTA, A.; ZOTTINI, M. Chloroplast-specific in vivo Ca^{2+} imaging using Yellow Cameleon fluorescent protein sensors reveals organelle-autonomous Ca^{2+} signatures in the stroma. **Plant Physiology**, v. 171, p. 2317–2330, 2016.

LUETHY, M.H.; MIERNYK, J.A.; RANDALL, D.D. The mitochondrial pyruvate dehydrogenase complex: nucleotide and deduced amino-acid sequences of a cDNA encoding the *Arabidopsis thaliana* E1 α-subunit. **Gene**, v. 164, n. 2, p.251-254, 1995.

MA, B.; GAO, L.; ZHANG, H.; CUI, J.; SHEN, Z. Aluminum-induced oxidative stress and changes in antioxidant defenses in the roots of rice varieties differing in Al tolerance. **Plant Cell Reports**, v. 31, p. 687-696, 2012.

MA, J.F. Syndrome of aluminum toxicity and diversity of aluminum resistance in higher plants. **International Review of Cytology**, v. 264, p. 225-252, 2007.

MAEDA, H.A.; FERNIE, A.R. Evolutionary history of plant metabolism. **Annual Review of Plant Biology**, v. 72, n. 1, p.185-216, 2021.

MAGALHAES, J.V.; LIU, J.; GUIMARAES, C.T.; LANA, U.G.; ALVES, V.M.; WANG, Y.H.; SCHAFFERT, R.E.; HOEKENGA, O.A.; PINEROS, M.A.; SHAFF, J.E.; KLEIN, P.E. A gene in the multidrug and toxic compound extrusion (*MATE*) family confers aluminum tolerance in sorghum. **Nature Genetics**, v. 39, n. 9, p. 1156-1161, 2007.

MAGNAN, F.; RANTY, B.; CHARPENTEAU, M.; SOTTA, B.; GALAUD, J-P.; ALDON, D. Mutations in AtCML9, a calmodulin-like protein from *Arabidopsis thaliana*, alter plant responses to abiotic stress and abscisic acid. **The Plant Journal**, v. 56, n. 575–589, 2008.

MAILLARD, A.; DIQUELOU, S.; BILLARD, V.; LAINE, P.; GARNICA, M.; PRUDENT, M.; GARCIA-MINA, J.M.; YVIN, J.C.; OURRY, A. Leaf mineral nutrient remobilization during leaf senescence and modulation by nutrient deficiency. **Frontier in Plant Science**, v. 6, p. 317, 2015.

MAIR, A.; PEDROTTI, L.; WURZINGER, B.; ANRATHER, D.; SIMEUNOVIC, A.; WEISTE, C.; VALERIO, C.; DIETRICH, K.; KIRCHLER, T.; NÄGELE, T.; VICENTE-CARBAJOSA, J. SnRK1-triggered switch of bZIP63 dimerization mediates the low-energy response in plants. **eLife**, v. 4, p. e05828, 2015.

MARON, L.G.; GUIMARÃES, C.T.; KIRST, M.; ALBERT, P.S.; BIRCHLER, J.A.; BRADBURY, P.J.; BUCKLER, E.S.; COLUCCIO, A.E.; DANILOVA, T.V.; KUDRNA, D.; MAGALHAES, J.V. Aluminum tolerance in maize is associated with higher *MATE1* gene copy number. **Proceedings of the National Academy of Sciences**, v. 110, n. 13, p. 5241-5246, 2013.

MARSCHNER, H. Mineral nutrition of higher plants. **2nd Academic Press**, pp.15-22, 1995.

MATA-PÉREZ, C.; SPOEL, S.H. Thioredoxin-mediated redox signalling in plant immunity. **Plant Science**, v. 279, p. 27-33, 2019.

MATTILA, H.; KHOROBRYKH, S.; HAVURINNE, V.; TYYSTJÄRVI, E. Reactive oxygen species: reactions and detection from photosynthetic tissues. **Journal of Photochemistry and Photobiology B: Biology**, v. 152 p. 176–214, 2015.

MCDONALD, A.E.; VANLERBERGHE, G.C. The organization and control of plant mitochondrial metabolism. **Annual Plant Reviews**, v. 22, pp.290-324, 2006.

MENG, L.; WONG, J.H.; FELDMAN, L.J.; LEMAUX, P.G.; BUCHANAN, B.B. A membrane-associated thioredoxin required for plant growth moves from cell to cell, suggestive of a role in intercellular communication. **Proceedings of the National Academy of Sciences**, v. 107, n. 8, p. 3900-3905, 2010.

MEYER, A. J.; BRACH, T.; MARTY, L.; KREYE, S.; ROUHIER, N; JACQUOT, J.P.; HELL, R. Redox-sensitive GFP in *Arabidopsis thaliana* is a quantitative biosensor for the redox potential of the cellular glutathione redox buffer. **The Plant Journal**, v. 52, n. 5, p. 973–86, 2007.

MEYER, Y.; BUCHANAN, B.B.; VIGNOLS, F.; REICHHELD, J.P. Thioredoxins and glutaredoxins: unifying elements in redox biology. **Annual Review of Genetics**, v. 43, p. 335-367, 2009.

MICHALSKA, J.; ZAUBER, H.; BUCHANAN, B.B.; CEJUDO, F.J.; GEIGENBERGER, P. NTRC links built-in thioredoxin to light and sucrose in regulating starch synthesis in chloroplasts and amyloplasts. **Proceedings of the National Academy of Sciences**, v. 106, n. 24, p. 9908-9913, 2009.

MILLAR, A.H.; WHELAN, J.; SOOLE, K.L.; DAY, D.A. Organization and regulation of mitochondrial respiration in plants. **Annual Review of Plant Biology**, v. 62, pp.79-104, 2011.

MITTLER, R., ZANDALINAS, S.I., FICHMAN, Y.; VAN BREUSEGEM, F. Reactive oxygen species signalling in plant stress responses. **Nature reviews Molecular cell biology**, v. 23, n. 10, p. 663–679, 2022.

MIYAWAKI, A.; LLOPIS, J.; HEIM, R.; MCCAFFERY, J.M.; ADAMS, J.A.; IKURA, M.; TSIEN, R.Y. Fluorescent indicators for Ca^{2+} based on green fluorescent proteins and calmodulin. **Nature**, v. 388, p. 882–887, 1997.

MØLLER, I.M.; RASMUSSON, A.G.; VAN AKEN, O. Plant Mitochondria - Past, Present and Future. **The Plant Journal**, v. 108, n. 4, p. 912–959, 2021.

MURCHA, M.W.; KMIEC, B.; KUBISZEWSKI-JAKUBIAK, S.; TEIXEIRA, P.F.; GLASER, E.; WHELAN, J. Protein import into plant mitochondria: signals, machinery, processing, and regulation. **Journal of Experimental Botany**, v. 65, n. 22, pp.6301-6335, 2014.

NARANJO, B.; DIAZ-ESPEJO, A.; LINDAHL, M.; CEJUDO, F.J. Type-*f* thioredoxins have a role in the short-term activation of carbon metabolism and their loss affects growth under short-day conditions in *Arabidopsis thaliana*. **Journal of Experimental Botany**, v. 67, n. 6, p.1951-1964, 2016.

NEGISHI, T.; OSHIMA, K.; HATTORI, M.; KANAI, M.; MANO, S.; NISHIMURA, M.; YOSHIDA, K. Tonoplast-and plasma membrane-localized aquaporin-family transporters in blue hydrangea sepals of aluminum hyperaccumulating plant, **PLoS ONE**, v. 7, n. 8, p. e43189, 2012.

NIKKANEN, L.; TOIVOLA, J.; RINTAMÄKI, E. Crosstalk between chloroplast thioredoxin systems in regulation of photosynthesis. **Plant, Cell & Environment**, v. 39, n. 8, p.1691-1705, 2016.

NOCTOR, G.; MHAMDI, A.; FOYER, C. Oxidative stress and antioxidative systems: recipes for successful data collection and interpretation, **Plant Cell & Environment**, v. 39, n. 5, p. 1140-1160, 2016.

NUNES-NESI, A.; BRITO, D.S.; INOSTROZA-BLANCHETEAU, C.; FERNIE, A.R.; ARAÚJO, W.L. The complex role of mitochondrial metabolism in plant aluminum resistance. **Trends in Plant Science**, v. 19, n. 6, p. 399-407, 2014.

NUNES-NESI, A.; CARRARI, F.; GIBON, Y.; SULPICE, R.; LYTOVCHENKO, A.; FISAHN, J.; GRAHAM, J.; RATCLIFFE, R.G.; SWEETLOVE, L.J.; FERNIE, A.R. Deficiency of mitochondrial fumarase activity in tomato plants impairs photosynthesis via an effect on stomatal function. **The Plant Journal**, v. 50, n. 6, p.1093-1106, 2007.

OFOE, R.; THOMAS, R.H.; ASIEDU, S.K.; WANG-PRUSKI, G.; FOFANA, B.; ABBEY, L. Aluminum in plant: Benefits, toxicity and tolerance mechanisms. **Frontiers in Plant Science**, v. 13, p. 1085998, 2023.

OKEGAWA, Y.; MOTOHASHI, K. Chloroplastic thioredoxin m functions as a major regulator of Calvin cycle enzymes during photosynthesis *in vivo*. **The Plant Journal**, v. 84, n. 5, p. 900-913, 2015.

OKUMOTO, S.; JONES, A.; FROMMER, W.B. Quantitative imaging with fluorescent biosensors. **Annual Review of Plant Biology**., v. 63, p. 663–706, 2012.PANDA, S.K.; YAMAMOTO, Y.; KONDO, H.; MATSUMOTO, H. Mitochondrial alterations related to programmed cell death in tobacco cells under aluminium stress. **Comptes Rendus Biologies**, v. 331, n. 8, p. 597-610, 2008.

PEROCHON, A.; ALDON, D.; GALAUD, J.P.; RANTY, B. Calmodulin and calmodulin-like proteins in plant calcium signaling. **Biochimie**, v. 93, n. 12, p.2048-2053, 2011.

RASMUSSON, A.G.; SOOLE, K.L.; ELTHON, T.E. Alternative NAD(P)H dehydrogenases of plant mitochondria. **Annual Review of Plant Biology**., v. 55, pp.23-39, 2004.

RAY, J.G.; GEORGE, K.J. Calcium accumulation in grasses in relation to their root cation exchange capacity. **Journal of Agronomy**, v. 9, p.70-74, 2010.

REICHHELD, J.P.; KHAFIF, M.; RIONDET, C.; DROUX, M.; BONNARD, G.; MEYER, Y. Inactivation of thioredoxin reductases reveals a complex interplay between thioredoxin and glutathione pathways in Arabidopsis development. **The Plant Cell**, v. 19, n. 6, pp.1851-1865, 2007.

REICHHELD, J.P.; MEYER, E.; KHAFIF, M.; BONNARD, G.; MEYER, Y. AtNTRB is the major mitochondrial thioredoxin reductase in Arabidopsis thaliana. **FEBS letters**, v. 579, n. 2, pp.337-342, 2005.

REN, J.; YANG, X.; ZHANG, N.; FENG, L.; MA, C.; WANG, Y.; YANG, Z.; ZHAO, J. Melatonin alleviates aluminum-induced growth inhibition by modulating carbon and nitrogen metabolism, and reestablishing redox homeostasis in *Zea mays* L. **Journal of Hazardous Materials**, v. 423, p. 127159, 2022.

RIBEIRO, C.; CAMBRAIA, J.; PEIXOTO, P.H.P.; FONSECA- JÚNIOR, É.M.D. Antioxidant system response induced by aluminum in two rice cultivars. **Brazilian Journal of Plant Physiology**, v. 24, p. 107-116, 2012.

RÍO, L.A.; SANDALIO, L.M.; ALTOMARE, D.A.; ZILINSKAS, B.A. Mitochondrial and peroxisomal manganese superoxide dismutase: differential expression during leaf senescence. **Journal of Experimental Botany**, v. 54, n. 384, p.923-933, 2003.

RIZZUTO, R.; DE STEFANI, D.; RAFFAELLO, A.; MAMMUCARI, C. Mitochondria as sensors and regulators of calcium signalling. **Nature Reviews Molecular Cell Biology**, v. 13, p. 566–578, 2012.

ROSENWASSER, S.; ROT, I.; MEYER, A. J.; FELDMAN, L.; JIANG, K.; FRIEDMAN, H. A fluorometer-based method for monitoring oxidation of redox-sensitive GFP (roGFP) during development and extended dark stress. **Physiologia Plantarum**, v. 138, n. 4, p. 493–502, 2010.

ROUSSEAUX, MC.; BALLARÉ, CL.; JORDAN, ET.; VIERSTRA, RD. Directed overexpression of PHYA locally suppresses stem elongation and leaf senescence responses to far-red radiation. **Plant, Cell & Environment,** v. 20, p.1551–1558, 1997.

RUBERTI, C.; FEITOSA-ARAUJO, E.; XU, Z.; WAGNER, S.; GRENZI, M.; DARWISH, E.; LICHTENAUER, S.; FUCHS, P.; PARMAGNANI, A.S.; BALCEROWICZ, D.; SCHOENAERS, S. MCU proteins dominate in vivo mitochondrial Ca^{2+} uptake in Arabidopsis roots. **The Plant Cell**, v. 34, n. 11, p.4428-4452, 2022.

RYAN, P.R.; DELHAIZE, E.; RANDALL, P.J. Malate efflux from root apices and tolerance to aluminium are highly correlated in wheat. **Functional Plant Biology**, v. 22, n. 4, p. 531-536, 1995.

RYAN, P.R.; LIU, Q.; SPERLING, P.; DONG, B.; FRANKE, S.; DELHAIZE, E. A higher plant Δ8 sphingolipid desaturase with a preference for (Z)-isomer formation confers aluminum tolerance to yeast and plants. **Plant Physiology**, v. 144, n. 4, p. 1968-1977, 2007.

SADANANDOM, A.; NAPIER, R.; M. Biosensors in plants, **Current Opinion in Plant Biology**, v. 13, n. 6, p. 736-743, 2010.

SADE, H.; MERIGA, B.; SURAPU, V.; GADI, J.; SUNITA, M.S.L.; SURAVAJHALA, P.; KAVI KISHOR, P.B. Toxicity and tolerance of aluminum in plants: tailoring plants to suit to acid soils. **Biometals**, v. 29, p. 187-210, 2016.

SADOINE, M.; ISHIKAWA, Y.; KLEIST, T. J.; WUDICK, M. M; NAKAMURA, M.; GROSSMANN, G.; FROMMER, W. B.; CHENG-HSUN, H. Designs, applications, and limitations of genetically encoded fluorescent sensors to explore plant biology, **Plant Physiology**, v. 187, n. 2, p. 485–503, 2021.

SAKURABA, Y.; JEONG, J.; KANG, M.Y.; KIM, J.; PAEK, N.C.; CHOI, G. Phytochrome-interacting transcription factors PIF4 and PIF5 induce leaf senescence in *Arabidopsis*. **Nature Communications**, v. 5, n. 1, p.4636, 2014.

SASAKI, T.; YAMAMOTO, Y.; EZAKI, B.; KATSUHARA, M.; AHN, S.J.; RYAN, P.R.; DELHAIZE, E.; MATSUMOTO, H. A wheat gene encoding an aluminum-activated malate transporter. **The Plant Journal**, v. 37, n. 5, p. 645-653, 2004.

SAWAKI, Y.; IUCHI, S.; KOBAYASHI, Y.; KOBAYASHI, Y.; IKKA, T.; SAKURAI, N.; FUJITA, M.; SHINOZAKI, K.; SHIBATA, D.; KOBAYASHI, M.; KOYAMA, H. *STOP1* regulates multiple genes that protect Arabidopsis from proton and aluminum toxicities. **Plant Physiology**, v. 150, n. 1, p. 281-294, 2009.

SCHMIDTMANN, E.; KÖNIG, A.C.; ORWAT, A.; LEISTER, D.; HARTL, M.; FINKEMEIER, I. Redox regulation of Arabidopsis mitochondrial citrate synthase. **Molecular Plant**, v. 7. n. 1, p.156-169, 2014.

SCHÜRMANN, P.; BUCHANAN, B.B. The ferredoxin/thioredoxin system of oxygenic photosynthesis. **Antioxidants & Redox Signaling**, v. 10, n. 7, p. 1235-1274, 2008.

SCHÜRMANN, P.; JACQUOT, J.P. Plant thioredoxin systems revisited. **Annual Review of plant biology**, v. 51, n. 1, p. 371-400, 2000.

SCHWARZLÄNDER, M.; FINKEMEIER, I. Mitochondrial Energy and Redox Signaling in Plants, **Antioxidants & Redox Signaling**, v. 18, n. 16, p. 2122-2144, 2013.

SCHWARZLÄNDER, M.; WAGNER, S.; ERMAKOVA, Y. G.; BELOUSOV, V. V.; RADI, R.; BECKMAN, J. S.; BUETTNER, G. R.; DEMAUREX, N.; DUCHEN, M. R.; FORMAN, H. J.; FRICKER, M.D. The 'mitoflash' probe cpYFP does not respond to superoxide. **Nature**, v.514, p. E12–E14, 2014.

SERRATO, A.J.; PÉREZ-RUIZ, J.M.; SPÍNOLA, M.C.; CEJUDO, F.J. A novel NADPH thioredoxin reductase, localized in the chloroplast, which deficiency causes hypersensitivity to abiotic stress in *Arabidopsis thaliana*. **Journal of Biological Chemistry**, v. 279, n. 42, p. 43821-43827, 2004.

SHIMOMURA, O.; JOHNSON, F. H.; SAIGA, Y. Extraction, purification and properties of aequorin, a bioluminescent protein from the luminous hydromedusan, Aequorea. **Journal of Cellular and Comparative Physiology**, v. 59, p. 223–239, 1962.

SINGH, S.; TRIPATHI, D.K.; SINGH, S.; SHARMA, S.; DUBEY, N.K.; CHAUHAN, D.K.; VACULÍK, M. Toxicity of aluminium on various levels of plant cells and organism: a review. **Environmental and Experimental Botany**, v. 137, p. 177-193, 2017.

SIQUEIRA, J.A.; FERREIRA-SILVA, M.; WAKIN, T.; NUNES-NESI, A.; ARAÚJO, W.L. Metabolic and DNA checkpoints for the enhancement of Al tolerance. **Journal of Hazardous Materials**, v. 430, p.128366, 2022.

SMART, C.M. Gene expression during leaf senescence. **New phytologist**, v. 126, n. 3, p.419-448, 1994.

SMITH, D.R.; KEELING, P.J. Mitochondrial and plastid genome architecture: reoccurring themes, but significant differences at the extremes. **Proceedings of the National Academy of Sciences**, v. 112, n. 33, p.10177-10184, 2015.

SONG, Y.; YANG, C.; GAO, S.; ZHANG, W.; LI, L.; KUAI, B. Age-triggered and dark-induced leaf senescence require the bHLH transcription factors PIF3, 4, and 5. **Molecular plant**, v. 7, n. 12, p.1776-1787, 2014.

SOUZA, P.V.; HOU, L.Y.; SUN, H.; POEKER, L.; LEHMAN, M.; BAHADAR, H.; DOMINGUES-JUNIOR, A.P.; DARD, A.; BARIAT, L.; REICHHELD, J.P.; SILVEIRA, J.A.G.; FERNIE, A.; TIMM, S.; GEIGENBERGER, P.; DALOSO, D.M. Plant NADPH-dependent thioredoxin reductases are crucial for the metabolism of sink leaves and plant acclimation to elevated CO_2. **Plant, Cell & Environment**, v. 46, n. 8, 2023.

SPÍNOLA, M.C.; PÉREZ-RUIZ, J.M.; PULIDO, P.; KIRCHSTEIGER, K.; GUINEA, M.; GONZÁLEZ, M.; CEJUDO, F.J. NTRC new ways of using NADPH in the chloroplast. **Physiologia Plantarum**, v. 133, n. 3, p. 516-524, 2008.

STAEL, S.; WURZINGER, B.; MAIR, A.; MEHLMER, N.; VOTHKNECHT, UC.; TEIGE, M. Plant organellar calcium signalling: an emerging field. **Journal of Experimental Botany**, v. 63, p. 1525–1542, 2012.

SWEETLOVE, L.J.; BEARD, K.F.; NUNES-NESI, A.; FERNIE, A.R.; RATCLIFFE, R.G. Not just a circle: flux modes in the plant TCA cycle. **Trends in plant science**, v. 15, n. 8, pp.462-470, 2010.

SWEETMAN, C.; MILLER, TK.; BOOTH, NJ.; SHAVRUKOV, Y.; JENKINS, CL.; SOOLE, KL.; DAY, DA. Identification of alternative mitochondrial electron transport pathway

components in chickpea indicates a differential response to salinity stress between cultivars. **International Journal of Molecular Sciences**, v.21, n. 3844, 2020.

TAJ, G.; AGARWAL, P.; GRANT, M.; KUMAR, A. MAPK machinery in plants: recognition and response to different stresses through multiple signal transduction pathways. **Plant Signaling & Behavior**, v. 5, n. 11, p.1370-1378, 2010.

TEARDO, E.; CARRARETTO, L.; WAGNER, S.; FORMENTIN, E.; BEHERA, S.; DE BORTOLI, S.; LAROSA, V.; FUCHS, P.; LO SCHIAVO, F.; RAFFAELLO, A.; RIZZUTO, R. Physiological characterization of a plant mitochondrial calcium uniporter *in vitro* and *in vivo*. **Plant Physiology**, v. 173, p. 1355–1370, 2017.

THORMÄHLEN, I.; ZUPOK, A.; RESCHER, J.; LEGER, J.; WEISSENBERGER, S.; GROYSMAN, J.; ORWAT, A.; CHATEL-INNOCENTI, G.; ISSAKIDIS-BOURGUET, E.; ARMBRUSTER, U.; GEIGENBERGER, P. Thioredoxins play a crucial role in dynamic acclimation of photosynthesis in fluctuating light. **Molecular Plant**, v. 10, n. 1, p. 168-182, 2013.

TOKIZAWA, M.; KOBAYASHI, Y.; SAITO, T.; KOBAYASHI, M.; IUCHI, S.; NOMOTO, M.; TADA, Y.; YAMAMOTO, Y.Y.; KOYAMA, H. Sensitive to proton rhizotoxicity1, calmodulin binding transcription activator2, and other transcription factors are involved in aluminum-activated malate transporter1 expression. **Plant Physiology**, v. 167, n. 3, p. 991-1003, 2015.

TOMAZ, T.; BAGARD, M.; PRACHAROENWATTANA, I.; LINDÉN, P.; LEE, C.P.; CARROLL, A.J.; STRÖHER, E.; SMITH, S.M.; GARDESTRÖM, P.; MILLAR, A.H. Mitochondrial malate dehydrogenase lowers leaf respiration and alters photorespiration and plant growth in *Arabidopsis*. **Plant Physiology**, v. 154, n. 3, pp.1143-1157, 2010.

UMENA. Y.; KAWAKAMI, K.; SHEN, J-R.; KAMIYA, N. Crystal structure of oxygen-evolving photosystem II at a resolution of 1.9 Å. **Nature**, v. 473, p. 55–60, 2011.

USLU, V.; GROSSMANN, G.; The biosensor toolbox for plant developmental biology, **Current Opinion in Plant Biology**, v. 29, p.138-147, 2016.

VAN AKEN, O.; GIRAUD, E.; CLIFTON, R.; WHELAN, J. Alternative oxidase: a target and regulator of stress responses. **Physiologia Plantarum**, v. 137, n. 4, p.354-361, 2009.

VAN GESTEL, K.; KÖHLER, R.H.; VERBELEN, J.P. Plant mitochondria move on F-actin, but their positioning in the cortical cytoplasm depends on both F-actin and microtubules. **Journal of Experimental Botany**, v. 53, n. 369, p.659-667, 2002.

VERCESI, A.E.; BORECKÝ, J.; MAIA, I.D.G.; ARRUDA, P.; CUCCOVIA, I.M.; CHAIMOVICH, H. Plant Uncoupling Mitochondrial Proteins. **Annual Review in Plant Biology**, v. 57, p.383–404, 2006.

VON UEXKÜLL, H.R.; MUTERT, E. Global extent, development and economic impact of acid soils. **Plant and Soil**, 171, pp.1-15, 1995.

WAGNER, S.; BEHERA, S.; DE BORTOLI, S.; LOGAN, DC.; FUCHS, P.; CARRARETTO, L.; TEARDO, E.; CENDRON, L.; NIETZEL, T.; FÜßL, M.; DOCCULA, F.G. The EF-Hand

Ca^{2+} binding protein MICU choreographs mitochondrial Ca^{2+} dynamics in *Arabidopsis*. **Plant Cell**, v. 27, p. 3190–3212, 2015.

WAGNER, S.; DE BORTOLI, S.; SCHWARZLÄNDER, M.; SZABÒ, I. Regulation of mitochondrial calcium in plants versus animals. **Journal of Experimental Botany**, v. 67, p. 3809–3829, 2016.

WALIA, A.; WAADT, R.; JONES, A, M. Genetically Encoded Biosensors in Plants: Pathways to Discovery. **Annual Review of Plant Biology**, v. 691, p. 497-524, 2018.

WANG, Y.; LI, R.; LI, D.; JIA, X.; ZHOU, D.; LI, J.; LYI, S.M.; HOU, S.; HUANG, Y.; KOCHIAN, L.V.; LIU, J. NIP1; 2 is a plasma membrane-localized transporter mediating aluminum uptake, translocation, and tolerance in *Arabidopsis*. **Proceedings of the National Academy of Sciences**, v. 114, n. 19, p. 5047-5052, 2017.

WASZCZAK, C.; CARMODY, M.; KANGASJÄRVI, J. Reactive Oxygen Species in Plant Signaling, **Annual Review of Plant Biology**, v. 69, n. 1, p. 209-236, 2018.

WEAVER, L.M.; AMASINO, R.M. Senescence is induced in individually darkened *Arabidopsis* leaves, but inhibited in whole darkened plants. **Plant Physiology**, v. 127, n. 3, p.876-886, 2001.

WEN, K.; PAN, H.; LI, X.; HUANG, R.; MA, Q.; NIAN, H. Identification of an ATP-binding cassette transporter implicated in aluminum tolerance in wild soybean (*Glycine soja*). **International Journal of Molecular Sciences**, v. 22, n. 24, p. 13264, 2021.

WERNIMONT, AK.; ARTZ, JD.; FINERTY, P.; LIN, Y-H.; AMANI, M.; ALLALI-HASSANI, A.; SENISTERRA, G.; VEDADI, M.; TEMPEL, W.; MACKENZIE, F.; CHAU, I. Structures of apicomplexan calcium-dependent protein kinases reveal mechanism of activation by calcium. **Nature Structural & Molecular Biology**, v. 17, p. 596–601, 2010.

WHITE, P.J. The pathways of calcium movement to the xylem. **Journal of Experimental Botany,** v. 52, n. 358, p.891-899, 2001.

WHITE, P.J.; BROADLEY, M.R. Calcium in plants. **Annals of Botany**, v. 92, n. 4, p.487-511, 2003.

WILLEMS, P.; MHAMDI, A.; STAEL, S.; STORME, V.; KERCHEV, P.; NOCTOR, G.; GEVAERT, K.; BREUSEGEM, F. The ROS Wheel: Refining ROS Transcriptional Footprints, **Plant Physiology**, v. 171, n. 3, p. 1720–1733, 2016.

WONG, M.T.F.; ASSENG, S.; ROBERTSON, M.J.; OLIVER, Y. Mapping subsoil acidity and shallow soil across a field with information from yield maps, geophysical sensing and the grower. **Precision Agriculture**, v. 9, p. 3–15, 2008.

YAMAMOTO, Y.; KOBAYASHI, Y.; DEVI, S.R.; RIKIISHI, S.; MATSUMOTO, H. Aluminum toxicity is associated with mitochondrial dysfunction and the production of reactive oxygen species in plant cells. **Plant Physiology**, v. 128, n. 1, p. 63-72, 2002.

YAN, L.; RIAZ, M.; LIU, J.; YU, M.; CUNCANG, J. The aluminum tolerance and detoxification mechanisms in plants; recent advances and prospects. **Critical Reviews in Environmental Science and Technology,** v. 52, p. 1491-1527, 2022.

YANG, H.; JIE, Y. Uptake and transport of calcium in plants. **Journal of Plant Physiology and Molecular Biology,** v. 31, n. 3, p. 227, 2005.

YANG, J.L.; YOU, J.F.; LI, Y.Y.; WU, P.; ZHENG, S.J. Magnesium enhances aluminum-induced citrate secretion in rice bean roots (*Vigna umbellata*) by restoring plasma membrane H^+-ATPase activity. **Plant and Cell Physiology**, v. 48, n. 1, p. 66-73, 2007.

YOKOSHO, K.; YAMAJI, N.; FUJII-KASHINO, M.; MA, J.F. Retrotransposon-mediated aluminum tolerance through enhanced expression of the citrate transporter OsFRDL4. **Plant Physiology**, v. 172, n. 4, p. 2327-2336, 2016.

YOSHIDA, K.; HARA, S.; HISABORI, T. Thioredoxin selectivity for thiol-based redox regulation of target proteins in chloroplasts. **Journal of Biological Chemistry**, v. 290, n. 23, p.14278-14288, 2015.

YOSHIDA, K.; HISABORI, T. Two distinct redox cascades cooperatively regulate chloroplast functions and sustain plant viability. **Proceedings of the National Academy of Sciences**, v. 113, n. 27, p. E3967-E3976, 2016.

ZHANG, C.J.; ZHAO, B.C.; GE, W.N.; ZHANG, Y.F.; SONG, Y.; SUN, D.Y.; GUO, Y. An apoplastic *h*-type thioredoxin is involved in the stress response through regulation of the apoplastic reactive oxygen species in rice. **Plant Physiology**, v. 157, n. 4, p.1884-1899, 2011.

ZHANG, Y.; FERNIE, A.R. On the role of the tricarboxylic acid cycle in plant productivity. **Journal of Integrative Plant Biology**, v. 60, n. 12, p.1199-1216, 2018.

ZHANG, Y.; FERNIE, A.R. The role of TCA cycle enzymes in plants. **Advanced Biology**, v. 7, n. 8, p.2200238, 2023.

ZHANG, Z.; LIU, D.; MENG, H.; LI, S.; WANG, S.; XIAO, Z.; SUN, J.; CHANG, L.; LUO, K.; LI, N. Magnesium alleviates aluminum toxicity by promoting polar auxin transport and distribution and root alkalization in the root apex in populus. **Plant and Soil**, v. 448, p. 565-585, 2020.

ZHOU, Q.; SON, K.; LIU, Y.; REVZIN, A. Biosensors for Cell Analysis. **Annual Review of Biomedical Engineering**, v. 17, p.165-190, 2015.

ZHOU, X.; JIANG, Y.; YU, D. *WRKY22* transcription factor mediates dark-induced leaf senescence in *Arabidopsis*. **Molecules and Cells**, v. 31, p.303-313, 2011.

ZHU, X.; DUNAND, C.; SNEDDEN, W.; GALAUD, J-P. CaM and CML emergence in the green lineage. **Trends in Plant Science**, v. 20, p. 483–489, 2015.

ZHU, Y.; LU, J.; WANG, J.; CHEN, F.; LENG, F.; LI, H. Regulation of thermogenesis in plants: the interaction of alternative oxidase and plant uncoupling mitochondrial protein. **Journal of Integrative Plant Biology**, v. 53, n. 1, p.7-13, 2011.

CHAPTER 1: Deciphering the significance of the thioredoxin system in aluminum stress response

ABSTRACT

Toxicity triggered by aluminum (Al), mainly Al^{3+}, is a critical factor that limits agricultural production in acidic soils (pH < 5.0). Its main symptom is root growth inhibition. Being a highly reactive element, Al can alter the energetic state, disturbing cellular redox homeostasis, and altering membrane potential, therefore affecting cellular metabolism. To prevent or mitigate the effects of these toxicity plants display two mechanisms. These include tolerance mechanisms – which are based on the internal sequestration and detoxification of Al, and exclusion mechanisms – which prevent the entry of toxic Al species into the root tip. Both strategies involve the presence of organic acids, that come from mitochondrial processes to complex Al. In this context, mitochondrial metabolism is crucial to supporting cellular processes mitigating the effect of Al; therefore, maintaining mitochondrial metabolic and redox homeostasis is essential in responses to Al stress. Evidence suggests that the thioredoxin (TRX) system mitigates oxidative damage through the control of reactive oxygen species (ROS), which makes TRX important to fulfill the requirements to sustain plant growth and development under different environmental conditions, including abiotic stress. To understand to which extent the TRX system is related to mitigating Al stresses we used *Arabidopsis thaliana* mutants for NADP-dependent TRX reductase A and B double mutant (*ntra/b*), the mitochondrially TRX*o1* (*trxo1*) mutant and the GLUTATHIONE REDUCTASE 1 (*gr1-1*). Our data demonstrate the *trxo1* mutants did not show drastic changes in phenotype compared to the wide type, which indicates a degree of redundancy within the mitochondrial TRXs acting during stress. Surprisingly, the *ntra/b* double mutant displayed a "tolerant" behavior, being less affected by the Al stress in root growth, which could be associated with a better function of the glutathione (GSH) redox system, overlapping the lack of NTR in these genotypes. Thus, in agreement, the *gr1-1* displayed a more sensitive phenotype. Collectively, our data led us to propose that the redox status of the glutathione redox system is essential to deal with toxicity caused by aluminum, and in the lack of the NTR system, the reductant power of NADPH can be exclusively used by GR for the GSH redox system, leading to a better Al mitigation.

INTRODUCTION

Acidic soils (pH < 5.0) are a global problem that severely impacts agricultural production (YAN et. al, 2022). Being approximately 50% of the arable land available in the world (von UEXKÜLL & MUTERT, 1995), these soils account for a quarter of the areas used for food crops, such as rice and maize (DELHAIZE & RYAN, 1995). On a national level, around two-thirds of the Brazilian territory is covered by acidic soils; in numbers, approximately 500 million hectares of potentially arable areas, compromising maximum crop productivity (VITORELLO et al., 2005). Such soils are characterized by nutrient deficiency and metal toxicity, with Al toxicity being the main factor limiting plant growth in these soils (KOCHIAN et al., 2004; GUPTA et al., 2013; BOJÓRQUEZ -QUINTAL et al., 2017).

Al is an important mineral constituent in soils and is not toxic as a metal if present in the pH range of 6.0 to 8.0. In this condition, it has low solubility and exists in the form of oxides and aluminosilicates, such forms of Al are harmless to plants (von UEXKÜLL & MUTERT, 1995; MA et al., 2007; YAN et al., 2022). When soil pH is low (pH < 5.5), Al solubilizes and exists in the forms of aluminum hydroxide ($Al(OH)^{2+}$), and cation aluminum (Al^{3+}) (LIU et al., 2022; ZHONGJIE et al., 2023). Present in ionic forms, Al becomes toxic to all living cells (von UEXKÜLL & MUTERT, 1995; MA et al., 2007). Solubilized Al becomes extremely toxic to plants (LIU et al., 2022), with Al^{3+} being the form that has the greatest capacity to interfere with the growth and root development of several plants, resulting in severe Al toxicity in acidic soils (KOCHIAN et al., 2004).

There are several symptoms caused by Al toxicity, all associated with serious changes in the root system, with the initial symptom of toxicity being the inhibition of root elongation (KOCHIAN et al., 2002; RENGEL et al., 2003). This effect drastically reduces the volume of soil explored by the root system, impairing the absorption of water and nutrients and, ultimately, affecting cellular maintenance and growth (SETOTAW et al., 2015). Al interacts with the large number of negative charges in cell wall pectins, which increases the rigidity of the cell wall and interferes with cell division, which can lead to callus and atrophy of root hairs (ZHU et al., 2012). Furthermore, it leads to a distortion of the cytoskeletal actin network and depolymerization of microtubules (PANDA et al., 2007), depolarization of membranes, which can affect a series of physiological mechanisms (OFOE et al., 2022). Furthermore, it increases the rigidity of the double helix, leading to a reduction in DNA replication (EEKHOUT et al., 2017).

As it is a highly reactive element, Al induces oxidative stress, rapidly forming reactive oxygen species (ROS) that can lead to cell death (CHAUHANA et al., 2021). In non-photosynthetic cells, the mitochondrial electron transport chain is the main source of ROS production, and in the presence of Al, the content of superoxide radicals and hydrogen peroxide is significantly increased in isolated mitochondria (PANDA et al., 2007). In tobacco cells and pea root tip meristematic cells there are similar redox changes accompanied by an inhibition in cellular respiration (YAMAMOTO et al., 2002). In effect, Al leads to a disturbance of the surface charge of the plasma membrane, leading to ATP depletion (YAMAMOTO et al., 2002).

Although mitochondria are one of the organelles affected by Al stress, mitochondrial metabolism plays a fundamental role in the strategies that plants provide to prevent or mitigate the effects of this toxicity (NUNES-NESI et al., 2014). Such mechanisms include (*i*) tolerance mechanisms – which are based on the internal sequestration and detoxification of Al, and (*ii*) exclusion mechanisms – which prevent the entry of toxic Al species into the root tip (RYAN et al., 2007; KOCHIAN et al., 2002; KOCHIAN et al., 2004; KOCHIAN et al., 2015). Both mechanisms involve different transporters and the formation of Al complexes with organic acids (OA), more specifically malate, citrate, and, in some species, oxalate (NUNES-NESI et al., 2014) all originating from mitochondrial processes. In the tolerance mechanism, Al enters the cytoplasm and can be complexed with OA and/or phenolic compounds inside the cell, thus mitigating their toxic effects (KOCHIAN et al., 2015). Several compounds, including OAs and proteins, can form specific complexes with Al inside the cell, which will later be sequestered into the vacuole (SIMÕES et al., 2012). On the other hand, the Al exclusion mechanism is associated with the transport of organic compounds from the interior of the cell to the rhizosphere, mainly in the root apex, in the presence of solubilized Al. In *Arabidopsis thaliana*, the main OA exuded by the roots is malate and involves the ALMT transporter (Al-ACTIVATED MALATE TRANSPORTER), encoded by the gene of the same name (KOBAYASHI et al., 2007). Once complexed with OA, Al:OA forms non-toxic compounds and cannot be absorbed by the roots (GUPTA et al., 2013; NUNES-NESI et al., 2014). Therefore, increased mitochondrial activity is fundamental for OA synthesis under Al stress (BOJÓRQUEZ-QUINTAL et al., 2017).

Mitochondrial metabolism is also critical in underpinning key cellular processes including photosynthesis, photorespiration, nitrogen metabolism, redox regulation, and stress signaling (ARAÚJO et al., 2011; BARROS et al., 2017; BAUWE et al., 2012; DUTILLEUL et al., 2005; NUNES-NESI et al., 2005; 2007). Moreover, the redox regulation of plant metabolism is fundamental to coordinating and integrating the responses of different plant

compartments (FOYER & NOCTOR, 2013; FONSECA-PEREIRA, et al., 2019). As said before, Al is a highly reactive element that can alter the energetic state, disturbing redox homeostasis (GIANNAKOULA et al., 2010). Recent studies suggested that TRX may have crucial importance in controlling the redox state in different cell compartments during abiotic stress (KEECH et al., 2016), providing a mechanism for the regulation of plant metabolism in general.

TRX are thiol-oxidoreductases with two reactive cysteines in a common CxxC redox center (MEYER et al., 2012) that generally function in the redox regulation of diverse cellular processes in most organisms (SCHMIDTMANN et al., 2014). In photosynthetic cells, various processes such as modulation of the Calvin-Benson-Bassham cycle (CBBC) (MICHELET et al., 2013; OKEGAWA; MOTOHASHI, 2015), the response to oxidative stress (KAPOOR, 2015; MARTÍ et al., 2011), and the regulation of the TCA cycle in leaves (DALOSO et al., 2015) are redox-regulated by TRXs. More than 20 genes coding for TRX have been found in the *Arabidopsis* genome (THORMÄHLEN et al., 2015). The isoforms are grouped in several TRX families, differing in amino acid sequence and subcellular localization (HÄGGLUND et al., 2016). TRXs *f, m, x, y*, and *z* are located in chloroplasts and are reduced by electrons from the ferredoxin-TRX reductase (FTR) enzyme or employing the flavoenzyme NADPH-dependent TRX reductase C (NTRC). In its turn, TRX *o* is in the mitochondrion and most TRXs *h* are in the cytosol and both can be found in the nucleus (DELORME-HINOUX et al., 2016). Specific NADPH-dependent thioredoxin reductases A and B (NTRA and NTRB) occur in both mitochondria and cytosol and NTRA in nucleus where they are responsible for the reduction of TRX proteins (REICHHELD et al., 2007).

Studies have demonstrated that several proteins related to stress tolerance are targets of the plant TRX system (BALMER et al., 2004; YOSHIDA; HARA; HISABORI, 2015; ORTIZ-ESPÍN et al., 2017), which suggests that this system is involved in the regulation of stress acclimation in higher plants. Taken together, these results indicate that the regulation of plant stress responses is, at least partially, mediated by the TRX system. Many abiotic stress conditions can affect plant physiology; thus, it will cause widespread changes in metabolism and cellular processes (ZHANG et al., 2022).

Several approaches have been used to evaluate the redox potential indirectly through the quantification of specific compounds, indicative of potential changes in the redox state (QUEVAL; NOCTOR, 2007). Despite being widely used in research, these techniques have several technical limitations, such as: (*i*) the need for cell tissue homogenization that includes mixing between cell types and subcellular pools, not reflecting the *in vivo* conditions; (*ii*)

possible alterations in the redox status of these molecules during their extraction; and (iii) analytical quantification of these molecules in different compartments requires non-aqueous fractionation techniques since standard organelle isolations do not allow to retain the cofactors and metabolites (SCHWARZLÄNDER et al., 2016). Sensors based on the redox sensibility of fluorescent proteins have been developed (HANSON et al., 2004; ØSTERGAARD et al., 2001; SCHWARZLÄNDER, et al., 2016). This allows a sensitivity of the real-time redox potential through the disulfide bridge formed by the fluorescent protein. In this way, real-time monitoring of the dynamics of the redox potential in living cells is possible (SCHWARZLÄNDER, M. et al., 2008).

In this context, to understand how the TRX redox system is related to mitigating Al stress we used two *TRXo1* lines; NADPH-TRX reductase A and B double mutant, *ntra/b* and GLUTATHIONE REDUCTASE 1, *gr1-1*. Considering the interdependent relationship between TRXs and redox homeostasis following stress conditions, we observed in our experiments that the double mutant *ntra/b* displayed was less impacted in the growth under stress conditions, while the *gr1-1* mutant appears more affected in terms of root development, which could be related with the glutaredoxins, acting as a potential source of redundancy in *ntra/b*. Furthermore, using genetically encoded biosensors we could monitor the alterations in the GSH/GSSG ratio, H_2O_2, and pH in response to Al, where the results demonstrate that pH drops rapidly and fast after the Al stress, in cytosol and mitochondria, while the H_2O_2 increases, and the GS pool starts to be more oxidized. In the end, it is possible to infer that GSH plays a major role in the metal mitigation process by maintaining the growth through pH variation in the environment. Bearing this in mind, elucidating the role of the antioxidant system as a source of redox power under Al stress conditions will likely be highly revealing and can be a resourceful power for future crop improvement.

MATERIAL AND METHODS

Plant materials

All genotypes of *Arabidopsis thaliana* plants used in this study are described in Table 1. All mutant plants have Columbia (Col-0) ecotype as background. All sensor lines were generated via *Agrobacterium tumefaciens* mediated transformation via floral dip (CLOUGH & BENT, 1998) and kindly provided by Plant Energy Biology Lab (Münster, Germany).

Table 1. *Arabidopsis thaliana* genotypes used in this study.

Plant line	Mutation	Sensor	Collection	Reference
Col-0	-	-	-	-
Col-0	-	Cytosolic **GRX1-roGFP2** (Ex = 400 ± 5 and 482 ± 16 nm/Em = 520 ± 10 nm)	-	-
Col-0	-	Cytosolic **ORP-roGFP2** (Ex = 400 ± 5 and 482 ± 16 nm/Em = 520 ± 10 nm)	-	-
Col-0	-	Mitochondrial **GRX1-roGFP2** (Ex = 400 ± 5 and 482 ± 16 nm/Em = 520 ± 10 nm)	-	-
Col-0	-	Mitochondrial **ORP-roGFP2** (Ex = 400 ± 5 and 482 ± 16 nm/Em = 520 ± 10 nm)	-	-
Col-0	-	Cytosolic **cpYFP** (Ex = 400 ± 5 and 482 ± 16 nm/Em = 520 ± 10 nm)	-	-
Col-0	-	Mitochondrial **cpYFP** (Ex = 400 ± 5 and 482 ± 16 nm/Em = 520 ± 10 nm)	-	-
trxo1.1	T-DNA insertion mutant in the *trxo1* gene (At2g35010)	-	SALK 042792	DALOSO et al. (2015)
trxo1.2	T-DNA insertion mutant in the *trxo1* gene (At2g35010)	-	SALK 143294	FONSECA-PEREIRA et al. (2019b)
ntra/b	NADPH dependent thioredoxin reductase double-KO mutant (At*NTRA At2g17420* x At*NTRB At4g35460*)	-	SALK 539152 / SALK 545978	REICHHELD et al. (2007)
ntra/b	NADPH dependent thioredoxin reductase double-KO mutant (At*NTRA At2g17420* x At*NTRB At4g35460*)	Cytosolic **GRX1-roGFP2** (Ex = 400 ± 5 and 482 ± 16 nm/Em = 520 ± 10 nm)	-	-
ntra/b	NADPH dependent thioredoxin reductase double-KO mutant (At*NTRA At2g17420* x At*NTRB At4g35460*)	Mitochondrial **ORP-roGFP2** (Ex = 400 ± 5 and 482 ± 16 nm/Em = 520 ± 10 nm)	-	-
cad-2	EMS mutated seeds with reduced glutathione content - defects in *GSH1* (At4g23100) approximately 30% GSH levels	-	-	HOWDEN et al. (1995) BANGASH et al. (2019)
zir1	EMS mutated seeds with reduced glutathione content - defects in *GSH1* (At4g23100) approximately 15% GSH levels	-	-	SHANMUGAM et al. (2012) BANGASH et al. (2019)

gr1-1	T-DNA insertion knockout mutant of glutathione reductase 1 (At3g24170)	-	SALK 105794	MHAMDI et al. (2010)
gr1-1	T-DNA insertion knockout mutant of glutathione reductase 1 (At3g24170)	Cytosolic **GRX1-roGFP2** (Ex = 400 ± 5 and 482 ± 16 nm/Em = 520 ± 10 nm)		-

Experimental conditions and root growth assays

Seeds were surface-sterilized and vernalized at 4 º C for 72 h. Then it was placed on a half-strength Murashige and Skoog (MS) medium (MURASHIGE & SKOOG, 1962) nutrient solution and 0.8% (w/v) agar (Sigma-Aldrich) pH 5.0. After 5 days, the seedlings were carefully transferred to a new square petri dish with different treatments: mock MS pH 4,0; MS pH 4.0 supplemented with aluminum (300 µM $AlCl_3$); MS pH 4.0 supplemented with Buthionine-sulfoximine (500 µM BSO). Appropriate amounts of the filter-sterilized stock solution containing these substances were added to sterile Petri dishes, and molten half-strength MS medium that had been cooled to 50 °C was added to the sterile plates. Supplementation of the growth medium with BSO (Sigma-Aldrich); Aluminum $AlCl_3$ (anhydrous stock solution - Sigma-Aldrich). The pH was adjusted with a KOH solution. All genotypes for the assay were placed side-by-side on freshly prepared plates, at least eight plates per treatment. Plates were sealed with Micropore surgical tape (3M).

Then, all dishes were placed back in a growth chamber under long-day conditions (16 h/8 h of light/dark), irradiance of 150 µmol photons m^{-2} s^{-1}, temperature of 20 ± 2 °C and humidity of 70 ± 5%. After 10 days, the Petri dish plates were subjected to photographic documentation, and the plants were harvested for further analysis. For root growth measurements, seeds were germinated on vertical plates, and the position of the root tip was marked on the underside of the plate. Every day after the transfer, root growth was measured at 15 roots per plate, being the average length of each plate one repetition. The increase in primary root length was quantified from images with ImageJ software v 1.52 (https://imagej.nih.gov/ij/). In addition, shoot and root dry weight was determined by placing the plants in a forced air circulation oven at 70 °C for 2 days.

Histochemical Al localization assay

At the end of the experiment, after 10 days of the seedlings growing with Al, roots were stained for Al localization with hematoxylin and Chrome Azurol S. For hematoxylin staining seedlings were dipped in deionized water for 30 min. Afterward, it was dipped in iron hematoxylin 0.2% (m/v) solution with sodium iodide ($NaIO_3$) for 30 min, then back into

deionized water for 30 min, as previously described by Souza et al. (2016). Then samples were observed under a stereomicroscope (Zeiss model Stemi 2000-C) and photographed.

For Chrome Azurol S (KUKACHKA & MILLER, 1980) seedlings were dipped in deionized water for 30 min, then stained for 1 h with 0.5% Chrome Azurol S solution, and afterward dipped again in deionized water for 30 min. Then samples were observed under Olympus stereomicroscopic (model SZX7) and photographed with an Olympus camera (model EP50).

Histochemical ROS assays

Qualitative evaluation of hydrogen peroxide (H_2O_2) and superoxide (O^{2-}) was performed by histochemical staining as previously described by Kong et al., (2011) with modifications. For the H_2O_2 detection, 1.0 mg mL-^{1} 3,3'-diaminobenzidine (DAB) was used, whereas for the O^{2-} detection, 0.1 mg ml^{-1} nitrobluetetrazolium (NBT) was used. The exposure time was 3 hours for DAB and 1 hour for NBT. Afterwards, seedlings stained were registered using a stereomicroscope (Zeiss model Stemi 2000-C) and photographed.

***In vivo* sensor measurement of physiological dynamics**

To understand the physiological dynamics responses of cytosolic and mitochondrial GSH redox pool (E_{GSH}), H_2O_2, and pH, 5-week-old plants leaf discs, 10-days-old roots, and 10-days-old seedlings of *A. thaliana* plants expressing fluorescent biosensors (Table 1) were monitored in a CLARIOstar® (BMG Labtech, Ortenberg, Germany) microplate reader performed according to Wagner et al. (2019).

For the plate reader assays using leaf discs, the seeds were sow on soil, the soil (VMV 800, Classic Profisubstrat, Einheitserde®) previously sterilized at 80 °C, stratified at 4 ºC for 48 hours in the dark and then transferred to growth chambers running under long-day conditions (16 h at 22 ˚C and 80–100 µmol m^{-2} s^{-1}, 8 h at 18 ˚C and darkness, 65% RH). For the root and seedlings assays, the seeds were surface sterilized for 1 min in 70% Ethanol, 15 min in 5% sodium hypochlorite and washed seven times with deionized sterile H_2O. Then, the seeds were placed in Petri dishes with 0.8% agar supplemented with 1/2-strength MS medium 10 mM MES, followed by stratification for 48 hours at 4 ºC. The plates were then transferred to the growth chamber under the same conditions mentioned earlier.

For the different treatments, wells from transparent 96-well plates were filled with 180 µL of MS medium pH 4.0. Leaf discs of 5-week-old plants, grown in a substrate and 10-day-

old seedlings (five per well) and roots (eight per well) of each genotype grown in MS medium agar plates were submerged in the wells before inserting the plate into a CLARIOstar® plate reader pre-equilibrated to 25 °C for recording the fluorescence in the steady-state. For this, the top optic was used as well as a protocol with 30 excitation flashes per well and cycle, an orbital averaging with a 3 mm diameter, and 0.1 s settling time. The excitation and emission wavelengths were adjusted to the sensor *reduction–oxidation-sensitive green fluorescent protein2* (roGFP2) and *yellow fluorescent protein* (YFP): Ex = 400 ± 5 and 482 ± 16 nm/Em = 520 ± 10 nm. The gain settings for each wavelength and the focal height were set at the beginning of each experiment and maintained for identical experiments. The treatments were imposed one-to-two hours after the start of the measurement, the treatments were 20 µL of mock solution (only MS medium pH 4.0) or 20 µL of MS medium pH 4.0 with aluminum ($AlCl_3$ 2.5 mM) were added manually in the dark (under green light) in each well. The bars graphs were generated with the points after 4 h of the application.

Data and statistical analyses

The growth measurements were subjected to ANOVA followed by Tukey's multiple-comparison posttest ($P \leq 0.05$). All statistical tests were performed with GraphPad Prism 5.0 (GraphPad Software, Inc., San Diego, CA). The program was also used to plot the data as mean and standard deviation. For the analysis of the data obtained from the plate reader, the data were transferred to the data analysis software MARS (V3.32, BMG Labtech GmbH, Ortenberg, Germany). The raw data of each well with the fluorescence intensities for each channel were then exported to Microsoft Excel (2016, Microsoft Corporation, Redmond, WA, USA) for analysis. The intensities of the background or Col-0 without the sensor were used to subtract the chlorophyll autofluorescence from the corresponding intensities of each replicate at each time point. The data were log10-transformed. The bars graphs of the dynamics responses of cytosolic and mitochondrial GSH redox pool (E_{GSH}), H_2O_2, and pH were generated with the points after 4 h of the application.

RESULTS

Lack of a functional mitochondrial TRX reductase system leads to a greater Al tolerance

Decreases in root growth were observed for all genotypes with 300 µM of Al after 10 days (Fig. 1 A), the most known symptom of Al toxicity. The *trxo1* lines showed the same pattern of Col-0 in terms of the reduction (~ 35% of root loss) whereas the *ntra/b* double mutant

presented a less drastic change in root growth phenotype losing only 15.5% of its length during the stress (Fig. 1 A). This can suggest a better mitigation of the toxicity caused by Al. It is important to notice that the double mutation in the NTRs leads to a smaller seedling, even in the absence of Al (Fig. 1).

However, this result was not repeated in terms of biomass partition, even with the different root lengths the Al did not significantly affect the biomass partitioning for any of the genotypes (Fig. 1 B), what can be associated with the short time of Al exposure to affect this parameter in seedlings. The same result was observed for the germination assay; no significant decrease in seed germination rate was observed in the presence of Al or the low pH condition of the mock, pH 4.0 (Supplemental Fig. 1 and 2).

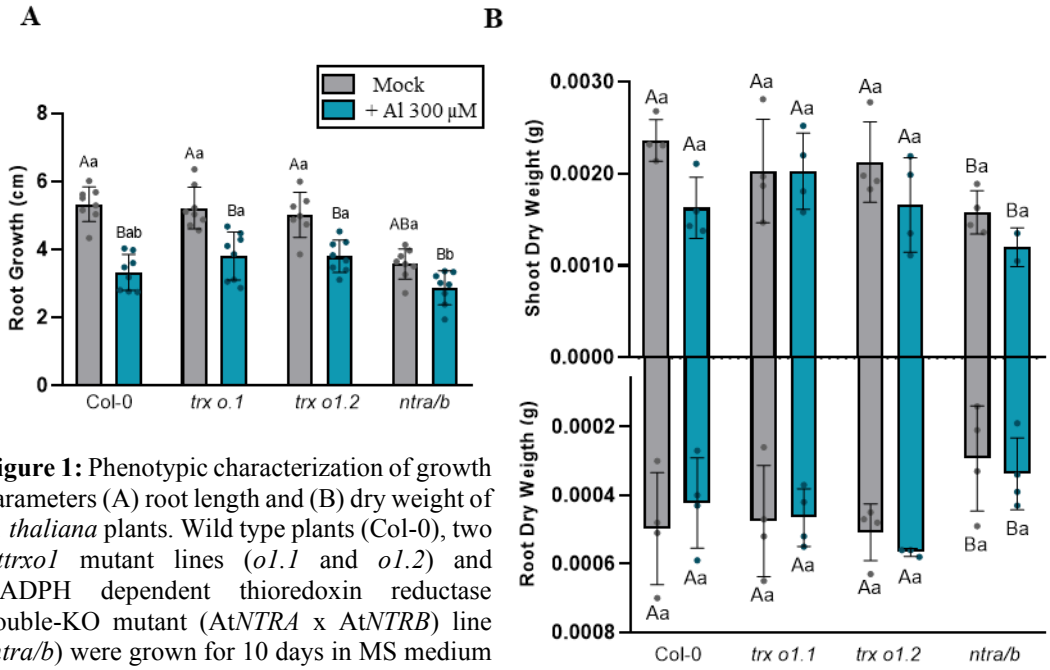

Figure 1: Phenotypic characterization of growth parameters (A) root length and (B) dry weight of *A. thaliana* plants. Wild type plants (Col-0), two *Attrxo1* mutant lines (*o1.1* and *o1.2*) and NADPH dependent thioredoxin reductase double-KO mutant (At*NTRA* x At*NTRB*) line (*ntra/b*) were grown for 10 days in MS medium pH 4.0 in the absence (Mock) and presence of aluminum - $AlCl_3$ (+ Al 300 µM). Values or means ±SD (n=4 - 8). Different letters indicate significant differences ($p < 0.05$) according to the Tukey's test, capital case letters compare each condition within the same genotype and lower-case letters compares the conditions among all genotypes.

Since *trxo1* lines did not show a differential response in response to Al treatment, we then decided to do further investigation only with the *ntra/b* double mutant. Al localization in roots surface was evaluated by hematoxylin staining for Col-0 and *ntra/b* and we observed that seedlings treated with Al showed more intense purplish staining (Fig. 2 B and D) with iron hematoxylin than those non-treated ones (Fig 2 A and C). Surprisingly, both genotypes

presented similar shades of the stain, suggesting that the better mitigation effect observed for *ntra/b* in root growth (Fig. 1) is not due to OA exudation.

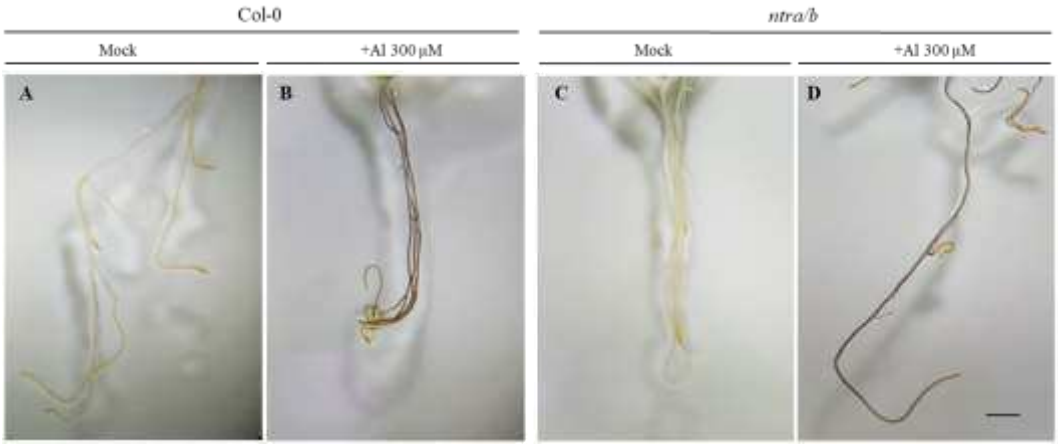

Figure 2. Differential superficial Al localization in *A. thaliana* roots stained with ferric hematoxylin. Wild-type (Col-0) and NADPH-dependent thioredoxin reductase double-KO mutant (At*NTRA* x At*NTRB*) line (*ntra/b*) were grown for 10 days in MS medium pH 4.0 in the absence (Mock) and presence of aluminum - $AlCl_3$ (+Al 300 µM). Scale bar = 1cm.

Al localization was also performed using Chrome Azurol S dye, and in this case, the positive reaction for Al could be observed by the dark blue color. Again, roots treated with Al showed a more intense blue color for both genotypes (Fig. 3 B and D) which corroborates the result with hematoxylin. However, clear anatomical damage was observed in the root apex for the Col-0 (Fig. 3 F), while for the *ntra/b* is possible to observe a blue dot in the root tip (Fig. 3 H), but the overall morphological structure of the root apex stayed conserved.

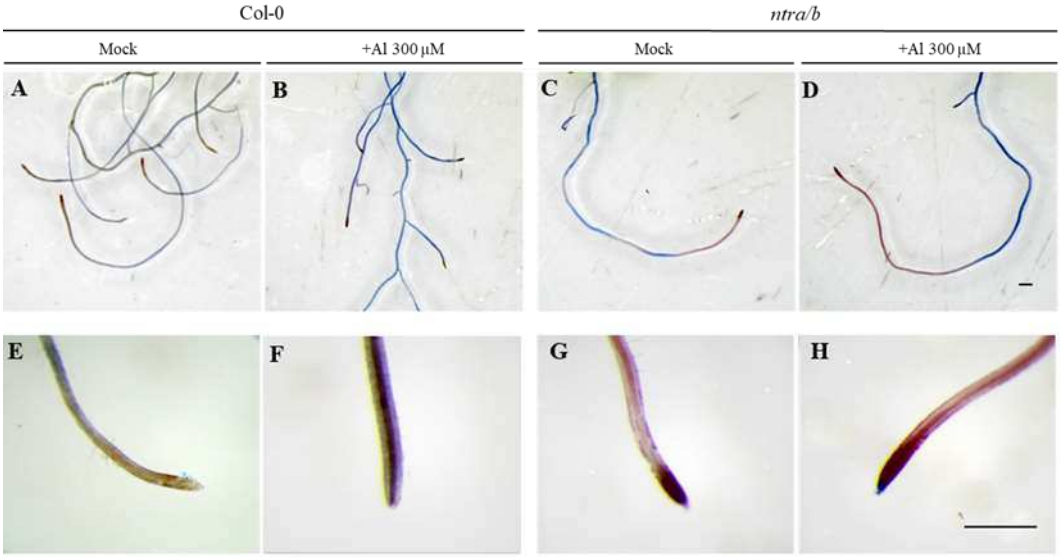

Figure 3. Differential superficial Al localization in roots (A – D) and root's apex (E – H). Representative images of wild-type (Col-0) and NADPH-dependent thioredoxin reductase double-KO mutant (At*NTRA* x At*NTRB*) line (*ntra/b*) that were grown for 10 days in MS medium pH 4.0 (Mock – A, C, E, G) and MS medium with aluminum - $AlCl_3$ (+Al 300µM – B, D, F, H) stained with Chrome Azurol S for aluminum localization. Scale bar = 250 µm.

Alterations in histochemical ROS staining in *A. thaliana* under Al stress

Histochemical assays allowed us to observe a distinct staining with NBT (nitroblue tetrazolium) and DAB (diaminobenzidine tetrahydrochloride), as a qualitative evaluation of superoxide (O^{2-}), and hydrogen peroxide (H_2O_2), respectively. By exposing the seedlings samples of plates with and without Al we noticed a differential stain pattern for NBT. Col-0 NBT staining was clear in all root apex of the seedlings treated with Al (Fig. 4 B), while the *ntra/b* double mutant presented a light color even in the stressed seedling (Fig. 4 D), suggesting a lower accumulation of superoxide in the NTR double mutant line. However, the DAB staining showed no clear pattern comparing both genotypes (Fig 4. E – H).

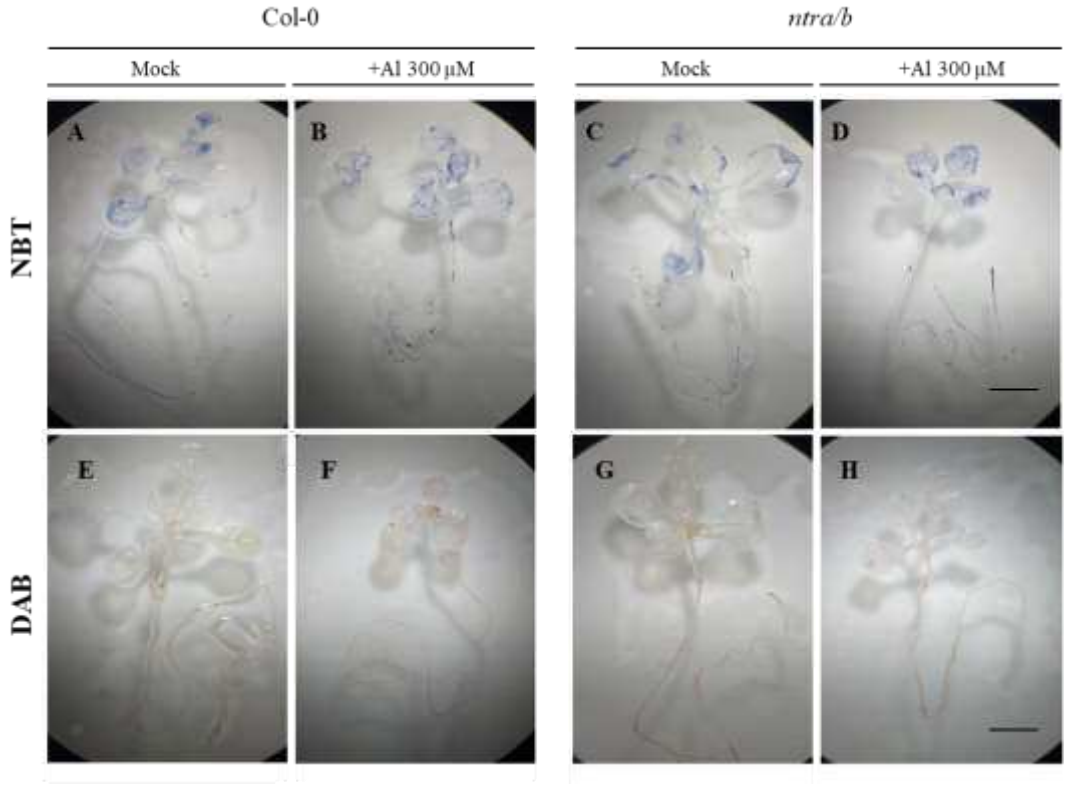

Figure 4: Histochemical reactive oxygen species (ROS) localization of *A. thaliana* plants. Wild-type (Col-0) and NADPH-dependent thioredoxin reductase double-KO mutant (At*NTRA* x At*NTRB*) line (*ntra/b*) were grown for 10 days in MS medium (Mock) and MS medium with aluminum - $AlCl_3$ (+Al 300µM). Images of stained O^{2-} superior bar – NBT (A – D) and H_2O_2 inferior bar – DAB (E – H). Scale bar = 2 mm. Abbreviations: NBT, nitroblue tetrazolium; DAB, Diaminobenzidine tetrahydrochloride.

Once the Al localization (Fig. 2 and 3) revealed that the *ntra/b* better root growth mitigation effect (Fig. 1) was not directly related to a higher OA exudation and ROS histochemical analyzes (Fig. 4) showed that *ntra/b* had a lower accumulation of superoxide (O^{2-}) when comparing to the Col-0, it could be associated with a compensation by glutathione (GSH) system like suggested before by REICHHELD et. al (2007). Hence, we then studied the impact of lowering the level of this other redox homeostasis system, glutathione, on the mitigation of Al stress. For that, we compared the root growth of Col-0 and *ntra/b* mutants

grown in an acid medium (pH 4.0) supplemented with glutathione synthesis inhibitor buthionine sulfoximine (BSO).

The Col-0 root growth was slightly affected by the low concentration of BSO (500 µM) (Fig. 5 A and C) and the association of BSO and Al showed a worse seedling development (Fig. 5 A) than just Al (Fig. 5 A). The root length in the presence of Al and BSO showed a ~60% reduction when compared with the control and a ~45% reduction compared with the mock with BSO (Fig. 5 A). For the *ntra/b* mutant, the same concentration of BSO showed a drastic inhibition on seedling development (Fig. 5 B), culminating in almost no root growth in the medium supplemented with the glutathione inhibitor (Fig. 5 C). Again, the *ntra/b* mutant showed a less reduction of root growth in the presence of only Al (Fig. 6 C), like presented here before (Fig. 1 A). For the biomass partition (Fig. 5 D), neither Al nor BSO seems to affect this parameter.

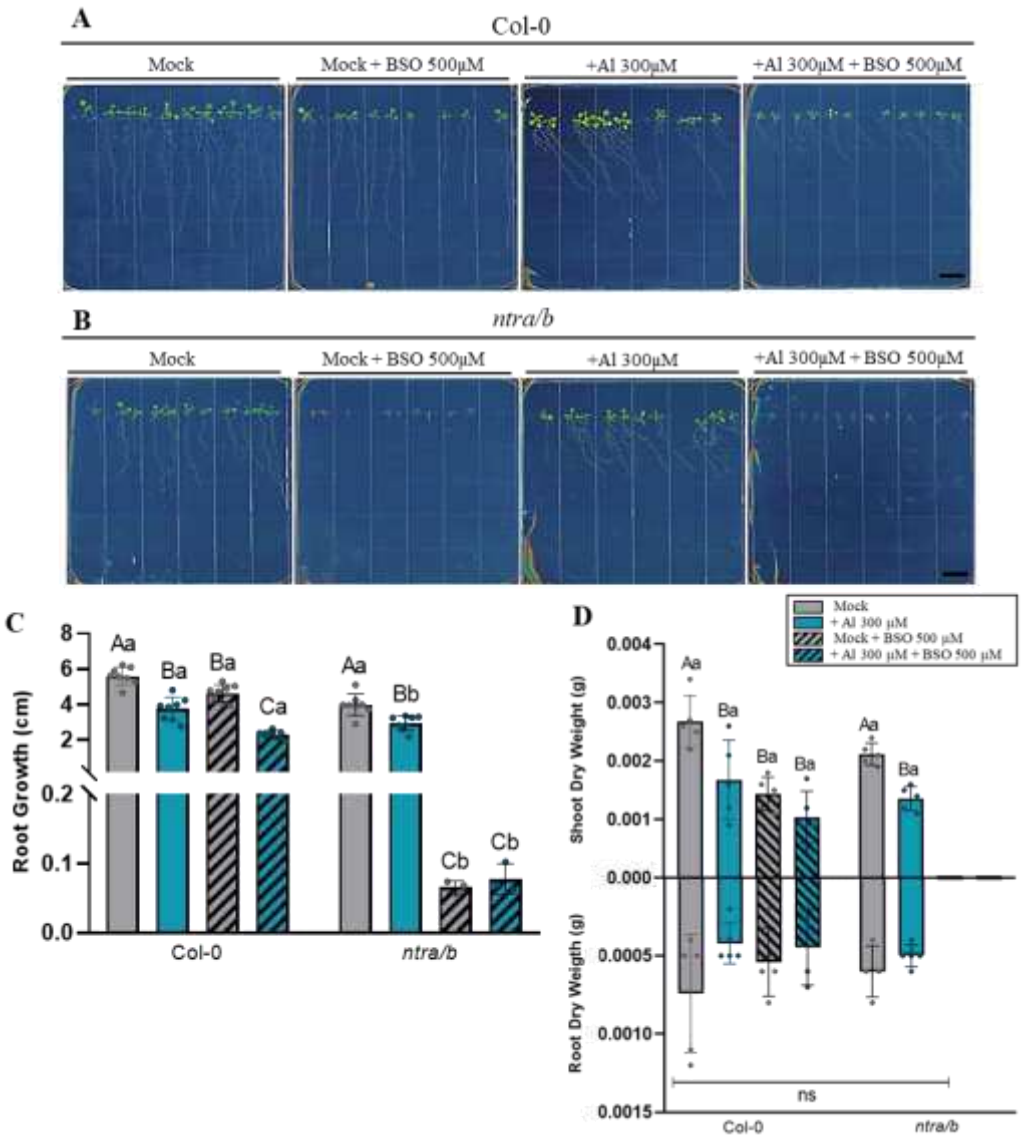

Figure 5: Phenotypic characterization of *A. thaliana* plants in response to aluminum and BSO. (A and B) representative images of the seedling's plates. Growth parameters (C) root length and (D) dry weight of Wild-type (Col-0) and NADPH dependent thioredoxin reductase double-KO mutant (At*NTRA* x At*NTRB*) line (*ntra/b*) were grown for 10 days in the absence of aluminum and glutathione inhibitor-BSO (Mock) – MS medium pH 4.0; the presence of only BSO (Mock + BSO 500 µM); in aluminum (300 µM) and with aluminum and BSO (300 µM and 500 µM respectively). Values or means ± SD (n = 4 - 8). Means followed by the same uppercase (for the genotypes) and lowercase (for aluminum/BSO concentration) letters do not have significant statistical differences according to Tukey's test ($p<0.05$). Abbreviations: BSO, Buthionine-sulfoximine.

Glutathione synthesis impairment strongly affect Al mitigation process

We observed that the impairment of GSH production by BSO affects the root growth in the presence of Al, to better understand if this impairment was caused by less GSH or by the redox state of the pool, we used GSH-defected mutants (*cad-2* - 30% remaining GSH levels and *zir1*15% remaining GSH levels) and a glutathione reductase 1 mutant (*gr1-1*).

Even though the mutant *zir1* is a smaller plant, virtually it showed the same result as Col-0 and *cad-2* in terms of root growth inhibition after 10 days in the presence of 300 µM of Al (Fig. 6 A). Nevertheless, the *gr1-1* showed a more drastic decrease in root development during Al stress (Fig. 6 A) two-fold decrease compared to Col-0. In terms of biomass partitioning, no significant difference was observed (Fig. 6 B).

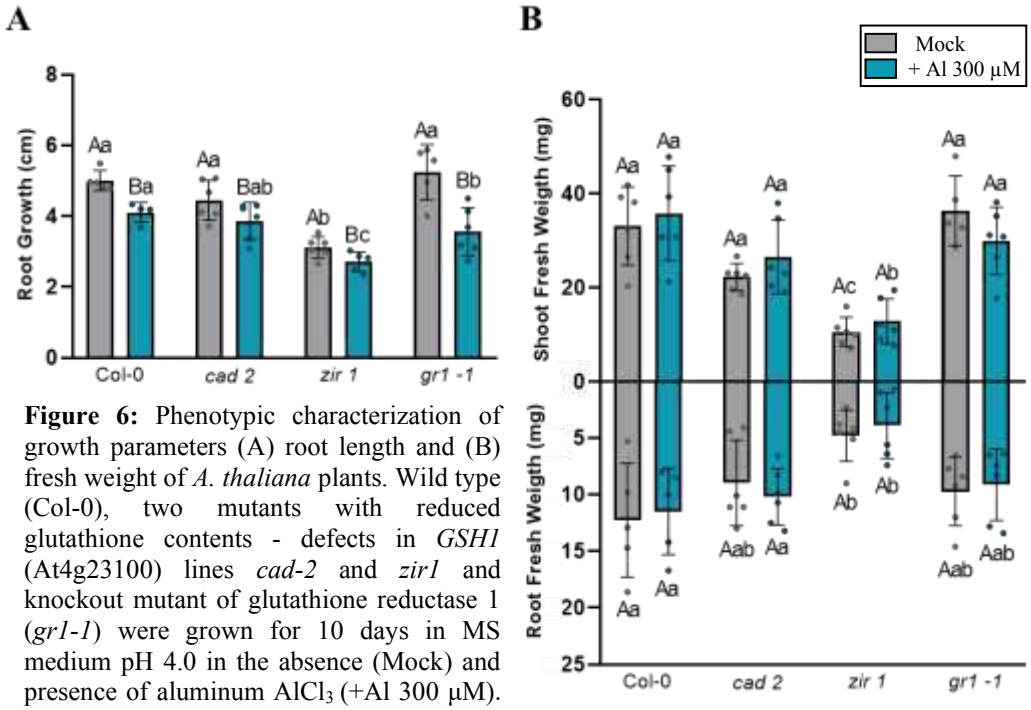

Figure 6: Phenotypic characterization of growth parameters (A) root length and (B) fresh weight of *A. thaliana* plants. Wild type (Col-0), two mutants with reduced glutathione contents - defects in *GSH1* (At4g23100) lines *cad-2* and *zir1* and knockout mutant of glutathione reductase 1 (*gr1-1*) were grown for 10 days in MS medium pH 4.0 in the absence (Mock) and presence of aluminum $AlCl_3$ (+Al 300 µM). Values or means ±SD (n=6). Different letters indicate significant differences ($p < 0.05$) according to the Tukey's test, capital case letters compare each condition within the same genotype and lower-case letters compares the conditions among all genotypes.

Since the impairment of the redox status of the GSH pool showed a difference in root growth, we performed an *in vivo* assay to determine the steady-state redox status of Col-0, *gr1-1,* and *ntra/b*. As expected, the redox pool (E_{GSH}) of glutathione is more oxidized for the mutant *gr1-1* than for Col-0 or *ntra/b* in seedlings (Fig. 7 A), roots (Fig. 7 B) and leaf discs (Fig. 7 C). Even though similar, a slight difference is observed for the pool between *ntra/b* and Col-0 in seedlings and roots, being the *ntra/b* a little more oxidized in roots and more reduced in seedlings.

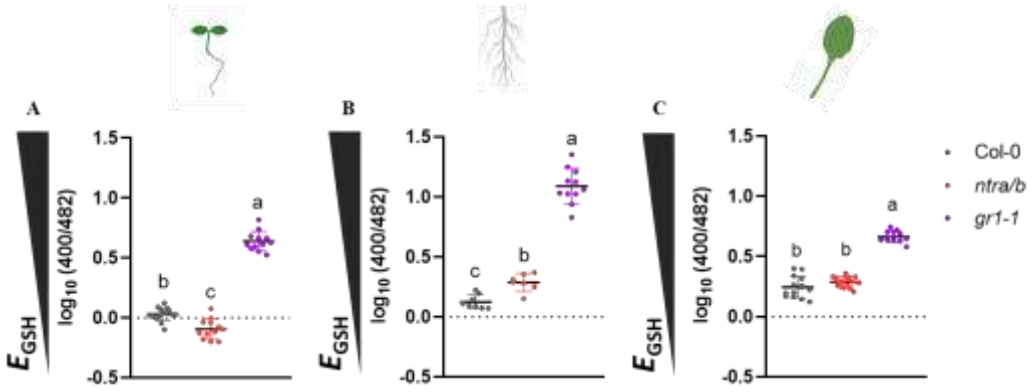

Figure 7: Phenotypic characterization of glutathione redox status (E_{GSH}) of *A. thaliana* plants in steady state. Wild-type (Col-0), NADPH dependent thioredoxin reductase double-KO mutant (At*NTRA* x At*NTRB*) line (*ntra/b*) and knockout mutant of glutathione reductase 1 (*gr1-1*) expressing cytosolic Grx1-roGFP2 to monitor glutathione redox status in (A) ten-day-old seedlings, (B) ten-day-old roots and (C) five-week-old leaf discs. Values are displayed as mean ± SD (n = 7 – 12). All the fluorescence intensities were recorded from the plant material in MS pH 4.0 medium and the autofluorescence from corresponding Col-0 control without a sensor was used for background subtraction. Reduction–oxidation-sensitive green fluorescent protein2 (roGFP2): Ex = 400 ± 5 and 482 ± 16 nm/Em = 520 ± 10 nm. Means followed by the same letters do not have significant statistical differences according to Tukey's test ($p<0.05$).

To better understand the implications of the glutathione redox pool, *in vivo* time series dynamics of seedlings, roots, and leaf discs of Col-0, *gr1-1,* and *ntra/b* were evaluated with Al stress. For seedlings, it was clear that oxidation of the cytosolic pool starts to occur hours after the application of the stress for Col-0 and *gr1-1* (Fig. 8 A and B), while for the *ntra/b* the application of the Al seems to not disturb the pool in seedlings (Fig. 8 C). Differently, in roots the response of oxidization of the glutathione pool occurs faster and more drastically in *ntra/b* mutants (Fig. 8 F), while for Col-0 and *gr1-1* the response exists but is not with high amplitude (Fig. 8 D and E). For leaf discs, we could only observe a response for *gr1-1* (Fig. 8 H), Col-0, and *ntra/b* leaves seem virtually not disturbed by Al application (Fig. 8 G and I).

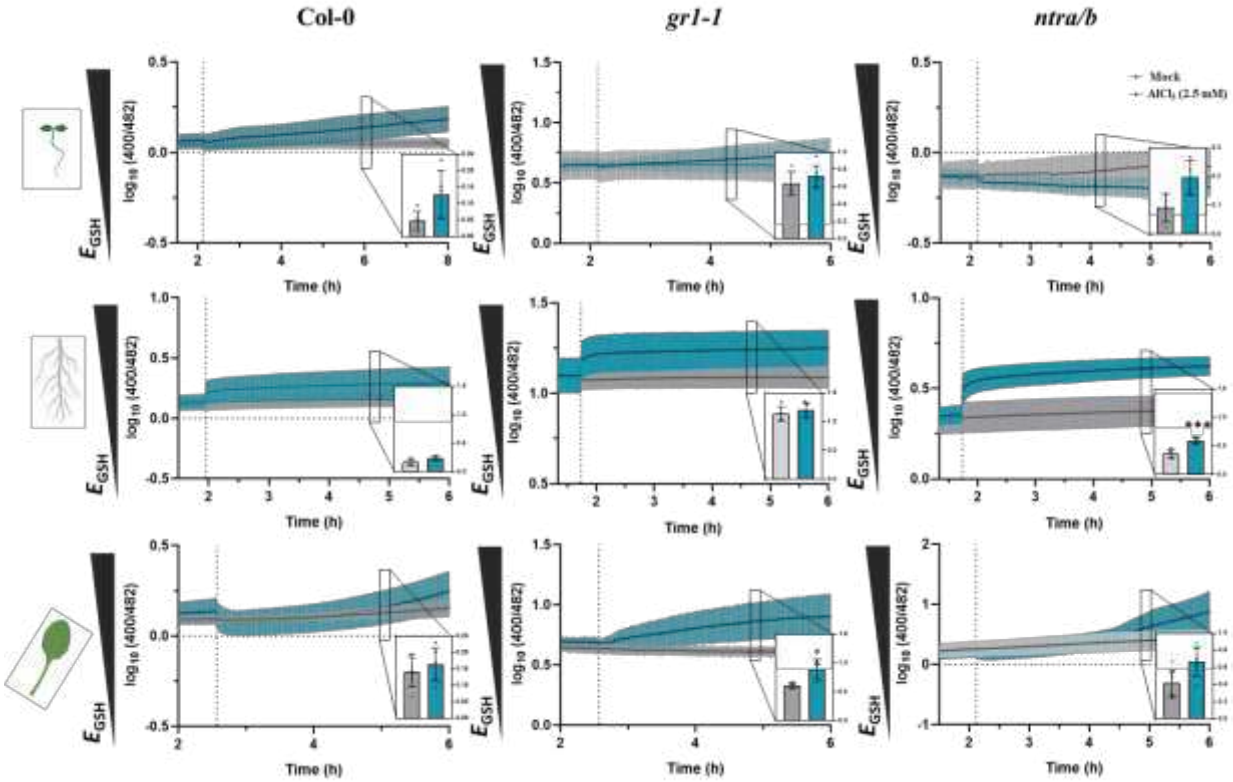

Figure 8: Monitoring the cytosolic glutathione redox status (E_{GSH}) responses to aluminum in *Arabidopsis thalia*na. Time series of wild-type (Col-0), NADPH dependent thioredoxin reductase double-KO mutant (At*NTRA* x At*NTRB*) line (*ntra/b*) and knockout mutant of glutathione reductase 1 (*gr1-1*) expressing cytosolic Grx1-roGFP2 to monitor glutathione redox status in (A - C) ten-day-old seedlings, (D - F) ten-day-old roots and (G - I) five-week-old leaf discs. Values are displayed as mean ± SD (n = 6 – 8). Subjected to mock MS pH 4.0 (gray dots) or 2.5 mM $AlCl_3$ (blue dots). Dashed line indicates the moment of aluminum application after the steady state. All the fluorescence intensities were recorded from the plant material in MS pH 4.0 medium and the autofluorescence from corresponding Col-0 controls without a sensor were used for background subtraction. Reduction–oxidation-sensitive green fluorescent protein2 (roGFP2): Ex = 400 ± 5 and 482 ± 16 nm/Em = 520 ± 10 nm. N = 5 - 8 ± SD. Asterisks * indicate a significant difference in relation to control as determined by Student's t-test *P < 0.05; **P < 0.01; *** P <0.005.

H_2O_2 and pH rapidly changes in response to Al stress

The pool of GSH tends to be oxidized within time after the application of the Al stress. By using cytosolic sensors for ROS and pH *in vivo,* we verified the dynamics of those in Col-0. Surprisingly, for seedlings no clear response was observed for H_2O_2 (Fig. 9 A), nevertheless, for roots a clear gradual increase in ROS could be observed after Al application (Fig. 9 B); the same also happened for leaf disc, but slower than in roots (Fig. 9 C). Interestingly, the cytosolic pH drops fast, right after the stress application for both roots (Fig. 9 D) and leaf discs (Fig. 9 E).

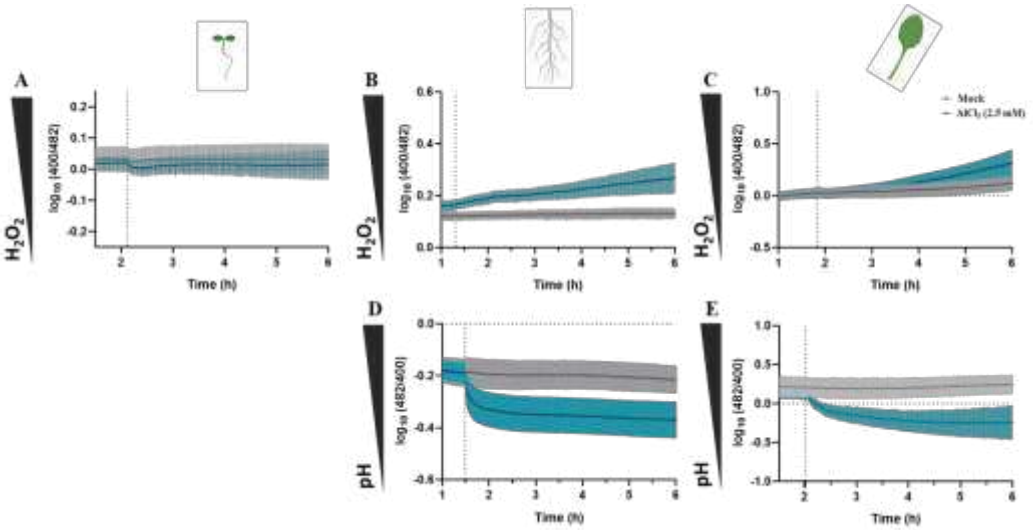

Figure 9. Monitoring the cytosolic responses of H_2O_2 and pH to aluminum in *Arabidopsis thalia*na. Time series of wild-type (Col-0) expressing cytosolic roGFP2-ORP and cpYFP (A) ten-day-old seedlings, (B and D) ten-day-old roots, and (C and E) five-week-old leaf discs. Values are displayed as mean ± SD (n = 6 – 8). Subjected to mock MS pH 4.0 (gray dots) or 2.5 mM $AlCl_3$ (blue dots). Dashed line indicates the moment of aluminum application after the steady state. All the fluorescence intensities were recorded from the plant material in MS pH 4.0 medium and the autofluorescence from corresponding Col-0 controls without a sensor were used for background subtraction. Reduction–oxidation-sensitive green fluorescent protein2 (roGFP2) and yellow fluorescent protein (YFP): Ex = 400 ± 5 and 482 ± 16 nm/Em = 520 ± 10 nm.

The dynamics of ROS and pH in cytosol showed that even though the pH drops rapidly the ROS increase happens gradually. To better understand if the roots *in vivo* dynamics of both parameters inside the mitochondria are similar to the cytosolic one we used a mitochondrial target sensor for Col-0 and *ntra/b*. Once again, the pH rapidly drops in the organelle for Col-0 (Fig. 10 A), and as observed for the cytosolic response, the ROS in the Col-0 mitochondria gradually increase (Fig. 10 B). However, for the *ntra/b* the ROS response was faster (Fig. 10 C); however, it seems slowly increase, while for Col-0 even though we observed a slow increase immediately after Al application it seems to continue to increase in a higher slope within time after the application.

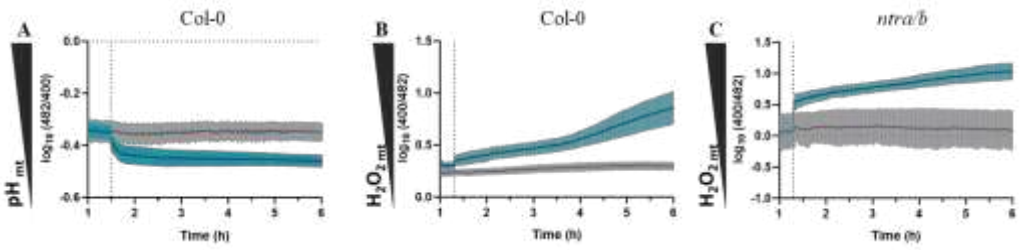

Figure 10: Monitoring the mitochondrial pH and H_2O_2 responses to aluminum in *Arabidopsis thalia*na. Time series of wild-type (Col-0), NADPH dependent thioredoxin reductase double-KO mutant (At*NTRA* x At*NTRB*) line (*ntra/b*) expressing mitochondrial (A) cpYFP to monitor pH; (B–C) roGFP2-ORP to monitor H_2O_2 in ten-day-old roots. Values are displayed as mean ± SD (n = 6 – 8). Subjected to mock MS pH 4.0 (gray dots) or 2.5 mM $AlCl_3$ (blue dots). Dashed line indicates the moment of aluminum application after the steady state. All the fluorescence intensities were recorded from the plant material

in MS pH 4.0 medium and the autofluorescence from corresponding Col-0 controls without a sensor were used for background subtraction. Reduction–oxidation-sensitive green fluorescent protein2 (roGFP2) and yellow fluorescent protein (YFP): Ex = 400 ± 5 and 482 ± 16 nm/Em = 520 ± 10 nm.

DISCUSSION

In the present study, we evaluated how the lack of two key components of mitochondrial redox systems, NTR and GR, affects molecular responses to Al^{3+} stress. Both *TRXo1* single knockout mutant lines did not show any visible phenotypic alterations in response to Al stress compared with the Col-0, which was in part expected since a certain degree of redundancy in mitochondria redox systems was described before (REICHHELD et al., 2005). Accordingly, it is possible that the glutaredoxins can compensate for the lack of *TRXo1*, acting on its protein targets, therefore no significant phenotype was observed for Al stress conditions (ROUHIER et al., 2005). The double mutant *ntra/b* showed a smaller seedling even in the absence of Al, as observed before (REICHHELD et al., 2007), and it is suggested that this is the reflection of the metabolic adjustments required in the primary metabolism to cope with the absence of one key regulatory enzyme that determines the redox state of the TRX system, which regulates the TCA cycle (DALOSO et al., 2015). In contrast, this same mutant (*ntra/b*) showed greater tolerance to Al stress, since it presented lower loss in root growth, a parameter used to describe and evaluate the Al tolerance (KOCHIAN et al., 2002).

One mechanism to deal with Al in *Arabidopsis thaliana* is the root malate exudation through ALMT transporter (KOBAYASHI et al., 2007), this, and others, TCA cycle intermediary are increased in *ntra/b* (DALOSO et al., 2015), however, the Al histolocalization did not show less Al content in the root surface for the *ntra/b*, suggesting no higher OA exudation than the Col-0. Nevertheless, the Al detoxification by OA can also occur internally, the NIP1;2 transporter was shown to facilitate the removal of Al from the root to shoot only when it is an Al-malate complex (WANG et al., 2017), reinforcing the importance of malate cellular content to Al tolerance. Moreover, an increase in the intracellular levels of malate was associated with a more tolerant phenotype observed for NADP-dependent malic enzyme (NADP-ME1) mutants (BADIA et al., 2019). Another interesting observation in the Al stain assay was the morphological anomaly in the Col-0 root apex. It is well established that root growth inhibition occurs in sensitive plants in response to Al (DAWOOD et al., 2022), and it occurs in part because the Al interacts with a large number of negative charges in the cell wall, leading to a rigidity that will interfere with cell division (ZHU et al., 2013; FURLAN et al. 2020) and ultimately cause structural damage, as observed for the Col-0 root apex. This data

also corroborates with the Al tolerance of *ntra/b*, once is clear the non-morphological disturbance in the root apex, the most affected site by Al in plants (LI et al., 2021).

Keeping this in mind, Al tolerance can also be related to better ROS scavenge machinery detoxification (FURLAN et al., 2020). Our results showed less O_2^- staining in the root apex of *ntra/b* in the presence of Al, which can be highly related to the overlapping of functions between TRXs and Glutaredoxins that may be overcompensating the absence of the NTRs (REICHHELD et al., 2007). Glutathione was shown crucial to *ntra/b* survival (REICHHELD et al., 2007), consistently the artificial glutathione biosynthesis inhibition by BSO supplementation in the medium impaired the *ntra/b* seedling development. Interestingly, the BSO supplementation also appears to increase the Al toxic effect in the Col-0, reducing even more the root growth, suggesting the direct relation between the Al stress and glutathione. Root growth is directed to lateral upon Al stress in both Col-0 and *ntra/b* and this change directions can be strongly related to low pH that can directly affect polar auxin transport (LI et al., 2021).

GSH cycle is an important antioxidant response machinery during stress, including Al stress (LIU et al., 2018; KUSUNOKI et al., 2018). Although, mutants deficient in GSH content, *cad-2* (HOWDEN et al., 1995) and *zir1* (SHANMUGAM et al., 2012), which contain approximately 30 and 15% total GSH levels compared to the Col-0, respectively (BANGASH et al., 2019), did not show a more affect phenotype when exposed to Al. Accordingly, double mutant *ntra/b* does not show higher levels of GSH (REICHHELD et al., 2007), which leads us to infer that the better mitigation in *ntra/b* and the more sensitive phenotype observed for the *gr1-1* is strongly related to the redox status of the GSH system and not with the GSH content.

Using Nernst equation, we can calculate the glutathione redox potential (E_{GSH}) with the mathematical equation $[GSH]^2/[GSSG]$, based on the quantification of the molecules in the cell extract, however, since the extraction can alter some metabolites features and does not allow subcellular localization it might lead to incorrect assumptions of the biological environment (FLOHÉ, 2013). To overcome this challenge the roGFP-probe genetically encoded can monitor real-time E_{GSH} *in vivo* (SCHWARZLÄNDER et al., 2016).

Monitoring the redox status of GSH with the roGFP-probe, as expected, the steady state of E_{GSH} is more oxidized in the *gr1-1* mutant; in agreement, previous works showed a higher GSSG accumulation in this mutant (MHAMDI et al., 2010). This fact aside, no generalized oxidative stress was observed (MHAMDI et al., 2010), which can corroborate with no visual phenotype in seedling development in mock conditions, being similar in size and biomass to

the Col-0 even with its function not overcome by *AtGR2* nor by other thiol systems (MHAMDI et al., 2010). It is important to notice that even with the absence of NTRs A and B, the *ntra/b* mutant showed a very similar E_{GSH} to Col-0, being a little more oxidized in roots, a fact that can be a reflection of the redundancy between these redox systems described before (REICHHELD et al., 2005).

We could observe that the redox response to Al occurs rapidly when evaluating the time series response of the E_{GSH} to Al application. That is coherent with the Al effects on the roots, which can be perceived in the first hours of exposure (KOCHIAN et al., 2005). Consistently the malate exudation response starts after 2 to 4 h of Al stress imposed (KOBAYASHI et al., 2007). Taking that into account, we monitor the cellular responses *in vivo* for 6 to 8 h. In general, the GSH pool was oxidized for all genotypes and organs upon Al stress. That can be strongly associated with the ROS production by Al and the subsequent detoxification of H_2O_2 to H_2O (FOYER & NOCTOR, 2005). This process is highly related to GR, once it can occur through ascorbate peroxidase (APX) or glutathione peroxidase (GPX), both depend on GR activity coupled to NADPH oxidation (MHAMDI et al., 2010; DAWOOD et al., 2022). NADPH links the respiratory and redox metabolism in the mitochondria and is the main reductant source for a thiol-redox network (SCHWARZLÄNDER & FINKEMEIER, 2013). In stress conditions, there is a higher request for NADPH than NADH in plant cells (OBATA et al., 2011). *In vitro* studies demonstrated that GRX can reduce TRX using NAD(P)H, hence the same may occur in the *ntra/b*. Bearing that in mind, it is possible to infer that in this mutant all the NAD(P)H reductant power goes to the GR pathway, which can explain the strong and rapid oxidizing of E_{GSH} in *ntra/b* roots exposed to Al. Considering that this rapid and strong oxidizing of the E_{GSH} is necessary for better cellular mitigation responses to Al, that can explain, at least partially, the strong sensitive phenotype observed in *gr1-1*, which already has the pool oxidized with little space for more oxidation in quick response to Al. Corroborating with that, it was shown that GR levels are increased in Al-tolerant rice genotypes (RIBEIRO et al., 2022).

Roots, especially the root-apex, are the main site for Al effects (LI et al., 2021), some species, like rice, also present an influx Al transporters (HUANG et al., 2009), therefore it is expected a higher response in this organ. While for shoots the Al that is translocated to it is already complexed with OA (WANG et al., 2017) and can be sequestered into the vacuole (ZHANG et al., 2019), which can justify why leaf discs seem to have no clear responses in the E_{GSH} upon directly Al application. Monitoring the H_2O_2 levels in Col-0 plants, it is clear the gradual increase in ROS after the application in roots. Al is related to ROS increase in roots

and studies related to the capacity of the scavenging systems to tolerance (GIANNAKOULA et al., 2010). Al-tolerant plants show less H_2O_2 than sensitive ones, which can be related to an improvement in the scavenging system or to a decreased production of H_2O_2 itself (BADIA et al., 2019). Accordingly, overexpression of antioxidant enzymes, or use of external components to stimulate antioxidant enzymes, like melatonin, are also mechanisms related to increased root growth during Al stress (SUN et al, 2020; ROSA-SANTOS, et al., 2020). Even though H_2O_2 can also act as a signal molecule inside the cell (WILLEMS et al., 2016), in excess it can significantly damage cell structures and function (FURLAN et al., 2020). The continuous increase in H_2O_2 levels over time after Al application for Col-0 roots can indicate its sensibility to Al that culminates in the root growth impairment, once ROS is suggested to be involved in signaling pathways that lead to root growth restriction (BADIA et al., 2019).

The pH drops inside the cell immediately after the Al exposure in roots. This fact can be strongly related to root growth inhibition, once it can directly affect polar auxin transport (LI et al., 2021). Consistently, elevation of pH in the root mediated by magnesium could alleviate Al symptoms in *Populus* (ZHANG et al., 2020). The Col-0 internal mitochondrial pH also showed a rapid decrease in roots, which can interfere directly with the respiratory metabolism, once the supercomplexes dissociate with pH drops (RAMÍREZ-AGUILAR et al., 2011). The disbalance in mitochondrial metabolism can affect the mitigation process, hence OA is an essential player in Al-resistance. Also, concomitant with the pH decrease we can observe an H_2O_2 increase inside root mitochondria for Col-0 and *ntra/b*. Regardless of the fast increase of the H_2O_2 in the *ntra/b*, homeostasis is seemingly reached, whereas a continuum increase of ROS in the mitochondria is observed for the WT, showing a higher slope even after 4 h. This subcellular data corroborates with the possible scenario, that despite the absence of NTRs the scavenging machine is compensated using all NAD(P)H reductant power by the GR pathway to cope with the ROS generated following Al stress conditions.

CONCLUSIONS

In summary, our results highlight the importance of the GR in mitigating Al stress responses. The evidence that contributes to this conclusion includes a more sensitive genotype present in the *gr1-1* mutant, that is not observed in the GSH mutants. The rapid and strong oxidation of the E_{GSH} pool in response to Al was associated with a more tolerant phenotype showed by *ntra/b*. Although this more tolerant phenotype does not present the NTRs that use

the NADPH pool to regulate the TRX function, it seems reasonable to suggest that most of the NADHP reductant power can go to thiol-redox regulation mediated by GR to deal with the H_2O_2 generated following Al stress. The results described here further contribute to the elucidation of the internal detoxification mechanism of Al tolerance in plants, which could assist crop breeding with a better understanding of the cellular physiology responses to Al.

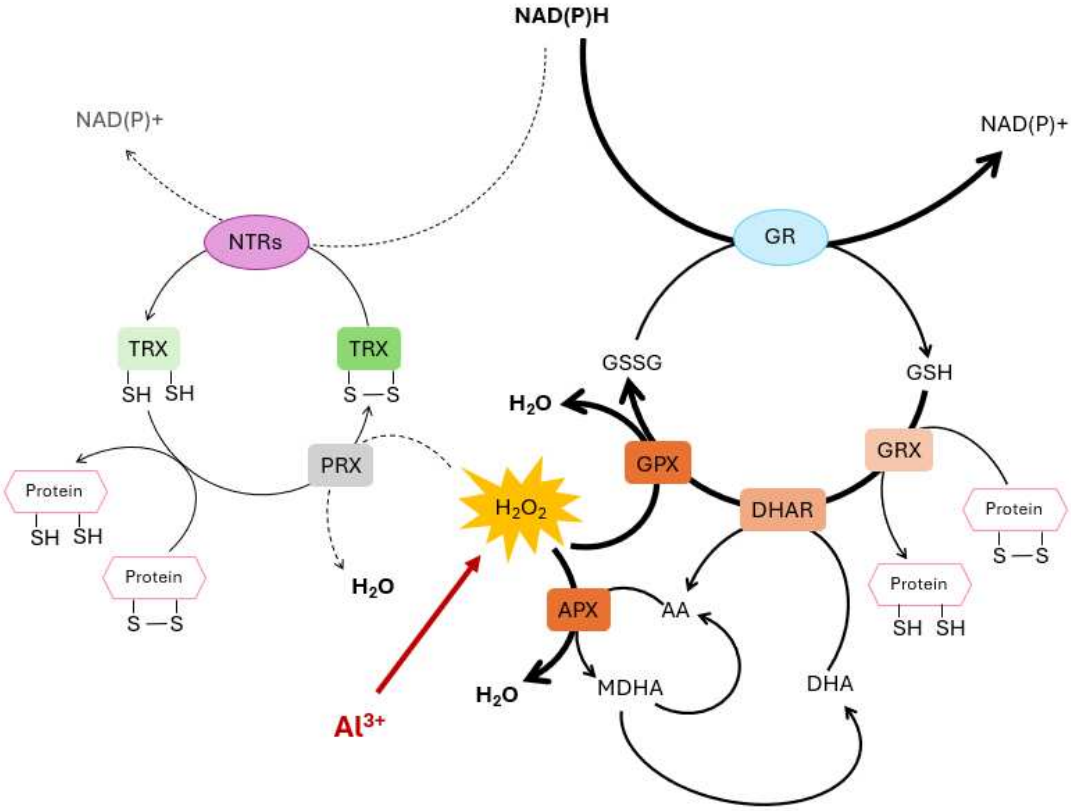

Figure 10: Schematic representation of the role of NAD(P)H dependent redox system in *Arabidopsis thaliana* roots response to Al stress. The GR activity plays a key role in allowing a better ROS detoxification, leading to a more tolerant phenotype mostly linked to the reductant power generated by the NAD(P)H oxidation going preferentially to the GR pathway and ultimately favoring the ROS scavenging machinery associated with APX and GRX. Abbreviations: GR, glutathione reductase; GSSG, glutathione disulfide; GSH, glutathione; GPX, glutathione peroxidase; DHAR, dehydroascorbate reductase; GRX, glutaredoxins; APX, ascorbate peroxidase; AA, ascorbate; MDHA, Monodehydroascorbate; DHA, dehydroascorbic acid; NTR, NADPH-dependent thioredoxin reductase; TRX, thioredoxin; PRX, peroxidase.

SUPPLEMENTAL DATA

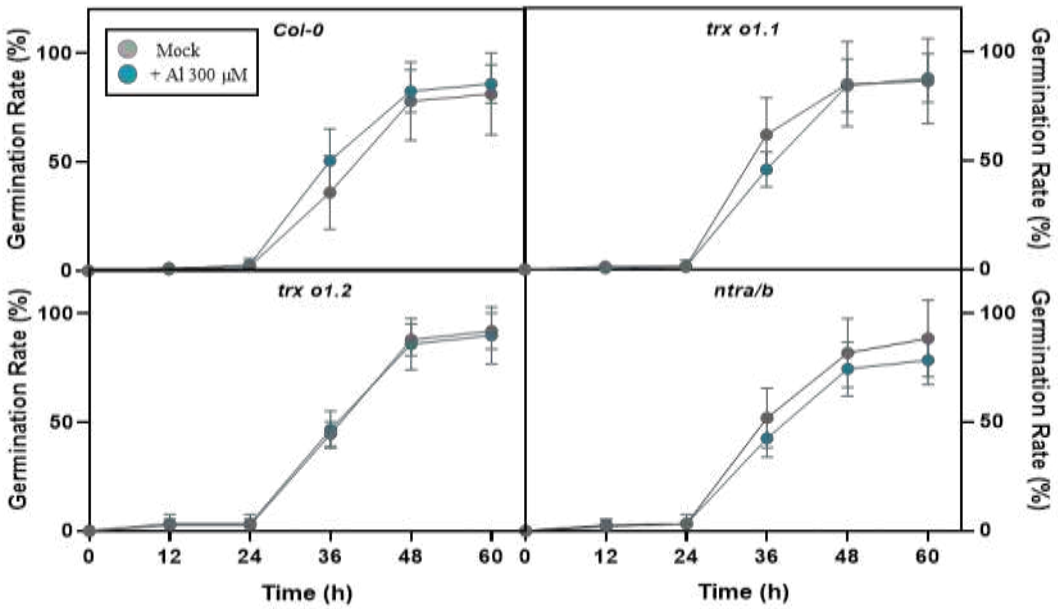

Supplemental Figure 1. Effect of aluminum on *Arabidopsis thaliana* germination of wild type plants (Col-0), two T-DNA insertion mutants in thioredoxin gene (*ATTRXO1)* lines (*trx o1.1* and *trx o1.2*) and a NADPH dependent thioredoxin reductase double-KO mutant (*AtNTRA x AtNTRB)* line (*ntra/b*). Germinated in 1/2 MS plates with MS medium pH 4.0 without (Mock) or with aluminum $AlCl_3$ (+Al 300 µM). Values or means ±SD (n=6).

REFERENCES

ARAÚJO, W. L.; NUNES-NESI, A.; OSORIO, S.; USADEL, B.; FUENTES, D.; NAGY, R.; BALBO, I.; LEHMANN, M.; STUDART-WITKOWSKI, C.; TOHGE, T.; MARTINOIA, E.; JORDANA, X.; DAMATTA, F. M.; FERNIE, A. R. Antisense inhibition of the iron-sulphur subunit of succinate dehydrogenase enhances photosynthesis and growth in tomato via an organic acid–mediated effect on stomatal aperture. **The Plant Cell,** v. 23, n. 2, p. 600–627, 2011.

BADIA, M.B.; MAURINO, V.G.; PAVLOVIC, T.; ARIAS, C.L.; PAGANI, M.A.; ANDREO, C.S.; SAIGO, M.; DRINCOVICH, M.F.; WHEELER, M.C.G. Loss of function of *Arabidopsis* NADP-malic enzyme 1 results in enhanced tolerance to aluminum stress. **The Plant Journal**, v. 101, n. 3, p. 653-665, 2019.

BALMER, Y.; VENSEL, W.H.; TANAKA, C.K.; HURKMAN, W.J.; GELHAYE, E.; ROUHIER, N.; JACQUOT, J.P.; MANIERI, W.; SCHÜRMANN, P.; DROUX, M.; BUCHANAN, B.B. Thioredoxin links redox to the regulation of fundamental processes of plant mitochondria. **Proceedings of the National Academy of Sciences of the United States of America**, USA, v. 101, n. 8, p. 2642–2647, 2004.

BANGASH, S.A.K.; MÜLLER-SCHÜSSELE, S.J.; SOLBACH, D.; JANSEN, M.; FIORANI, F.; SCHWARZLÄNDER, M.; KOPRIVA, S.; MEYER, A.J Low-glutathione mutants are impaired in growth but do not show an increased sensitivity to moderate water deficit. **PLoS ONE**, v. 14, n. 10, 2019.

BARROS, J.A.; CAVALCANTI, J.H.F.; MEDEIROS, D.B.; NUNES-NESI, A.; AVIN-WITTENBERG, T.; FERNIE A. R.; ARAÚJO, W.L. Autophagy deficiency compromises alternative pathways of respiration following energy deprivation. **Plant Physiology**, v. 175, p. 62-76, 2017.

BAUWE, H.; HAGEMANN, M.; KERN, R.; TIMM, S. Photorespiration has a dual origin and manifold links to central metabolism. **Current Opinion in Plant Biology**, v. 15, n. 3, p. 269–275, 2012.

BOJÓRQUEZ-QUINTAL, E.; ESCALANTE-MAGAÑA, C.; ECHEVARRÍA-MACHADO, I.; MARTÍNEZ-ESTÉVEZ, M. Aluminum, a friend or foe of higher plants in acid soils. **Frontiers In Plant Science**, v. 8, p.1–18, 2017.

CHAUHANA, D. K.; YADAV, V.; VACULÍK, M.; GASSMANN, W.; PIKE, S.; ARIF, N.; SINGH, S. P.; RUPESH, D.; SAHI, S.; TRIPATHI, D. K. Aluminum toxicity and aluminum stress-induced physiological tolerance responses in higher plants. **Critical Reviews in Biotechnology**, v. 41, p. 715-730, 2021.

CLOUGH, S.J.; BENT, A.F. Floral dip: a simplified method for *Agrobacterium*-mediated transformation of *Arabidopsis thaliana*. **The Plant Journal**, v. 16, n. 6, p. 735-743, 1998.

DALOSO, D; MÜLLER, K.; OBATA, T; FLORIAN, A.; TOHGE, T.; BOTTCHER, A.; RIONDET, C.; BARIAT, L.; CARRARI, F.; NUNES-NESI, A.; BUCHANAN, B.; REICHHELD, J-P.; ARAÚJO, W.L; FERNIE, A.R. Thioredoxin, a master regulator of the tricarboxylic acid cycle in plant mitochondria. **Proceedings of the National Academy of Sciences**, v. 112, n. 11, p. E1392-1400, 2015.

DAWOOD, M.F.; TAHJIB-UL-ARIF, M.; SOHAG, A.A.M.; ABDEL LATEF, A.A.H. Fluoride mitigates aluminum-toxicity in barley: morpho-physiological responses and biochemical mechanisms. **BMC Plant Biology**, v. 22, p. 1–17, 2022.

DELHAIZE, E.; RYAN, P.R. Aluminum Toxicity and Tolerance in Plants. **Plant Physiology**, v. 107, p. 315–307, 1995.

DUTILLEUL, C.; LELARGE, C.; PRIOUL, J. L.; DE PAEPE, R.; FOYER, C. H.; NOCTOR, G. Mitochondria-driven changes in leaf NAD status exert a crucial influence on the control of nitrate assimilation and the integration of carbon and nitrogen metabolism. **Plant Physiology**, v. 139, n. 1, p. 64–78, 2005.

EEKHOUT, T.; LARSEN, P.; DE VEYLDER, L. Modification of DNA Checkpoints to Confer Aluminum Tolerance. **Trends in Plant Science**, v. 22, n. 2, p.102–105, 2017.

FONSECA-PEREIRA, P.; DALOSO, D.M.; GAGO, J.; NUNES-NESI, A.; ARAÚJO, W.L. On the role of the plant mitochondrial thioredoxin system during abiotic stress. **Plant Signaling & Behavior**, v. 14, n. 6, p. 1592536, 2019a.

FONSECA-PEREIRA, P.; DALOSO, D. M.; GAGO, J.; SILVA, F. M. O.; CONDORI-APFATA, J.; FLOREZ-SARASA, I.; TOHGE, T.; REICHHELD, J-P.; NUNES-NESI, A.; FERNIE, A.; ARAÚJO, W. The Mitochondrial Thioredoxin System Contributes to the Metabolic Responses Under Drought Episodes in *Arabidopsis*. **Plant and Cell Physiology**, v. 60, n. 1, p. 213 – 229, 2019b.

FOYER, C. H.; NOCTOR, G. Redox signaling in plants. **Antioxidants & Redox Signaling**, v. 18, n. 16, p. 2087–2090, 2013.

FOYER, C.H.; NOCTOR, G. Stress-triggered redox signalling: What's in pROSpect? **Plant, Cell & Environment.** v. 39, n. 9, p. 51–64, 2016.

FURLAN, F.; BORGO, L.; RABÊLO, FHS.; ROSSI, ML.; LINHARES, FS.; MARTINELLI, AP.; AZEVEDO, RA.; LAVRES, J. Aluminum-induced toxicity in *Urochloa brizantha* genotypes: a first glance into root Al-apoplastic and-symplastic compartmentation, Al-translocation and antioxidant performance. **Chemosphere**, v. 243, n. 125362, 2020.

GIANNAKOULA, A.; MOUSTAKAS, M.; SYROS, T.; YUPSANIS, T. Aluminum stress induces up-regulation of an efficient antioxidant system in the Al-tolerant maize line but not in the Al-sensitive line. **Environmental and Experimental Botany**, v. 67, n. 3, p. 487 – 494, 2010.

GUPTA, N.; GAURAV, S. S.; KUMAR, A**.** Molecular Basis of Aluminium Toxicity in Plants: A Review. **American Journal of Plant Sciences,** v.4, p.21–37, 2013.

HÄGGLUND, P.; FINNIE, C.; YANO, H.; SHAHPIRI, A.; BUCHANAN, B.B.; HENRIKSEN, A.; SVENSSON, B. Seed thioredoxin *h*. **Biochimica et Biophysica Acta (BBA)-Proteins and Proteomics**, v. 1864, n. 8, p. 974–982, 2016.

HANSON, G.T.; AGGELER, R.; OGLESBEE, D.; CANNON, M.; CAPALDI, R. A.; TSIEN, R.Y.; REMINGTON, S.J. Investigating mitochondrial redox potential with redox-sensitive green fluorescent protein indicators. **Journal of Biological Chemistry**, v. 279, p.13044–13053, 2004.

HOWDEN, R; ANDERSEN, C.R.; GOLDSBROUGH, P.B; COBBETT, C.S. A cadmium-sensitive, glutathione-deficient mutant of *Arabidopsis thaliana*, **Plant Physiology**, v. 107, p. 1067–1073, 1995.

HUANG, C.F.; YAMAJI, N.; MITANI, N.; YANO, M.; NAGAMURA, Y.; MA, J.F. A bacterial-type ABC transporter is involved in aluminum tolerance in rice. **The Plant Cell**, v. 21, n. 2, p.655-667, 2009.

KAPOOR, D. Redox homeostasis in plants under abiotic stress: role of electron carriers, energy metabolism mediators and proteinaceous thiols. **Frontiers in Environmental Science**, v. 3, n. March, p. 1–12, 2015.

KEECH, O.; GARDESTRÖM, P.; KLECZKOWSKI, L.A.; ROUHIER, N. The redox control of photorespiration: From biochemical and physiological aspects to biotechnological considerations. **Plant, Cell & Environment**, v. 40, n. 4, p. 553-569, 2016.

KOBAYASHI, Y.; HOEKENGA, A.; ITOH, H.; NAKASHIMA, M.; SAITO, S.; SHAFF, JE.; MARON, L.; PIÑEROS M.; KOCHIAN, L.; KOYAMA, H. Characterization of At*ALMT1* expression in aluminum-inducible malate release and its role for rhizotoxic stress tolerance in *Arabidopsis*. **Plant Physiology**, v.145, n. 3, p.843-852, 2007.

KOCHIAN, L.V.; HOEKENGA, O.A.; PINEROS, M.A. How Do Crop Plants Tolerate Acid Soils? Mechanisms of Aluminum Tolerance and Phosphorous Efficiency. **Annual Review of Plant Biology,** v. 55, p. 459–493, 2004.

KOCHIAN, L.V.; PENCE, N.S.; LETHAM, D.L.; PINEROS, M.A.; MAGALHAES, J.V.; HOEKENGA, O.A.; GARVIN, D.F. Mechanisms of metal resistance in plants: aluminum and heavy metals. **Progress in Plant Nutrition: Plenary Lectures of the XIV International Plant Nutrition Colloquium**, v. 247, p.109–119, 2002.

KOCHIAN, L.V.; PINEROS, M.A.; HOEKENGA, O.A. The physiology, genetics and molecular biology of plant aluminum resistance and toxicity. **Plant and Soil**, v. 274, p.175-195, 2005.

KOCHIAN, L.V.; PIÑEROS, M.A.; LIU, J.; MAGALHAES, J.V. Plant adaptation to acid soils: the molecular basis for crop aluminum resistance. **Annual Review of Plant Biology**, v. 66, p. 571-598, 2015.

KONG, X.; SUN, L.; ZHOU, Y.; ZHANG, M.; LIU, Y.; PAN, J.; LI, D. *ZmMKK4* regulates osmotic stress through reactive oxygen species scavenging in transgenic tobacco. **Plant Cell Reports**, v. 30, p. 2097 2104, 2011.

KUKACHKA, B.F; MIIIER, R. B. A chemical spot-test for aluminum and its value in wood identification. **IAWA Journal** v. 1, n. 3, 1980.

KUSUNOKI, K.; KOBAYASHI, Y.; KOBAYASHI, Y.; KOYAMA, H. Comparative characterization of aluminum responsive transcriptome in Arabidopsis roots: comparison with other rhizotoxic ions at different stress intensities. **Soil Science and Plant Nutrition**, v. 64, n. 4, p. 469-481, 2018.

FLOHÉ, L. The fairytale of the GSSG/GSH redox potential. **Biochimica et Biophysica Acta (BBA)-General Subjects**, v. 1830, p. 3139–3142, 2013.

LI, C.; LIU, G.; GENG, X.; HE, C.; QUAN, T.; HAYASHI, K.I.; DE SMET, I.; ROBERT, H.S.; DING, Z.; YANG, Z.B. Local regulation of auxin transport in root-apex transition zone mediates aluminium-induced Arabidopsis root-growth inhibition. **The Plant Journal**, v. 108, p. 55-66, 2021.

LIU, H.; ZHU, R.; SHU, K.; LV, W.; WANG, S.; WANG, C.. Aluminum stress signaling, response, and adaptive mechanisms in plants. **Plant Signaling & Behavior,** v. 17, p. 2057060, 2022.

LIU, W.; XU, F.; LV, T.; ZHOU, W.; CHEN, Y.; JIN, C.; LU, L.; LIN, X. Spatial responses of antioxidative system to aluminum stress in roots of wheat (*Triticum aestivum L.*) plants. **Science of the Total Environment**, v. 627, p. 462–469, 2018.

MA, J. F. Syndrome of Aluminum Toxicity and Diversity of Aluminum Resistance in Higher **Plants International Review of Cytology,** v. 264, p. 225-252, 2007.

MARTÍ, M.C.; FLOREZ-SARASA, I.; CAMEJO, D.; RIBAS-CARBO, M.; LAZARO, J.J.; SEVILLA, F.; JIMENEZ, A. Response of mitochondrial thioredoxin PsTrxo1, antioxidant enzymes, and respiration to salinity in pea (*Pisum sativum* L.) leaves**. Journal of Experimental Botany**, v. 62, n. 11, p. 3863–3874, 2011.

MEYER, Y.; BELIN, C.; DELORME-HINOUX, V.; REICHHELD, J.P.; RIONDET, C. Thioredoxin and glutaredoxin systems in plants: molecular mechanisms, crosstalks, and functional significance. **Antioxidants and Redox Signaling**, v. 17, n. 8, p. 1124–1160, 2012.

MHAMDI, A.; HAGER, J.; CHAOUCH, S.; QUEVAL, G.; HAN, Y.; TACONNAT, L.; SAINDRENAN, P.; GOUIA, H.; ISSAKIDIS-BOURGUET, E.; RENOU, J.P.; NOCTOR, G. *Arabidopsis* GLUTATHIONE REDUCTASE1 plays a crucial role in leaf responses to intracellular hydrogen peroxide and in ensuring appropriate gene expression through both salicylic acid and jasmonic acid signaling pathways. **Plant Physiology**, v. 153, n. 3, p.1144-1160, 2010.

MICHELET, L.; ZAFFAGNINI, M.; MORISSE, S.; SPARLA, F.; PÉREZ-PÉREZ, M.E.; FRANCIA, F.; DANON, A.; MARCHAND, C.H.; FERMANI, S.; TROST, P.; LEMAIRE, S.D. Redox regulation of the Calvin-Benson cycle: something old, something new. **Frontiers in Plant Science**, v. 4, p. 470, 2013.

MURASHIGE, T.; SKOOG, F. A revised medium for rapid growth and bio assays with tobacco tissue cultures. **Physiologia Plantarum**, v. 15, n. 3, p. 473 497, 1962.

NUNES-NESI, A.; CARRARI, F.; GIBON, Y.; SULPICE, R.; LYTOVCHENKO, A.; FISAHN, J.; GRAHAM, J.; RATCLIFFE, R.G.; SWEETLOVE, L.J.; FERNIE, A. Deficiency of mitochondrial fumarase activity in tomato plants impairs photosynthesis via an effect on stomatal function. **The Plant Journal**, v. 50, p.1093–1106, 2007.

NUNES-NESI, A.; CARRARI, F.; LYTOVCHENKO, A.; SMITH, A.M.; EHLERS LOUREIRO, M.; RATCLIFFE, R.G.; SWEETLOVE, L.J.; FERNIE, A.R. Enhanced photosynthetic performance and growth as a consequence of decreasing mitochondrial malate dehydrogenase activity in transgenic tomato plants. **Plant Physiology**., v. 137, n. 2, p. 611–22, 2005.

NUNES-NESI, A.; BRITO, D.S.; INOSTROZA-BLANCHETEAU, C.; FERNIE, A.R.; ARAÚJO, W.L. The complex role of mitochondrial metabolism in plant aluminum resistance. **Trends in Plant Science**, v. 19, n. 6, p. 399–407, 2014.

OBATA, T.; MATTHES, A.; KOSZIOR, S.; LEHMANN, M.; ARAÚJO, W.L.; BOCK, R.; SWEETLOVE, L.J.; FERNIE, A.R. Alteration of mitochondrial protein complexes in relation to metabolic regulation under short-term oxidative stress in *Arabidopsis* seedlings. **Phytochemistry**, v. 72, n. 10, p. 1081-1091, 2011.

OFOE, R.; THOMAS, R. H.; ASIEDU, S. K.; WANG-PRUSKI, G.; FOFANA, B.; ABBEY, L. Aluminum in plant: Benefits, toxicity and tolerance mechanisms. **Frontiers in Plant Science,** v. 13, 2022.

OKEGAWA, Y.; MOTOHASHI, K. Chloroplastic thioredoxin m functions as a major regulator of Calvin cycle enzymes during photosynthesis *in vivo*. **The Plant Journal**, v. 84, n. 5, p. 900–913, 2015.

ORTIZ-ESPÍN, A.; IGLESIAS-FERNÁNDEZ, R.; CALDERÓN, A.; CARBONERO, P.; SEVILLA, F.; JIMÉNEZ, A. Mitochondrial *AtTrxo1* is transcriptionally regulated by AtbZIP9 and AtAZF2 and affects seed germination under saline conditions. **Journal of Experimental Botany**, v. 68, n. 5, p. 1025–1038, 2017.

ØSTERGAARD, H.; HENRIKSEN, A.; HANSEN, F.G.; WINTHER, J.R. Shedding light on disulfide bond formation: Engineering a redox switch in green fluorescent protein. **The EMBO Journal,** v. 20, n. 21, p. 5853–5862, 2001.

PANDA, S. K.; MATSUMOTO, H. Molecular physiology of aluminum toxicity and tolerance in plants. **The Botanical Review**, v. 73, p. 326–347, 2007.

QUEVAL, G.; NOCTOR, G. A plate reader method for the measurement of NAD, NADP, glutathione, and ascorbate in tissue extracts: application to redox profiling during *Arabidopsis* rosette development. **Analytical Biochemistry**, v. 363, n. 1, p. 58–69, 2007.

RAMÍREZ-AGUILAR, S.J.; KEUTHE, M.; ROCHA, M.; FEDYAEV, V.V.; KRAMP, K.; GUPTA, K.J.; RASMUSSON, A.G.; SCHULZE, W.X.; VAN DONGEN, J.T. The composition of plant mitochondrial supercomplexes changes with oxygen availability. **Journal of Biological Chemistry**, v. 286, n. 50, p. 43045-43053, 2011.

REICHHELD, J.P.; Meyer, E.; Khafif, M.; Bonnard, G.; Meyer, Y. *AtNTRB* is the major mitochondrial thioredoxin reductase in *Arabidopsis thaliana*. **FEBS Letters**., v. 579, n. 2, p. 337–342, 2005.

REICHHELD, J.P.; KHAFIF, M.; RIONDET, C.; DROUX, M.; BONNARD, G.; MEYER, Y. Inactivation of thioredoxin reductases reveals a complex interplay between thioredoxin and glutathione pathways in *Arabidopsis* development. **The Plant Cell**, v.19, n. 6, p. 1851–1865, 2007.

RENGEL, Z.; ZHANG, W. H. Role of dynamics of intracellular calcium in aluminium-toxicity syndrome. **New Phytologist**, v. 159, p. 295-314, 2003.

RIBEIRO, C.; DE MARCOS LAPAZ, A.; DE FREITAS-SILVA, L.; RIBEIRO, K.V.G.; YOSHIDA, C.H.P.; DAL-BIANCO, M.; CAMBRAIA, J. Aluminum promotes changes in rice

root structure and ascorbate and glutathione metabolism. **Physiology and Molecular Biology of Plants**, v. 28, n. 12, p. 2085-2098, 2022.

ROSA-SANTOS, T.M.; SILVA, R.G.D.; KUMAR, P.; KOTTAPALLI, P.; CRASTO, C.; KOTTAPALLI, K.R.; FRANÇA, S.C.; ZINGARETTI, S.M. Molecular mechanisms underlying sugarcane response to aluminum stress by RNA-Seq. **International Journal of Molecular Sciences**, v. 21, n. 21, p. 7934, 2020.

ROUHIER, N.; VILLAREJO, A.; SRIVASTAVA, M.; GELHAYE, E.; KEECH, O.; DROUX, M.; FINKEMEIER, I.; SAMUELSSON, G.; DIETZ, K.J; JACQUOT, JP.; WINGSLE, G. Identification of Plant Glutaredoxin Targets. **Antioxidants & Redox Signaling**, v. 7, p. 919–929, 2005.

RYAN, P. R.; LIU, Q.; SPERLING, P.; DONG, B.; FRANKE, S.; DELHAIZE, E. A Higher Plant Δ8 Sphingolipid Desaturase with a Preference for (Z) -Isomer Formation Confers Aluminum Tolerance to Yeast and Plants. **Plant Physiology,** v.144, p.1968–1977. 2007.

SCHMIDTMANN, E.; KÖNIG, A.C.; ORWAT, A.; LEISTER, D.; HARTL, M.; FINKEMEIER, I. Redox regulation of Arabidopsis mitochondrial citrate synthase. **Molecular Plant**, v. 7, n. 1, p. 156–169, 2014.

SCHWARZLÄNDER, M.; DICK, T.P.; MEYER, A.J.; MORGAN, B. Dissecting redox biology using fluorescent protein sensors. **Antioxidants & Redox Signaling**, v. 24, p. 680–712, 2016.

SCHWARZLÄNDER, M.; FINKEMEIER, I. Mitochondrial Energy and Redox Signaling in Plants, **Antioxidants & Redox Signaling**, v. 18, n. 16, p. 2122-2144, 2013.

SCHWARZLÄNDER, M.; FRICKER, M.D.; MÜLLER, C.; MARTY, L.; BRACH, T.; NOVAK, J.; SWEETLOVE, L.J.; HELL, R.; MEYER, A.J. Confocal imaging of glutathione redox potential in living plant cells. **Journal of microscopy**, v. 231, p. 299–316, 2008.

SETOTAW, T.A.; NUNES, C.F.; DE SOUZA, C.S.; RIBEIRO, A.P.; DE FARIA FREITAS, G.; DE AMORIM, D.A.; DOS SANTOS, D.N.; PASQUAL, M.; FERREIRA, J.L.; DE ALMEIDA CANÇADO, G.M. Assessment of tolerance to aluminum toxicity in olive (*Olea europaea*) based on root growth and organic acid Al^{3+} exclusion mechanism. **Australian Journal of Crop Science**, v. 9, n. 4, pp.264-270, 2015.

SHANMUGAM, V.; TSEDNEE, M.; YEH, K.C. Zinc tolerance induced by iron reveals the importance of glutathione in the cross-homeostasis between zinc and iron in *Arabidopsis thaliana*. **The Plant Journal**, v. 69, p.1006–1017, 2012.

SIMÕES, C.C.; MELO, J.O.; MAGALHAES, J.V.; GUIMARÃES, C.T. Genetic and molecular mechanisms of aluminum tolerance in plants. **Genetics and Molecular Research**, v. 11, n. 3, p. 1949-1957, 2012.

SOUZA, L. T.; CAMBRAIA, J.; RIBEIRO, C.; OLIVEIRA, J. A.; CAMPOS DA SILVA, L. Effects of aluminum on the elongation and external morphology of root tips in two maize genotypes. **Bragantia**, v. 75, p. 19 25, 2016.

SUN, C.; LV, T.; HUANG, L.; LIU, X.; JIN, C.; LIN, X. Melatonin ameliorates aluminum toxicity through enhancing aluminum exclusion and reestablishing redox homeostasis in roots of wheat. **Journal of Pineal Research**, v. 68, n. 4, p. e12642, 2020.

THORMÄHLEN, I.; MEITZEL, T.; GROYSMAN, J.; ÖCHSNER, A.B.; VON ROEPENACK-LAHAYE, E.; NARANJO, B.; CEJUDO, F.J.; AND GEIGENBERGER, P. Thioredoxin *f1* and NADPH-dependent thioredoxin reductase C have overlapping functions in regulating photosynthetic metabolism and plant growth in response to varying light conditions. **Plant Physiology**, v. 169, n. 3, p. 1766–1786, 2015.

VITORELLO, V.A.; CAPALDI, F.R.; STEFANUTO, V.A. Recent advances in alumium toxicity and resistance in higher plants. **Brazilian Journal of Plant Physiology,** v. 17, p.129–143, 2005.

VON UEXKÜLL, H. R.; MUTERT, E. Global extent, development and economic impact of acid soils. **Plant and Soil,** v. 171, p. 1–15, 1995.

WAGNER, S.; STEINBECK, J.; FUCHS, P.; LICHTENAUER, S.; ELSÄSSER, M.; SCHIPPERS, J.H.M.; NIETZEL, T.; RUBERTI, C.; VAN AKEN, O.; MEYER, A.J.; VAN DONGEN, J.T.; SCHMIDT, R.R.; SCHWARZLÄNDER, M. Multiparametric real-time sensing of cytosolic physiology links hypoxia responses to mitochondrial electron transport, **New Phytologist.** v. 224 p. 1668–1684, 2019.

WANG, Y.; LI, R.; LI, D.; JIA, X.; ZHOU, D.; LI, J.; LYI, S.M.; HOU, S.; HUANG, Y.; KOCHIAN, L.V.; LIU, J. NIP1; 2 is a plasma membrane-localized transporter mediating aluminum uptake, translocation, and tolerance in *Arabidopsis*. **Proceedings of the National Academy of Sciences**, v. 114, n. 19, p. 5047-5052, 2017.

WILLEMS, P.; MHAMDI, A.; STAEL, S.; STORME, V.; KERCHEV, P.; NOCTOR, G.; GEVAERT, K.; BREUSEGEM, F. The ROS Wheel: Refining ROS Transcriptional Footprints, **Plant Physiology**, v. 171, n. 3, p. 1720–1733, 2016.

YAMAMOTO, Y.; KOBAYASHI, Y.; DEVI, S. R.; RIKIISHI, S.; MATSUMOTO, H. Aluminum Toxicity Is Associated with Mitochondrial Dysfunction and the Production of Reactive Oxygen Species in Plant Cells. **Plant Physiology,** v. 128, n. 1, p. 63–72, 2002.

YAN, L.; RIAZ, M.; LIU, J.; YU, M.; CUNCANG, J. The aluminum tolerance and detoxification mechanisms in plants; recent advances and prospects. **Critical Reviews in Environmental Science and Technology,** v. 52, p. 1491-1527, 2022.

YOSHIDA, K.; HARA, S.; HISABORI, T. Thioredoxin selectivity for thiol-based redox regulation of target Proteins in Chloroplasts**. Journal of Biological Chemistry**, v. 290, n. 23, p. 14278–14288, 2015.

ZHANG, F.; YAN, X.; HAN, X.; TANG, R.; CHU, M.; YANG, Y.; YANG, Y.H.; ZHAO, F.; FU, A.; LUAN, S.; LAN, W. A defective vacuolar proton pump enhances aluminum tolerance by reducing vacuole sequestration of organic acids. **Plant Physiology**, v. 181, n. 2, p. 743-761, 2019.

ZHANG, H.; ZHU, J.; GONG, Z.; ZHU, J.K. Abiotic stress responses in plants. **Nature Reviews Genetics,** v. 23, n. 2, p. 104–119, 2022.

ZHANG, Z.; LIU, D.; MENG, H.; LI, S.; WANG, S.; XIAO, Z.; SUN, J.; CHANG, L.; LUO, K.; LI, N. Magnesium alleviates aluminum toxicity by promoting polar auxin transport and distribution and root alkalization in the root apex in populus. **Plant and Soil**, v. 448, p. 565-585, 2020.

ZHONGJIE, L.; ZHENG, T.; ZHENGYU, Y.; XINYING, Y.; RUI, D. Comparative transcriptomic analysis reveals coordinated mechanisms of different genotypes of common vetch root in response to Al stress. **Environmental and Experimental Botany**, v. 213, p. 105450, 2023.

ZHU, X.F.; SHI, Y.Z.; LEI, G.J.; FRY, S.C.; ZHANG, B.C.; ZHOU, Y.H.; BRAAM, J.; JIANG, T.; XU, X.Y.; MAO, C.Z.; PAN, Y.J. XTH31, Encoding an *in vitro* XEH/XET-Active enzyme, regulates aluminum a sensitivity by modulating in vivo XET action, cell wall xyloglucan content, and aluminum binding capacity in *Arabidopsis*. **The Plant Cell,** v. 24, n. 11, p. 4731–4747, 2012.

ZHU, X.F.; LEI, G.J.; WANG, Z.W.; SHI, Y.Z.; BRAAM, J.; LI, G.X.; ZHENG, S.J. Coordination between apoplastic and symplastic detoxification confers plant aluminum resistance. **Plant Physiology**, v. 162, p. 1947–1955, 2013.

CHAPTER 2: Deciphering the significance of the mitochondrial calcium uniport during leaf senescence

ABSTRACT

Plants have a flexible metabolism that helps them cope with environmental changes. Ca^{2+} signaling is directly involved in responses to environmental cues, and Ca^{2+} transient is unique and precise with specific time, duration, location, and sensing proteins, being the Ca transporters key participants in this process. Ca^{2+} regulation is mainly present in organelles and is closely related to the organelle function. In mitochondria it has been demonstrated that the mitochondrial calcium uniporter (*MCU*), which is Ca^{2+} influx transporter, is the main route for rapid Ca^{2+} influx into the matrix, therefore it modulates Ca responses within this organelle. Accordingly, triple knockout mutants of *MCU* (*mcu123*) showed reduced Ca levels in the mitochondrial matrix, while mutants for the *MCU* regulator, the EF-hand *MICU* (*micu*) were characterized by a disturbance with higher matrix Ca levels. When exposed to darkness the *mcu123* showed a delay in chlorophyll degradation, not observed for *micu* mutant plants. During dark-induced senescence, mitochondria are known to participate in nutrient remobilization. Interestingly, the mitochondrial enzyme glutamate dehydrogenase (GDH2) presents a predicted EF-hand motif, that could be affected by the Ca^{2+} levels inside the matrix. Moreover, it is a central enzyme in resource remobilization during dark, connecting carbon and nitrogen metabolism. Here, we investigate the possible regulation by Ca^{2+} of the matrix enzyme GDH2 through the predicted EF-hand motif as a reasonable connection between the delayed chlorophyll degradation and the lower mitochondrial Ca^{2+} matrix levels found in the *mcu123*. Our data showed that during the dark-induced senescence, Ca^{2+} levels drop in the mitochondria and cytosol, as do the expression levels of the *MCU*s. However, the results obtained here cannot unequivocally demonstrate the regulation of GDH2 by Ca^{2+}, and thus it remains unclear why *mcu123* mutant plants were characterized by lower chlorophyll degradation upon dark-induced senescence.

INTRODUCTION

To cope with environmental and developmental stimuli plants present a flexible metabolism, being able to adjust cell physiology (ZANDALINAS et al., 2022). One important strategy that allows a remarkable number of different responses to these stimuli is calcium (Ca^{2+}) signaling, possible due to the modulation of intracellular Ca^{2+} (KUDLA et al., 2018). Accordingly, Ca^{2+} signaling is directly involved in abiotic stress responses such as heat (KANG et al., 2023), cold (YUAN et al., 2018) and salt (MANISHANKAR et al., 2018), also mediates biotic interactions from pathogen attack (TIAN et al., 2019) to symbiosis (KOSUTA et al., 2008). The specificity of each Ca^{2+} signal is obtained through the precise modulation of time, duration, and location of these Ca^{2+} transients, and their combination with specific sensing proteins (ELÍES et al., 2020). Plants have several well elucidated Ca^{2+} responders, such as calmodulin (CaM) and CaM-like; calcineurin-B-like (CBL) and CBL-interacting protein kinase (CIPK); and Ca^{2+} dependent protein kinases (CDPK/CPK) (KUDLA et al., 2018). Ca^{2+} signaling also needs the channels that will mediate the Ca^{2+} transients between cellular compartments possible (KONG et al., 2020), those include cyclic nucleotide-gated channels (CHARPENTIER et al., 2016), reduced hyperosmolarity-induced Ca^{2+} increase channels (OSCAs) (HOU et al., 2014), touch sensing Ca^{2+} channel (NAKAGAWA et al., 2007) and glutamate receptor-like channels (TOYOTA et al., 2018).

It has been demonstrated that the main Ca^{2+} regulation process occurs in organelles, especially vacuole, endoplasmic reticulum (ER), chloroplasts, peroxisomes, and mitochondria (STAEL et al., 2012). In those, the organelle functions show a close connection with the Ca^{2+}-dependent proteins (RESENTINI et al., 2021). In the mitochondria matrix, the free Ca^{2+} concentrations are slightly higher than the cytosolic one (LOGAN & KNIGHT, 2003), and the Ca^{2+} transients have an exclusive signature, even though they follow the cytosolic Ca^{2+} transients (LORO et al., 2012; RUBERTI et al., 2022). Plants have the mitochondrial Ca^{2+} uniporter (*MCU*), and a homolog of animals' matrix influx channel specialized Ca^{2+} uniporter complexes (*MCUC*) (TEARDO et al., 2017). The *Arabidopsis thaliana* MCU system was shown to be the dominant protein to control the *in vivo* matrix rapid Ca^{2+} uptake (RUBERTI et al., 2022). MCU channels do not have a common amino acid sequence similarity with other Ca^{2+} transporters, it has a pore region with many negatively charged amino acids that are indispensable for the Ca^{2+} transport (De STEFANI et al., 2011). It is a 40kDa protein active in the inner mitochondrial membrane lipid bilayers, and the pore is formed by transmembrane domains organized in tetramers (De STEFANI et al., 2011). MCU homologs in other plant

species have been described, such as maize (MENG et al., 2015) and potato (WAGNER et al., 2015). Specific in Arabidopsis it was found six homologues (MCU 1 – 6), predicted to mitochondria (EMANUELSSON et al., 2000). This number of homologies within the same plant can provide a more flexible regulatory system for gene expression, from transcription, translation, and post-translational levels (STAEL et al., 2012). Also regulating MCU activity, the EF-hand protein MICU acts as a "lid" for the pore formation of MCU (WAGNER et al., 2016). MICU proteins are in the mitochondrial inner membrane, and they can negatively regulate the Ca^{2+} uptake, through the inhibitory function of MCU (WAGNER et al., 2015). MCU triple knockout mutants were generated to overcome redundancy between MCU family members, combining MCU1, MCU2, and MCU3 (*mcu123*) (RUBERTI et al., 2022). Such plants did not present an apparent phenotype, having size and development similar to the wild type (Col-0); however, such plants have lower levels of Ca in the mitochondrial matrix at rest (RUBERTI et al., 2022). Accordingly, MICU knockout mutants (*micu*) deregulated mitochondrial Ca^{2+} transients, once they presented higher Ca levels in the resting mitochondrial matrix (WAGNER et al., 2015). This demonstrates that it is possible to regulate Ca levels in the mitochondrial matrix, regulating the function or quantity of transporters, and such mutations did not lead to drastic phenotypic consequences in both cases (WAGNER et al., 2015; RUBERTI et al., 2022).

Due to mitochondria ability to rapidly and transiently accumulate Ca^{2+}, it underpins part of the intracellular Ca^{2+} regulation (DRAGO et al., 2012). Thus, mitochondria play a key role in the cellular responses to environmental and intracellular stimulus, not only by providing ATP but being active in the Ca^{2+} activities, allowing it to control essential processes within organelles as well as the entire cell (WAGNER et al., 2016). One process that affects the whole cell is senescence, which in plants can be prematurely imposed by dark (BUCHANAN-WOLLASTON et al., 2002). During dark-induced senescence (DIS) mitochondria go under multiple metabolic adjustments, mainly to allow nutrient recycling and remobilization (DIAZ et al., 2008). Keech et al., (2007) identified different patterns for chloroplasts and mitochondria during DIS, where mitochondria were strongly affected, presenting changes in the dimensions and volume. In this work, it was proposed that when the whole Arabidopsis rosettes are kept in darkness its metabolism enters a "stand-by" mode, where less mitochondria respiration was observed, as less degradation of chloroplasts and mitochondria itself. While for the treatment with only one leaf darkened the responses were rather different, in that case, the chloroplasts were degraded before mitochondria coupled with higher respiration rates, even higher than the

light control, suggesting that mitochondria directly participate in the efficient remobilization of nutrients (KEECH et al., 2007).

One enzyme that can be directly related to resource remobilization is glutamate dehydrogenase (GDH), as it is the link between nitrogen and carbon metabolism (GRZECHOWIAK et al., 2023). GDH is responsible for the oxidative deamination of glutamate (Glu) to 2-oxoglutarate (2OG), but it can also work in the opposite direction catalyzing the reductive amination (2OG → Glu) (LEA, 1993). GDH has different isoforms, that can be found in mitochondria and chloroplasts (FONTAINE et al., 2012). It is important to notice that all kingdoms of life have the GDH enzyme, however, its evolution is divergent (GRZECHOWIAK et al., 2020). For most plant species the GDH is NAD-dependent and can be encoded by different genes, that form different subunits (TURANO et al., 1997). In Arabidopsis was identified three genes (*GDH1*, *GDH2*, *GDH3*) that encode three subunits (α, β, γ, respectively) (MARCHI et al., 2014). These subunits can form homo or hetero hexamers with approximately 270 kDa (FONTAINE et al., 2012). They can also be separated into two groups, At*GDH1* and At*GDH3* belonging to type I and At*GDH2* to type II (GRZECHOWIAK et al., 2020). Another particularity of GDH2 is the predicted EF-hand loop motif (residue region 265DFNGGDAMNSDEL277) (TURANO et al., 1997; WAGNER et al., 2016). This predicted EF-hand is not present in GDH1 or GDH3 (TURANO et al., 1997) and even though there are some GDHs shown to be activated by calcium in other species, such as peas (*Pisum sativum* L.) (KINDT et al., 1980) and corn maize (*Zea mays*) (YAMAYA et al., 1984) it is not clear if this activation has physiological significance for Arabidopsis and if it is happening through the EF-hand predicted motive (GRZECHOWIAK et al., 2023). It should be noted that previous works related the GDH2 with a potential central participation in amino acid breakdown during dark treatments to supply the carbon skeletons to the mitochondria respiratory pathway (MIYASHITA et al., 2008).

Here, we attempted to enhance our understanding of the delay in chlorophyll degradation upon darkness, showed by mutants in the *MCU* family (previously reported by RUBERTI et al., 2022) and their possible correlation with the predicted EF-hand motif of GDH2. For that, we worked with *Arabidopsis thaliana* with differential mitochondrial matrix Ca^{2+} levels, from the less Ca^{2+} the triple *MCU* knockout line of *MCU1*, *MCU2*, and *MCU3* (*mcu123*), to more Ca^{2+} the knockout *MICU* line that negatively regulate the *MCU*s and the overexpression line *MCU2* OE. We evaluate their chlorophyll degradation upon dark-induced senescence, via a single darkened leaf (SDL) and only the less Ca^{2+} plants showed a phenotype.

Therefore, we further investigate the connection between nitrogen and carbon metabolism, which is essential for resource remobilization, and mainly related to mitochondria. We next explored the potential regulation by Ca^{2+} of the matrix enzyme *GDH2* through the predicted EF-hand motif as a reasonable connection between the delayed chlorophyll degradation and the lower levels of matrix Ca^{2+}. We also investigated the calcium levels in the matrix and the expression of *MCU*s and senescence markers during the SDL. It was possible to notice that the Ca levels for cytosol and mitochondria dropped during dark treatment as did the *MCU* expression; by contrast, the senescence marks were upregulated. Although our findings did not demonstrate a clear correlation between the lack of a mitochondrial Ca^{2+} uptake system and the delayed chlorophyll degradation in SDL, it seems reasonable to suggest that the *Arabidopsis thaliana GDH2* is seemingly not calcium-regulated.

MATERIAL AND METHODS

Plant materials

All genotypes of *Arabidopsis thaliana* plants used in this study are described in Table 1. All mutant plants have Columbia (Col-0) ecotype as background. All sensor lines were generated via *Agrobacterium tumefaciens* mediated transformation via floral dip (CLOUGH & BENT, 1998) and kindly provided by Plant Energy Biology Lab (Münster, Germany).

Table 1. *Arabidopsis thaliana* genotypes used in this study.

Plant line	Mutation	Sensor	Collection	Reference
Col-0	-	-		
mcu1	T-DNA insertion mutant in the *MCU1* gene (At1g09575)	-	SALK 082151	TEARDO et al., 2017
mcu2	T-DNA insertion mutant in the *MCU2* gene (At1g57610)	-	WiscDsLox 393-396L9	SELLES et al., 2018
mcu3	T-DNA insertion mutant in the *MCU3* gene (At2g23790)	-	SALK 019312	RUBERTI et al., 2020
mcu12	Double mutant generated by crossing *mcu1 mcu2*	-	-	RUBERTI et al., 2021
mcu13	Double mutant generated by crossing *mcu1 mcu3*	-	-	RUBERTI et al., 2022
mcu23	Double mutant generated by crossing *mcu2 mcu3*	-	-	RUBERTI et al., 2023
mcu123	Triple mutant generated by crossing *mcu1 mcu2 mcu3*	-	-	RUBERTI et al., 2024
micu	T-DNA insertion mutant in the MCU1 gene (At4g32060)	-	SALK 064052	ALONSO et al., 2003

pif-621	Point mutation (G/C to A/T) within *PIF5* gene (At3g59060)	-	EMS mutated seeds	LIEBSCH et al., 2022
Col-0	-	Citosolic (NES) **YC 3.6** (Ex = 400 ± 5 and 482 ± 16 nm/Em = 520 ± 10 nm)	-	-
mcu123	Triple mutant generated by crossing *mcu1 mcu2 mcu3*	Citosolic (NES) **YC 3.6** (Ex = 400 ± 5 and 482 ± 16 nm/Em = 520 ± 10 nm)	-	RUBERTI et al., 2024
micu	T-DNA insertion mutant in the MCU1 gene (At4g32060)	Citosolic (NES) **YC 3.6** (Ex = 400 ± 5 and 482 ± 16 nm/Em = 520 ± 10 nm)	-	WAGNER et al., 2015
Col-0	-	Mitochondrial (4mt) **YC 3.6** (Ex = 400 ± 5 and 482 ± 16 nm/Em = 520 ± 10 nm)	-	
mcu123	Triple mutant generated by crossing *mcu1 mcu2 mcu3*	Mitochondrial (4mt) **YC 3.6** (Ex = 400 ± 5 and 482 ± 16 nm/Em = 520 ± 10 nm)	-	RUBERTI et al., 2024
micu	T-DNA insertion mutant in the MCU1 gene (At4g32060)	Mitochondrial (4mt) **YC 3.6** (Ex = 400 ± 5 and 482 ± 16 nm/Em = 520 ± 10 nm)	-	WAGNER et al., 2015
MCU2 OE	*T-DNA insertion 35S:MCU2 (*MCU2 *gene - At1g57610)* BASTA selection	-	-	RUBERTI et al., 2023
MCU2 OE	*T-DNA insertion 35S:MCU2 (*MCU2 *gene - At1g57610)* BASTA selection	Mitochondrial (4mt) **YC 3.6** (Ex = 400 ± 5 and 482 ± 16 nm/Em = 520 ± 10 nm)	-	RUBERTI et al., 2024
gdh1	T-DNA insertion mutant in the *GDH1* gene (At5g18170)	-	SALK 042736	MIYASHITA & GOOD, 2008
gdh2	T-DNA insertion mutant in the *GDH2* gene (At5g07440)	-	SALK 102711	MIYASHITA & GOOD, 2008
gdh3	T-DNA insertion mutant in the GDH2 gene (At3g03910)	-	SALK 07617	FONTAINE et al., 2012
gdh12	Double mutant generated by crossing gdh*1* gdh2	-		
gdh13	Double mutant generated by crossing gdh*1* gdh*3*	-		
gdh123	Triple mutant generated by crossing gdh*1* gdh*2 gdh3*	-		

Experimental conditions and chlorophyll quantification

Seeds were surface-sterilized and vernalized at 4º C for 72 h. Then it was placed on soil (VMV 800, Classic Profisubstrat, Einheitserde®) previously sterilized at 80° C for two hours. The soil was humidified and placed in 0.1 L pots. The trays containing the pots were covered with a clear plastic dome, that was removed after 2 weeks. The trays were transferred to growth cabinets under short-day conditions (8 h/16 h of light/dark irradiance of 150 µmol photons m^{-2}. s^{-1}, temperature of 20 ± 2 °C and humidity kept at 70 ± 5%. Plants were watered every three to four days by adding tap water to the tray.

After 49 days the single darkened leaf (SDL) senescence was induced according to Keech et al. (2007). Briefly, SDL was imposed by covering the 7th leaf with 'mittens' made with a black plastic bag and covered with aluminum foil to reduce heat, whereas the rest of the plant remained in light and the 6th leaf was used as the light leaf control in the assays. Leaves were kept in the dark for 2, 3, 4, 7, or 10 days, depending on the analyses. For chlorophyll quantification, samples of the light and darkened leaves were harvested and flash-frozen in liquid nitrogen. Methanolic extraction was performed by rapid grinding in liquid nitrogen and the immediate addition of methanol. Chlorophyll determination was performed using a spectrophotometer (653 and 666 nm) according to Wellburn, (1994).

Phylogenetic analysis of *GDH2*

Protein sequences of representative plant species, with commercial and scientific importance (Tab. 2) were retrieved from http://phytozome.jgi.doe.gov using *Arabidopsis thaliana* GDH2 (UniProt identifier Q38946) as query sequence. Following manual curation, sequences were aligned with CLUSTAL_W in MEGAx software with default parameters and clustered in an unrooted maximum likelihood. Bootstrap values (on nodes) were calculated using 500 replicates. EF-hand motif prediction site was checked using the same protein sequences used for the alignment in the online software *ScanProsite* tool.

Table 2. The GDH2 sequence information used for phylogenetic analysis. Values written after each species show similarity in percentage with *A. thaliana* GDH2. The EF-hand calcium-binding domain, if positively predicted by the ScanProsite tool, is marked in orange.

Organism	Protein Sequence	Predict EF-hand
Arabidopsis thaliana	MNALAATNRNFRHASRILGLDSKIERSLMIPFREIKVECTIPKDD GTLVSYIGFRVQHDNARGPMKGGIRYHPEVDPDEVNALAQLMT WKTAVADIPYGGAKGGIGCSPRDLSLSELERLTRVFTQKIHDLIG IHTDVPAPDMGTNAQTMAWILDEYSKFHGHSPAVVTGKPIDLG GSLGREAATGRGVVFATEALLAEYGKSIQGLTFVIQGFGNVGT WAAKLIHEKGGKVVAVSDITGAIRNPEGIDINALIKHKDATGSL NDFNGGDAMNSDELLIHECDVLIPCALGGVLNKENAGDVKAKF IVEAANHPTDPDADEILSKKGVIILPDIYANAGGVTVSYFEWVQN IQGFMWEEEKVNLELQKYMTRAFHNIKTMCHTHSCNLRMGAF TLGVNRVARATQLRGWEA	Yes
Capsella rubella (91.6%)	MNALAATNRNFRHASRILGLDSKIEKSLMIPFREIKVECTIPKDD GTLVSYIGFRVQHDNARGPMKGGIRYHPEVDPDEVNALAQLMT WKTAVADIPYGGAKGGIGCSPRDLSLSELERLTRVFTQKIHDLIG IHTDVPAPDMGTNAQTMAWILDEYSKFHGHSPAVVTGKPIDLG GSLGREAATGRGVVYATEALLAEYGKSIEGLTFVIQGFGNVGT WAAKLIHEKGGKVVAVSDITGAVRNPEGIDINALLKHKDATGSL NDFTGGDAMNSDELLIHECDVLIPCALGGVLNKDNAGDVKAKF IIEAANHPTDPDADEILSKKGVIILPDIYANAGGVTVSYFEWVQNI QGFMWEEEKVNLELQKYMTRAFHNIKTMCHTHSCNLRMGAFT LGVNRVARATQLRGWEA	-

Brassica oleracea (75%)	MPQIQNHHPLSLSLSLSSPTNTLPFLLLSSSHQLSNQSDSNPLFDH FDSISCVIFSISAAMNALAATNRNFRHASRILGLDSKIERSLMIPFR EIKVECTIPKDDGTLVSFIGFRVQHDNARGPMKGGIRYHPEVDP DEVNALAQLMTWKTAVADIPYGGAKGGIGCNPRDLSLSELERL TRVFTQKIHDLIGIHTDVPAPDMGTNAQTMAWILDEYSKFHGHS PAVVTGKPIDLGGSLGREAATGRGVVYATEALLAEYGKSIQGLT FVLQGFGNVGTWAAKLIHEKGGKVVAVSDITGAVRNPEGIDIN ALLKHKDATGSLKDFSGGDAMDSEELLLHECDVLIPCALGGVL NKENAGDVKAKFIIEAANHPTDPDADEILSKKGVIILPDIYANAG GVTVSYFEWVQNIQGFMWEEEKVNLELQKYMTRAFHNIKSMC HTHSCNLRMGAFTLGVNRVARATQLRGWEA	Yes
Nicotiana tabacum (83.33%)	MNALAATNRNFRQAARILGLDSKLEKSLLIPFREIKVECTIPKDD GTLVSYVGFRVQHDNARGPMKGGIRYHPEVDLDEVNALAQLM TWKTAVADIPYGGAKGGIGCKPKDLSKSELERLTRVFTQKIHDL IGINTDVPAPDMGTNAQTMAWILDEYSKFHGHSPAIVTGKPIDL GGSLGREAATGRGVVYATEALLAEYGKNIKDLTFAIQGFGNVG AWAAKLIHERGGKVIAVSDITGAVKNPNGLDIPALLNHKEATGK LIDFSGGDVMNSDEVLTHECDVLIPCALGGVLNRENADNVKAK FIIEAANHPTDPEADEILSKKGIVILPDIYANAGGVTVSYFEWVQ NIQGFMWDEEKVNRELKKYMTKAFHKLKNMCQSHDCNLRMG AFTLGVNRVARATTLRGWEA	Yes
Glycine max (50%)	MNALAATNRNFRRAAHILGLDTKLENSLLIPFREIKVECTIPKDD GTLVSYVGFRIQHDNARGPMKGGIRYHPEVDPDEVNALAQLMT WKTAVADIPYGGAKGGIGCNPRDLSVSELERLTRVFTQKIHDLI GIQRDVPAPDMGTNSQTMAWILDEYSKFHGHSPAVVTGKPIDL GGSLGREAATGLGVIFATEALFAEYGKSISDMTFVIQGFGNVGT WAAKSIYERGGKVIAVSDISGAIRNPNGIDIPALLKHKEGNGNLK EFSGADIMDPDELLVHECDVLIPCALGGVLNKENAADVKAKFII EAANHPTDPDADEILSKKGVIILPDIYANAGGVTVSYFEWVQNIQ GFMWDEEKVNRELKKYMTKAFRNIKAMCQIHNCDLRMGAFSL GVNRVARATLLRGWEA	-
Vitis vinifera (50%)	MNALAATNRNFRHASRILGLDSKLEKSLLIPFREIKVECTIPKDD GSLATYVGFRVQHDNARGPMKGGIRYHPEVDPDEVNALAQLM TWKTAVVDIPYGGAKGGIGCTPKDLSMSELERLTRVFTQKIHDL IGTHTDVPAPDMGTNAQTMAWILDEYSKFHGHSPAVVTGKPIA LGGSLGREAATGRGVVFATEALLAQHGKSIKGLTFVIQGFGNVG SWVARLIGERGGKIIAVSDVTGAVKNQNGLDIVDLLRHKEETGC LTNFSGGDHMDPNELLTHECDVLIPCALGGVLNKENAADVKAK FIIEAANHPTDPEADEILSKKGGVILPDIYANAGGVTVSYFEWVQ NIQGFMWEEEKVNNELQKYMTKAFHNIKAMCQSHNCSLRMGA FTLAVNRVACATTLRGWE	-
Coffea arabica (41.6%)	MNALAATNRNFRQAARILGLDSKIEKSLLIPFREIKVECTIPKDD GGLVSFVGFRVQHDNSRGPMKGGIRYHPEVDPDEVNALAQLM TWKTAVADIPYGGAKGGIGCTPKELSTSELERLTRVFTQKIHDLI GINTDVPAPDMGTNAQTMAWILDEYSKFHGHSPAIVTGKPIDLG GSLGREAATGRGVVFATEALLAEHGKSIKDMTFAIQGFGNVGS WAAKLIHEKGGKVVAVSDITGGLKNPSGIDIPGLLTHKDTTGKL ANFSGGDALDPNDLLVHECDVLIPCALGGVLNRENADHVKAKF VIEAANHPTDPEADEILSKKGVIILPDIYANAGGVTVSYFEWVQN IQGFMWDEDKVNNELKKYMTRSFHNIKNMCQTHNCNLRMGAF TLGVNRVARATLLRGWEA	-
Populus trichocarpa (50%)	MNALAATNRNFRHAARILGLDSKVEKSLLIPFREIKVECTIPKDD GTLASYIGFRVQHDNARGPMKGGIRYHPEVDPDEVNALAQLMT WKSAVADIPYGGAKGGIGCNPGDLSKSELERLTRVFTQKIHDLI GVHTDVPAPDMGTNAQTMAWILDEYSKFHGHSPAVVTGKPIDL GGSLGREAATGRGVVFATEALLAEHGKSIKGLTFAVQGFGNVG SWAAKIIHERGGKVIAVSDISGAVKNPNGIDIPELIRHKESTGSLK NFQGGDSMDANELLVHECDVLIPCALGGVLNRENAADVKAKFI IEAANHPTDPEADEILAKKGVVVLPDIYANSGGVTVSYFEWVQN	-

	IQGFMWDEEQVNKTLQNYMTRAFHNIKVMCQTHDCNLRMGAF TLGVNRVARATLLRGWEA	
Tarenaya hasseleriana (75%)	*MNALAATSRNFRHAARILGLDSKIEKSLLIPFREIKVECTIPKDDGTL MSYIGFRVQHDNARGPMKGGIRYHPEVDPDEVNALAQLMTWKTAV ADIPYGGAKGGIGCSPRDLSMSELERLTRVFTQKIHDLIGIHTDVPAP DMGTNAQTMAWILDEYSKFHGHSPAVVTGKPIDLGGSLGREAATG RGVVFATQALLAEYGKSINGLTFVIQGFGNVGSWAARLIHEKGGKVI AVSDITGAVKNPDGIDIQALLKHKETTGSLTDFDGGDAMALDELLV HECDVLIPCALGGVLNRENAGDVKAKFIVEAANHPTDPEADEILSKK GVVILPDIYANAGGVTVSYFEWVQNIQGFMWEEEKVNIELQKYMTK AFHNIKSMCHSHSCNLRMGAFTLGVNRVARATLLRGWEA*	Yes
Zea mays (50%)	*MNALAATSRNFKQAAKLLGLDSKLEKSLLIPFREIKVECTIPKDDGTL ASYVGFRVQHDNARGPMKGGIRYHHEVDPDEVNALAQLMTWKTAV ANIPYGGAKGGIGCSPGDLSISELERLTRVFTQKIHDLIGIHTDVPAP DMGTNSQTMAWILDEYSKFHGYSPAVVTGKPVDLGGSLGRDAATG RGVLFATEALLAEHGKGIAGQRFVIQGFGNVGSWAAQLISEAGGKVI AISDVTGAVKNVDGLDIVQLVKHSAENKGIKGFKGGDAIAPDSLLTE ECDVLIPAALGGVINKDNANDIKAKYIIEAANHPTDPEADEILSKKGV LILPDILANSGGVTVSYFEWVQNIQGFMWDEEKVNAELRTYMTRAF GDVKQMCRSHSCDLRMGAFTLGVNRVARATVLRGWEA*	-
Oryza sativa (41.6%)	*MNALAATSRNFRQAARLLGLDSKLEKSLLIPFREIKVECTIPKDDGTL ASFIGFRVQHDNARGPMKGGIRYHPEVDPDEVNALAQLMTWKTAV AAIPYGGAKGGIGCAPGELSTSELERLTRVFTQKIHDLIGAHTDVPAP DMGTNSQTMAWILDEYSKFHGHSPAVVTGKPIDLGGSLGRDAATG RGVMYATEALLAEHGKSISGSTFVIQGFGNVGSWAARIIHEKGGKVI ALGDVTGSIRNKNGLDIPALMKHRNEGGALKDFHDAEVMDSSELLV HECDVLIPCALGGVLNRENAPDVKAKFIIEAANHPTDPEADEILAKK GVTILPDIYANSGGVIVSYFEWVQNIQGFMWDEEKVNMELHKYMNN SFQHIKAMCKSHDCNLRMGAFTLGVNRVARATLLRGWEA*	-
Triticum aestivum (41.6%)	*MNALAATSRNFRQAARLLGLDSKLEKSLLIPFREIKVECTIPKDDGTL ASFVGFRVQHDNARGPMKGGIRYHPEVDPDEVNALAQLMTWKTAV AAVPYGGAKGGIGCSPGDLSRSELERLTRVFTQKIHDLIGTHTDIPAP DMGTNSQTMAWIFDEYSKFHGHSPAVVTGKPIDLGGSLGRDAATG RGVMYATEALLAEYGKSISGSTFVIQGFGNVGSWAAQLIHEKGGKVI ALGDVSGTIRNKAGIDVPALMKHRNEGGQLKDFHGAEVMDASELL VHECDVLLPCALGGVLNRENAPEIKAKFIIEAANHPTDPEADEILTK KGVVVLPDIYANAGGVIVSYFEWVQNIQGFMWEEEKVNMELHKYM NSAFQNIKAMCKSQDCNLRMGAFTLGVNRVARATILRGWEA*	-
Sorghum bicolor (50%)	MNALAATSRNFKQAAKLLGLDSKLEKSLLIPFREIKVECTIPKDD GTLASYVGFRVQHDNARGPMKGGIRYHHEVDPDEVNALAQLM TWKTAVANIPYGGAKGGIGCSPGDLSISELERLTRVFTQKIHDLI GIHTDVPAPDMGTNSQTMAWILDEYSKFHGYSPAVVTGKPVDL GGSLGRDAATGRGVLFATEALLAEHGKGISGQRFVIQGFGNVGS WAAQLINEAGGKVIAISDVTGAVKNVNGLDIAQLVKHSAENRGI KGFNGGDAIDPNSLLTEECDVLIPAALGGVINKDNANDIKAKYII EAANHPSDPEADEILSKKGVIILPDILANSGGVTVSYFEWVQNIQ GFMWDEEKVNAELRTYMTRAFGDVKEMCRSHNCDLRMGAFT LGVNRVARATVLRGWEA	-

Amborella trichopoda (58.3%)	MNALVATSRNFRYAARILGLDSKLERSLLIPFREVKVECTIPKDD GSLVSYVGFRVQHDNARGPMKGGIRYHPEVDPDEVNALAQLM TWKTAVANVPYGGAKGGIGCNPKDLTTSELERLTRVFTQKIHD LIGINTDVPAPDMGTNSQIMAWILDEYSKFHGHSPAIVTGKPLDL GGSLGRDAATGRGVVFAMEALLAEYGKSISGLTFVIQGFGNVG SWAAQLIHEIGGKVVAVGDITGAIRNPNGIDIPALQKHKSASGSI KDFNGGDPVDMNELLLQECDVLIPCALGAVLNRENASDVKTKF IIEAANHPTDPEADEILHKKGVVILPDIYANAGGVIVSYFEWVQN IQGFMWDEKKVNRELQKYMKNSFATMKEMCETHNCNLRMGA FTLGVNRVARATLLRGWEA	-

Molecular cloning of GDH2

The coding sequence of *GDH2* was obtained from TAIR (http://arabidopsis.org) amplified, using S7 Fusion High-Fidelity DNA Polymerase (Biozym Scientific GmbH, Hessisch Oldendorf, Germany) for error-free amplification from *Arabidopsis* Col-0 cDNA (primers are listed in Table 3). Four different constructs were designed for Gateway® cloning, (i) $_{mt}$GDH2 having the mitochondrial targeting motif (MNALAATNRNFRHSRILGL, TURANO et. al 1997) and a functional predicted EF-hand motif; (ii) $_{mt}$GDH2ΔEF-hand having the mitochondrial targeting motif, but the G**A**T that synthesizes for the first aspartate (D) was changed into a G**C**T to an alanine (A), via KDL reaction, that did not interfere in the protein function and folding, but made the EF-hand to not be predicted anymore, tested in the *ScanProsite* tool; (iii) GDH2 without the mitochondrial targeting and with a regular functional EF-hand; and (iv) GDH2ΔEF-hand without the mitochondrial target and with the same point mutation to inactivate the EF-hand prediction. KLD-Reaction was used for an *in vitro* site-directed mutagenesis. Primers were designed in NEBaseChanger (https://nebasechanger.neb.com/). Then the PCR product was purified using a PCR Clean-up Kit (Macherey-Nagel) according to the manufacturer's instructions and inserted into the pDONR207 (gentamycin resistance) vector (Invitrogen, Carlsbad, CA, USA) using gateway BP-Clonase™ II (Invitrogen) according to the manufacturer's instructions. Later, the cloned constructs were transferred into the expression vector pETG10a by LR-Clonase™. The pETG10a is a bacterial expression vector with an N-terminal 6xHis-tag that can have its expression induced by IPTG.

Table 3. Primers used for GDH2 construct cloning. All gateway primers (Gtw) are already with the attL for binding in the pDONR207. In the forward primer for the non-mitochondrial target cloning and ATG was artificially added.

Primer	Sequence
mtGDH2_Gtw_Fwrd	GGGGACAAGTTTGTACAAAAAAGCAGGCTTCATGAATGCTTTAGCTGCAAC

mtGDH2_Gtw_Rev	GGGGACCACTTTGTACAAGAAAGCTGGGTTTTAAGCTTCCCAACCACG
GDH2_Gtw_Fwrd	GGGGACAAGTTTGTACAAA AAAGCAGGCTTCATGGATTCGAAGATCGAGAGA
GDH2_Gtw_Rev	GGGGACCACTTTGTACAAGAAAGCTGGGTTTTAAGCTTCCCAACCACG
ΔEF-hand_KDL_Fwrd	AGTCTCAATGcTTTCAATGGTGGAG
ΔEF-hand_KDL_Rev	TCCAGTTGCGTCCTTGTG

Protein expression and purification

Following the cloning process the constructs were transformed into the expression *Escherichia coli BL21 (DE3) Rosetta.* Transformation was performed in competent cells via heat shock. After the selection of the transformed strains, it was cultured in liquid LB, and the expression of (i) His:$_{mt}$GDH2; (ii) His:$_{mt}$GDH2ΔEF-hand; (iii) His:GDH2; and (iv) His:GDH2ΔEF-hand was induced with 0.1 mM isopropyl-β-thiogalactopyranoside (IPTG) for 16 h at 20°C. Cells were pelleted by centrifugation for protein purification. All steps in protein isolation were performed on ice. A nickel-NTA column (HiTrapTM Chelating HP, Cytiva Europe GmbH, Freiburg, Germany) was used for protein isolation of the protein construct that could bind to the nickel-loaded chromatography column via the 6xHis-tag. The column was washed with an imidazole gradient to elute the protein. To store the protein long-term, a ZebraTM Desalting Column (Thermo Fisher Scientific, Schwerte, Germany) was used according to the manufacturer's instructions. After, an SDS-Page gel was performed to confirm the protein purity and extraction. To measure protein concentration, a NanoDrop spectrophotometer was used.

Enzymatic GDH2 assay

The *in vitro* amination of glutamate activity of GDH2, purified from the cloning constructs, was determined spectrophotometrically, monitoring the NADH evolution, adapted from Sarasketa et al., (2015). Briefly, in a 96 well plate, 20µL of the purified enzyme (at 300ng/µL) was added to a 280 µL of reaction buffer (100 mM Tricine, pH 8, adjusted with KOH, 50 mM $(NH_4)_2SO_4$, 0.25 mM NADH and 13 mM 2-Oxoglutarate). After the establishment of a linear phase (i), 1mM of $CaCl_2$; (ii) 5mM of EGTA; or ddH_2O were added to the reaction well. The NADH kinetic consumption was monitored at 340 nm in the spectrophotometer for 20 min at 30 °C.

RNA extraction and RT–qPCR analysis

Total RNA was extracted from the light and darkened harvest leaves of Col-0, *mcu123,* and *MCU2*OE in the 0, 2, 4, or 7 days after the dark imposing using a NucleoSpin RNA Plant

kit, treated with DNase I (both from Macherey-Nagel, Düren, Germany). RNA integrity was checked with agarose gel and quantified in a NanoDrop spectrophotometer. 500 ng of RNA was reverse transcribed using an iScript cDNA Synthesis Kit (BioRad, Hercules, CA, USA) following the manufactory's instructions. RT–qPCR was performed with SYBR Green detection (KAPA SYBR Fast qPCR Master Mix, Roche, Mannheim, Germany) in a C1000 Touch Thermal Cycler using the CFX 96 Real-Time System (Bio-Rad, Hercules, CA, USA) and specific primers (Tab. 4). Data were analyzed using the DDCT method/comparative CT method. The transcript levels were normalized to that of the SAND family protein (SAND FP, At2g28390; CZECHOWSKI et al., 2005), and the relative expression levels for each analyzed gene were determined by comparative CT methods (SCHMITTGEN & LIVAK, 2008). The RT-qPCR analysis was performed to check the expression of the MCU genes during the SDL, the senescence-related genes (*SAG12* and *ORE1*), and to confirm the overexpression of *MCU2*, even after the dark treatment that revealed to decrease profoundly the *MCU2* expression.

Gene	Forward	Reverse	Primer Efficiency
SAND FAMILY	ATGAGGTTGCATCGGCTAAC	TTTCTGTGCACCAGCAAGAC	1.010
MCU1	CTCGTGTTCTTGACGATGCTG	CCACCTTGTCTGGGTGAAGA	1.005
MCU2	TCAACACCAACACGATTCCGA	ACAAGTGGAAGATAACGTCTTGC	1.039
MCU3	GGAGAGCAACAATGGCGATG	TCTGGTTCGTACGGCTAACG	1.005
MCU4	CGTCATGGTGATGATGAAGAAGC	GTTCGCATGGCTAACGAAGAA	0.929
MCU5	ACGCAGAGCAATCACTAAACG	CGACAATCCGGTCCGTAAGA	1.105
MICU	GACCGATCATTCCTTCTCATC	CCAGAGGACCAATAGAGAAACC	1.005
SAG12	ACAAAGGCGAAGACGCTACTTG	ACCGGGACATCCTCATAACCTG	1.380
ORE1	ACGTGCCGATGGTACAAAGGTTC	AGGTAAACCGGCTGGTTCCATTC	1.399

In vivo sensor measurement of Ca^{2+} dynamics

To monitor the steady state of Ca^{2+} levels in cytosol and mitochondria, during SDL we used genetically encoded Yellow Cameleon 3.6 (YC3.6) biosensor, for Col-0, *mcu123,* and *micu* plants. Leaf discs of the 7-week-old plants, after 0, 3, and 7 days of SDL were placed at the bottom of transparent 96-well plates filled with assay buffer (5 mM KCl, 10 mM MES, and 10 mM $CaCl^2$, Tris pH 5.8). Plates were inserted in the CLARIOstar® plate reader and pre-equilibrated to 25 °C for recording the fluorescence in the steady state. For this, the top optic was used as well as a protocol with 30 excitation flashes per well and cycle, an orbital averaging with a 3 mm diameter, and 0.1 s settling time. The excitation and emission wavelengths were adjusted to the sensor Ex = 485nm/Em = 540nm ± 10 nm. The gain settings for each wavelength and the focal height were set at the beginning of each experiment and maintained for identical

experiments. All the fluorescence intensities were recorded from the plant material and the autofluorescence from the corresponding Col-0 control without a sensor was used for background subtraction for each state of the single darkened leaf.

Confocal Laser Scanning Microscopy (CLSM)

For CLSM studies, a small leaf disc from Col-0 and *mcu123* light and darkened leaves were analysed under a ZEISS LSM 980 with Airyscan 2 Confocal Microscope (Carl Zeiss Microscopy Germany GmbH, Oberkochen, Germany). The following lasers were used for excitation: MitoTrackerTM Orange CMTMRos (30 min incubation, 1:2000 dilution): Excitation: 551 nm, emission: 560 to 590 nm. Chlorophyll autofluorescence: Excitation: 488 nm, emission above 650 nm.

Data and statistical analyses

The chlorophyll quantification measurements were subjected to ANOVA followed by Tukey's multiple-comparison posttest ($P \leq 0.05$). For the enzymatic assays, gene expression, and Ca^{2+} levels monitoring the data were analyzed with Student-t. All statistical tests were performed with GraphPad Prism 5.0 (GraphPad Software, Inc., San Diego, CA). The program was also used to plot the data as mean and standard deviation. For the analysis of the data obtained from the plate reader, the data were transferred to the data analysis software MARS (V3.32, BMG Labtech GmbH, Ortenberg, Germany). The raw data of each well with the fluorescence intensities for each channel were then exported to Microsoft Excel (2016, Microsoft Corporation, Redmond, WA, USA) for analysis. The intensities of the background or Col-0 without the sensor were used to subtract the chlorophyll autofluorescence from the corresponding intensities of each replicate at each time point. The data were $\log_{10}$-transformed.

RESULTS

Change in chlorophyll degradation can be related to the absence of *mcu* Ca^{2+} transporter

No difference was observed for the lightened leaves among genotypes and all single darkened leaves showed a massive chlorophyll degradation after 7 days (Fig. 1 B). Both *mcu123* and *pif 621* mutant plants were characterized by higher chlorophyll content after 7 days of darkness (Fig. 1 B), showing lower chlorophyll degradation. It is important to notice that all single and double mutants for *mcu* showed the same chlorophyll degradation behavior as Col-0 (Fig. 1 B; Supplemental Fig. 1), which leads us to infer that this less chlorophyll phenotype

is a cumulative effect, only happening in the triple mutant that has less calcium in the mitochondria matrix (RUBERTI et al., 2022; Fig. 2 A). Interestingly, the *micu* mutant, which was characterized by more Ca^{2+} levels in the mitochondrial matrix (WAGNER et al., 2015; Fig. 2 A), did not present an opposite effect, having a chlorophyll degradation pattern similar to Col-0 (Fig 1 A).

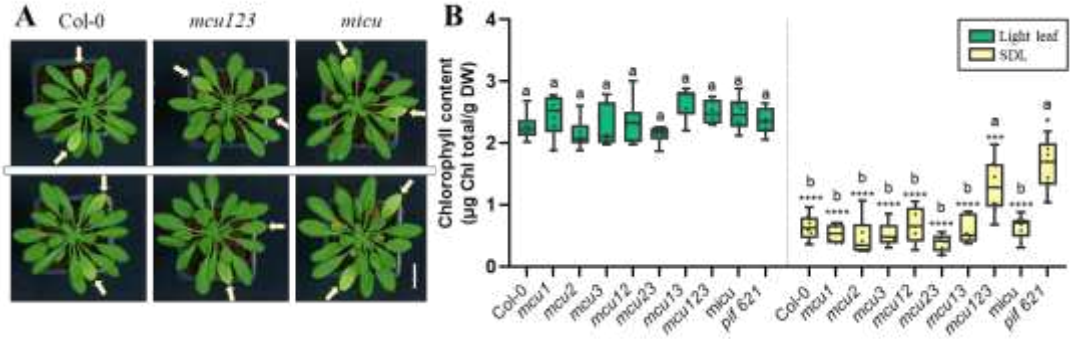

Figure 1: Phenotypic characterization of *Arabidopsis thaliana* lines during single-leaf dark-induced senescence. (A) Representative images of 7-week-old plants of wild type (Col-0), triple mutant for mitochondrial calcium uniporter (*mcu123)* and mutant for mitochondrial Ca^{2+} uptake protein (*micu*); after individually single darkened leaves (SDL) for 7 days. White arrows point to darkened leaves. (B) Chlorophyll quantification of seven-week-old *Arabidopsis thaliana* plants in the backgrounds Col-0, *mcus*, *micu,* and *pif 621* after single darkened leaves (SDL) for 7 days. Data were submitted to one-way ANOVA followed by multiple comparisons to Tukey`s test. Letters compare genotypes inside the treatment and different letters indicate significant differences ($P < 0.05$). An asterisk (*) compare an individual genotype between the two treatments. $*P < 0.05$; $**P < 0.01$; *** $P < 0.005$ $****P < 0.0001$; $N = 6\text{-}9 \pm$ SD.

Once no differences were observed for the knockout mutant plants, we next evaluated the overexpression of *MITOCHONDRIAL CALCIUM UNIPORTER 2* (*MCU2* OE). Using genetically encoded mitochondria Ca^{2+} sensors we performed an *in vivo* assay that determined the steady state of Ca^{2+} levels, where the *MUC2* OE showed clearly more matrix Ca^{2+} levels than the other genotypes (Fig. 2 A). We could also confirm that *mcu123* and *micu* have less and more Ca^{2+} levels in the mitochondria matrix, respectively (Fig. 2 A). To validate the SDL experiment with the overexpression mutants we analyzed the OE line after the darkened period (Supplemental Fig. 2), and we could confirm that even after the 7 days of the dark, the *MCU2* is still overexpressed in the OE line. When analysing the chlorophyll content, we observed the same result as in the first one, with the *mcu123* presenting a lower chlorophyll degradation (Fig. 2 B); however, the *MCU2* OE, even presenting more Ca^{2+} levels than the *micu* (Fig. 2 A), had the same pattern as Col-0 in terms of chlorophyll degradation (Fig. 2 B).

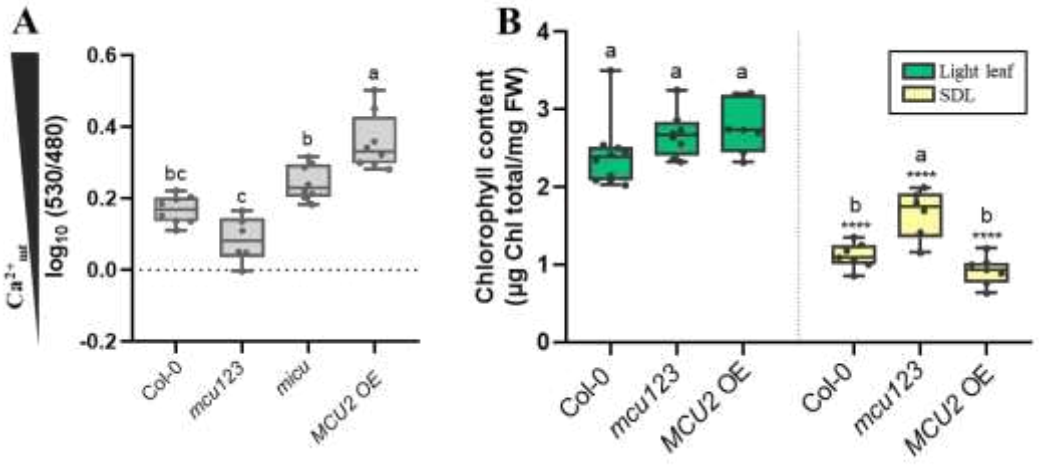

Figure 2: Phenotypic characterization of mitochondrial calcium in steady-state and chlorophyll of *Arabidopsis thaliana.* **(A)** Calcium levels in steady-state, wild-type (Col-0), *mcu123* and *MCU2 OE* expressing mitochondrial 4mt YC3.6 to monitor calcium levels in seven-week-old leaf discs. Values are displayed as mean ± SD (n = 6 – 8). All the fluorescence intensities were recorded from the plant material and the autofluorescence from the corresponding Col-0 control without the sensor was used for background subtraction. Yellow cameleon 3.6 (YC3.6): Ex = 485nm/Em = 540nm ± 10 nm. Means followed by the same letters do not have significant statistical differences according to the Tukey's test ($p<0.05$). **(B)** Chlorophyll quantification of *Arabidopsis thaliana* lines during single leaf dark-induced senescence. Seven-week-old *Arabidopsis thaliana* wide time (Col-0), *mcu123,* and *MCU2 OE #2* after single darkened leaves (SDL) for 7 days. Data were submitted to one-way ANOVA followed by multiple comparisons to Tukey`s test. Letters compare genotypes inside the treatment and different letters indicate significant differences ($P < 0.05$). An asterisk (*) compares an individual genotype between the two treatments. $*P < 0.05$; $**P < 0.01$; *** $P < 0.005$ $****P < 0.0001$; $N = 6\text{-}9 \pm$ SD.

Next, we investigate the impact of the number of days in the dark on the phenotype found for *mcu123*. After 3 days of darkness, little to no difference is observed in chlorophyll levels among all genotypes (Fig. 3). After 7 days the results are similar to what was observed here before, with only the *mcu123* mutant showing a different pattern (Fig. 3). It was possible to observe that the phenotype of less chlorophyll degradation seems to be related with a delay in the pathway since the degradation still happens in the *mcu123* mutant and after 10 days it reaches the chlorophyll levels that other evaluated genotypes had in 7 days (Fig. 3).

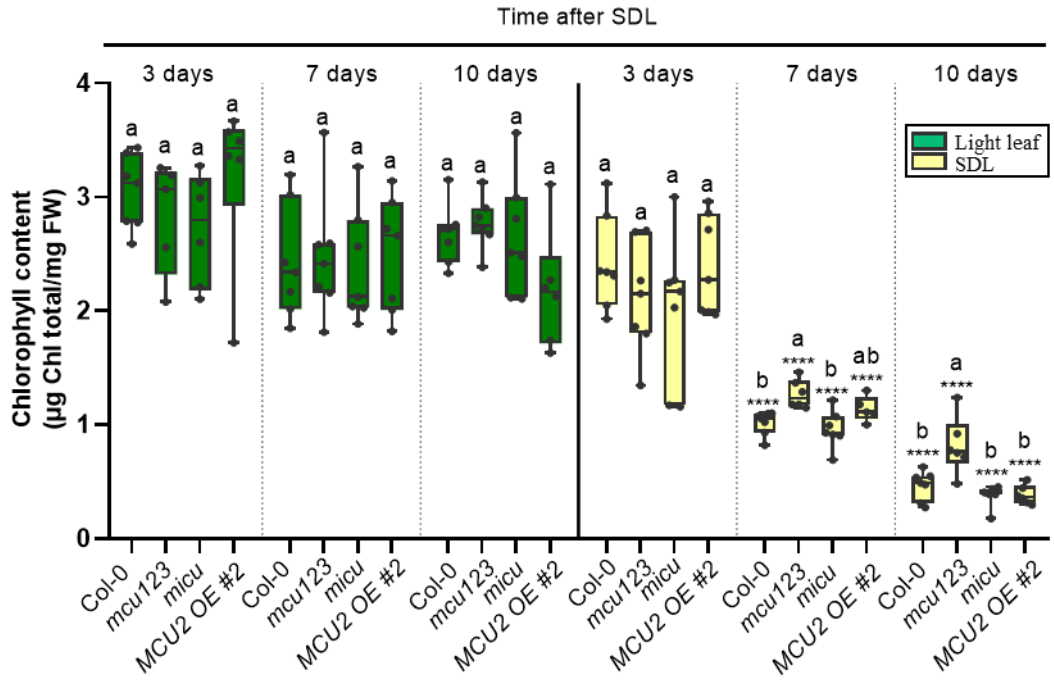

Figure 3: Chlorophyll quantification of *Arabidopsis thaliana* lines during single-leaf dark-induced senescence. Seven-week-old *Arabidopsis thaliana* wild type (Col-0), *mcu123*, *micu,* and *MCU2 OE #2* after single darkened leaves (SDL) for 7 days. Data were submitted to one-way ANOVA followed by multiple comparisons to Tukey`s test. Letters compare genotypes inside the treatment and different letters indicate significant differences ($P < 0.05$). An asterisk (*) compares an individual genotype between the two treatments. *$P < 0.05$; **$P < 0.01$; *** $P < 0.005$ ****$P < 0.0001$; $N = 6\text{-}9 \pm$ SD.

Arabidopsis thaliana GDH2 seems not to be regulated by calcium

The only mitochondrial condition that seems to lead to the delay in chlorophyll degradation is the lower calcium in the mitochondria matrix. The GDH2 is reported to be activated by calcium and bears the EF-hand calcium-activated motif, being a good candidate for one enzyme affected by the less Ca^{2+} in the matrix. It is also the mitochondrial protein that connects the carbon and nitrogen metabolism (FONTAINE et al., 2012). We built a phylogenetic tree and then checked the existence of the EF-hand motif among the species. It is possible to observe that GDH2 is highly conserved among the plant species, the monocotyledons and dicotyledons being the most separated group (Fig. 4). However, differently than what was expected, the prediction of the EF-hand motif is not abundant, even though it does not appear only in the closest group to *Arabidopsis* (Fig. 4).

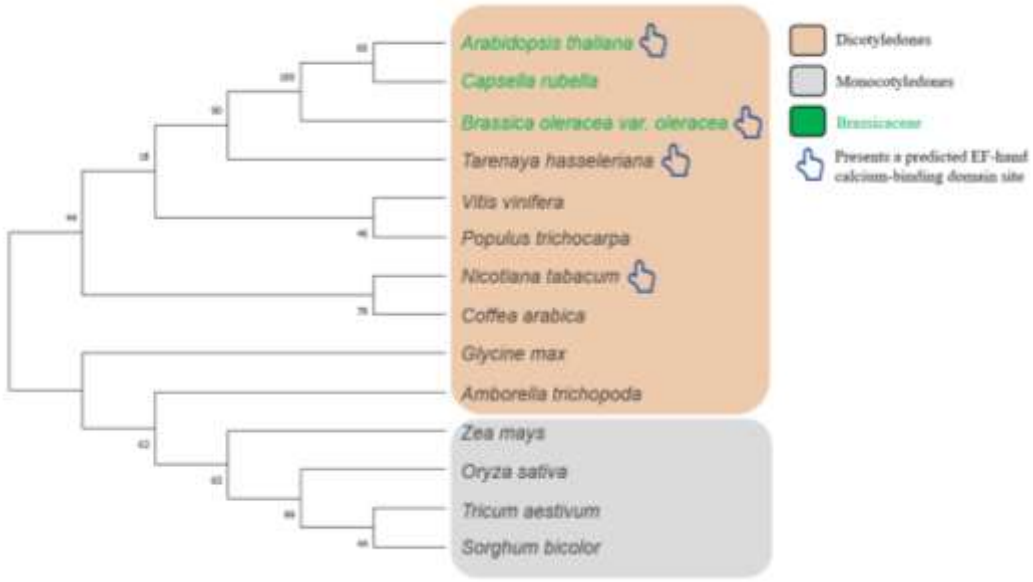

Figure 4: Phylogenetic tree of *GDH2* (glutamate dehydrogenase 2) in plants. Phylogenetic tree constructed using MEGAx software by the maximum likelihood (ML) of GDH2 homologs protein sequence from representative of commercial and scientific important plant species. Bootstrap values (on nodes) were calculated using 500 replicates. EF-hand motif prediction site was checked using the online software ScanProsite tool.

To confirm the activation of GDH2 by calcium we performed an enzymatic assay with purified GDH2 from the cloned constructs. It is possible to notice that all constructs can fulfill the reductive amination (2OG → Glu) activity (Fig. 5). No difference was observed in the reaction rate in any of the constructs after the application of Ca^{2+} (Fig. 5).

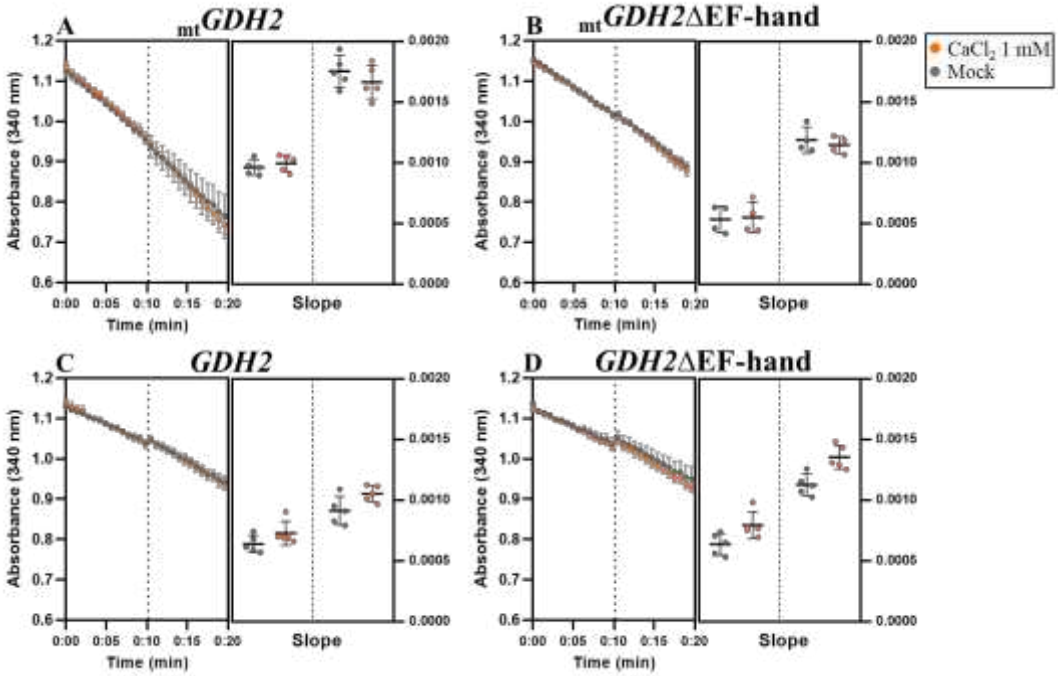

Figure 5: Enzymatic assay to determine reductive amination (2OG → Glu) activity of isolated *At*GDH2. Isolated constructs of *At*GDH2 (A) with the mitochondrial target; (B) with the mitochondrial target and a defective EF-hand motif; (C) without the mitochondrial target and (D) without the mitochondrial target and a defective EF-hand motif were used to characterize enzyme kinetics curves, responsiveness to the application of 1 mM Ca^{2+} (orange dots) after the linear phase and without adding Ca^{2+} (gray dots). The slope calculations were performed in the linear phases of the curve (NADH consumption evaluated by the absorbance in 340 nm). Data was submitted to Student-t test. An asterisk * compares an individual slope between the control and treatment. $*P < 0.05$; $**P < 0.01$; *** $P < 0.005$ **** $P < 0.0001$; $N = 4 - 6 \pm$ SD.

To continue the confirmation of the correlation between Ca^{2+} and GDH2 activity we next repeat the reductive amination activity in the presence of the potent calcium chelate EGTA (Fig. 6). Interestingly, the constructs bearing the mitochondrial target, with the functional EF-hand ($_{mt}$GDH2) and with the nonactive EF-hand ($_{mt}$GDH2ΔEF-hand) showed a decrease in the reaction rate upon EGTA application (Fig. 6 A and B), what was not observed for the constructs without mitochondrial target (Fig. 6 C and D).

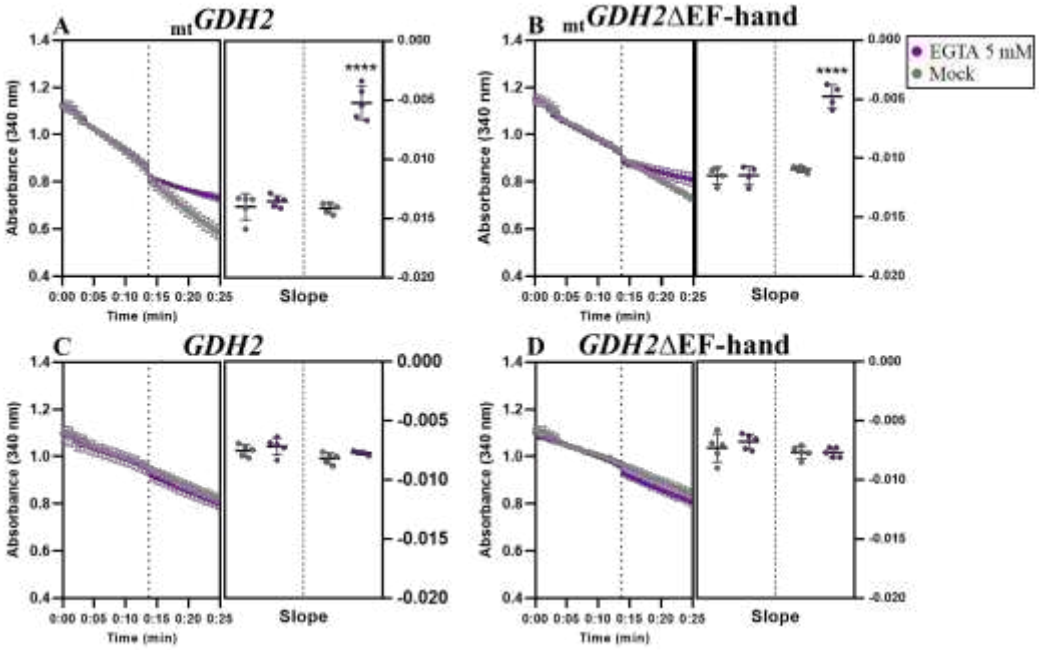

Figure 6: Enzymatic assay to determine reductive amination (2OG → Glu) activity of isolated *At*GDH2. Isolated constructs of *At*GDH2 (A) with the mitochondrial target; (B) with the mitochondrial target and a defective EF-hand motif; (C) without the mitochondrial target and (D) without the mitochondrial target and a defective EF-hand motif were used to characterize enzyme kinetics curves, responsiveness to the application of calcium ion chelator 5 mM EGTA (purple dots) after the linear phase and without adding it (gray dots). The slope calculations were performed in the linear phases of the curve (NADH consumption evaluated by the absorbance in 340 nm). Data were submitted Student-t test. An asterisk (*) compares an individual slope between the control and treatment. $*P < 0.05$; $**P < 0.01$; *** $P < 0.005$ **** $P < 0.0001$; $N = 4 - 6 \pm$ SD.

Even though the enzymatic assays did not present a positive correlation with GDH2, the predicted EF-hand motif, and Ca^{2+} activation, we performed an SDL assay to evaluate the relation between GDH and chlorophyll degradation upon dark-induced senescence. It is possible to see that the pattern of less chlorophyll degradation repeats itself once more in the

mcu123, although for the *gdh* singles, double and triple mutants, the chlorophyll degradation is similar to Col-0 (Fig. 7). That corroborates with the previous results, showing no direct relation between GDH2 and calcium levels.

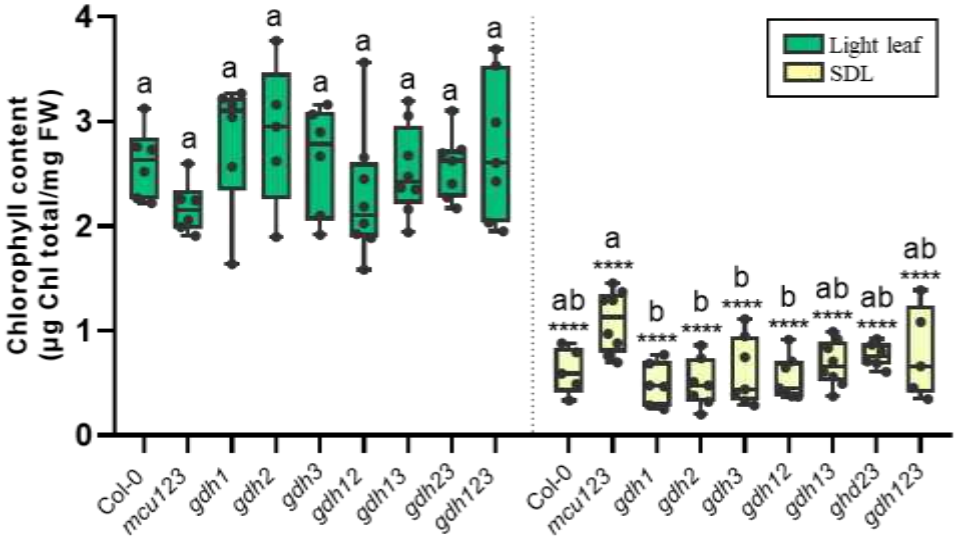

Figure 7: Phenotypic characterization of *Arabidopsis thaliana* lines during single-leaf dark-induced senescence. Chlorophyll quantification of seven-week-old *Arabidopsis thaliana* plants in the backgrounds Col-0, triple mutant for mitochondrial calcium uniporter (*mcu123),* single, double, and triple e mutants for *At*GDH1, *At*GDH2, and *At*GDH3 after single darkened leaves (SDL) for 7 days. Data were submitted to one-way ANOVA followed by multiple comparisons to Tukey`s test. Letters compare genotypes inside the treatment and different letters indicate significant differences (P < 0.05). An asterisk (*) compares an individual genotype between the two treatments. *$P < 0.05$; **$P < 0.01$; *** $P < 0.005$ ****$P < 0.0001$; $N = 6\text{-}9 \pm$ SD.

Cellular calcium levels decrease in single-darkened leaves

By using genetically encoded biosensors to cytosol and mitochondria we could monitor the Ca^{2+} levels during senescence (Fig. 8). Ca^{2+} cytosolic levels drop after the 7 days for all genotypes (Fig. 8 A-C), being this response in Col-0 the most dramatic one (Fig. 8 A). Surprisingly, the mitochondrial Ca^{2+} levels, also presented a decrease along time, that is not significant for *micu* (Fig. 8 E).

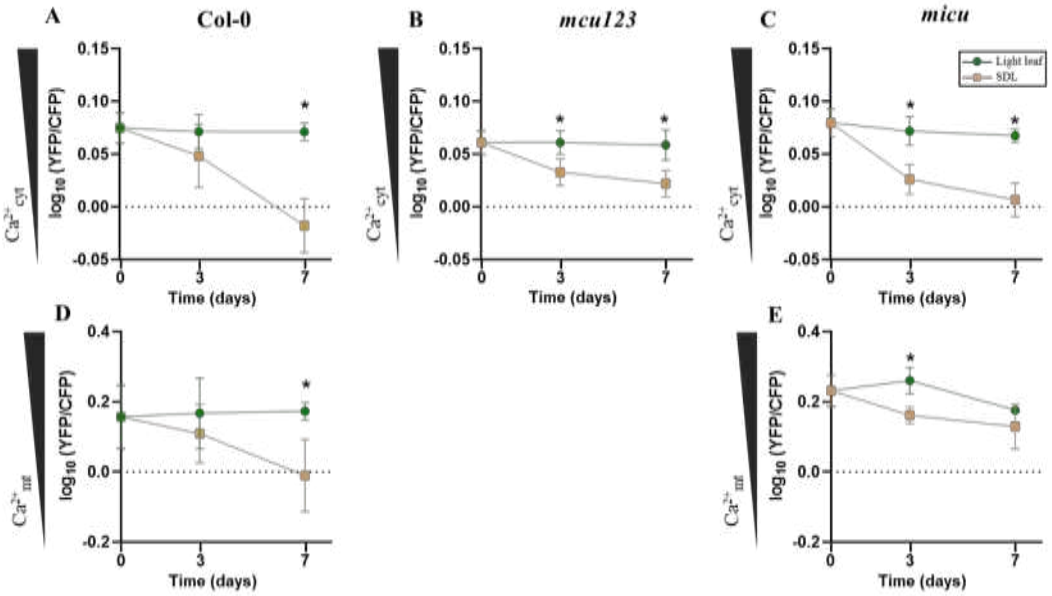

Figure 8: Phenotypic characterization of cytosolic and mitochondrial calcium in *Arabidopsis thaliana* using a single darkened leaf. **(A - C)** Cytosolic calcium and **(D – E)** mitochondrial calcium levels in, wild-type (Col-0), triple mutant for mitochondrial calcium uniporter (*mcu123)* and mutant for mitochondrial Ca^{2+} uptake protein (*micu*); expressing cytosolic and mitochondrial YC3.6 to monitor calcium levels in seven-week-old leaf discs. Values are displayed as mean ± SD (n = 6 – 8). All the fluorescence intensities were recorded from the plant material and the autofluorescence from corresponding Col-0 control without sensor was used for background subtraction for each state of a single darkened leaf (0, 3, and 7 days). Yellow cameleon 3.6 (YC3.6): Ex = 485nm/Em = 540nm ± 10 nm. An asterisk (*) indicate a significant difference comparing in the same time the light and darkened leaf as determined by Student's t-test ($P < 0.05$).

The MCU expression also decreased during the dark treatment for Col-0 (Fig. 9). We could observe that certain *MCU* are less expressed (e.g. *MCU1* and *MCU5*), even in the light, while *MCU2* and *3* are more expressed (Fig. 9). It is important to notice that for *MCU2* the expression immediately decreases after the dark is imposed, being able to see the difference in expression in the first 2 days (Fig. 9). For *MICU* expression, even though seem to have a difference in the middle of the treatment, with 4 days, does not have a significant impact in the expression after 7 days.

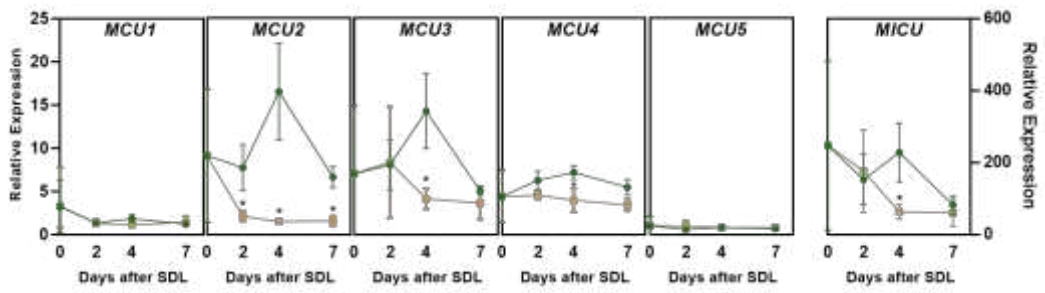

Figure 9: Relative transcript abundance of MCUs and MICU in light and single darkened leaves. Reverse transcription–quantitative PCR (RT–qPCR) analysis of *MCU1, MCU2, MCU3, MCU4, MCU5*, and *MICU* mRNA abundance in control (light leaf) and SDL leaves of 7-week-old *Arabidopsis thaliana* (Col-0) plants. Relative

expression of each gene was normalized to the *SAND* family housekeep gene. N = 4 ± SD. Asterisks * indicate a significant difference in relation to control as determined by Student's t-test (P < 0.05).

mcu123 modifies chlorophyll degradation pattern but does not delay the senescence

To investigate whether the mitochondria abundance was similar between *mcu123* and Col-0, even after the dark treatment, we did a confocal transmission imaging (Fig. 10). Corroborating our chlorophyll quantification, the amount of chlorophyll is lower in Col-0 darkened than in *mcu123* (Fig 10 E – H). The number of mitochondria seems similar for both genotypes (Fig. 10 I – L).

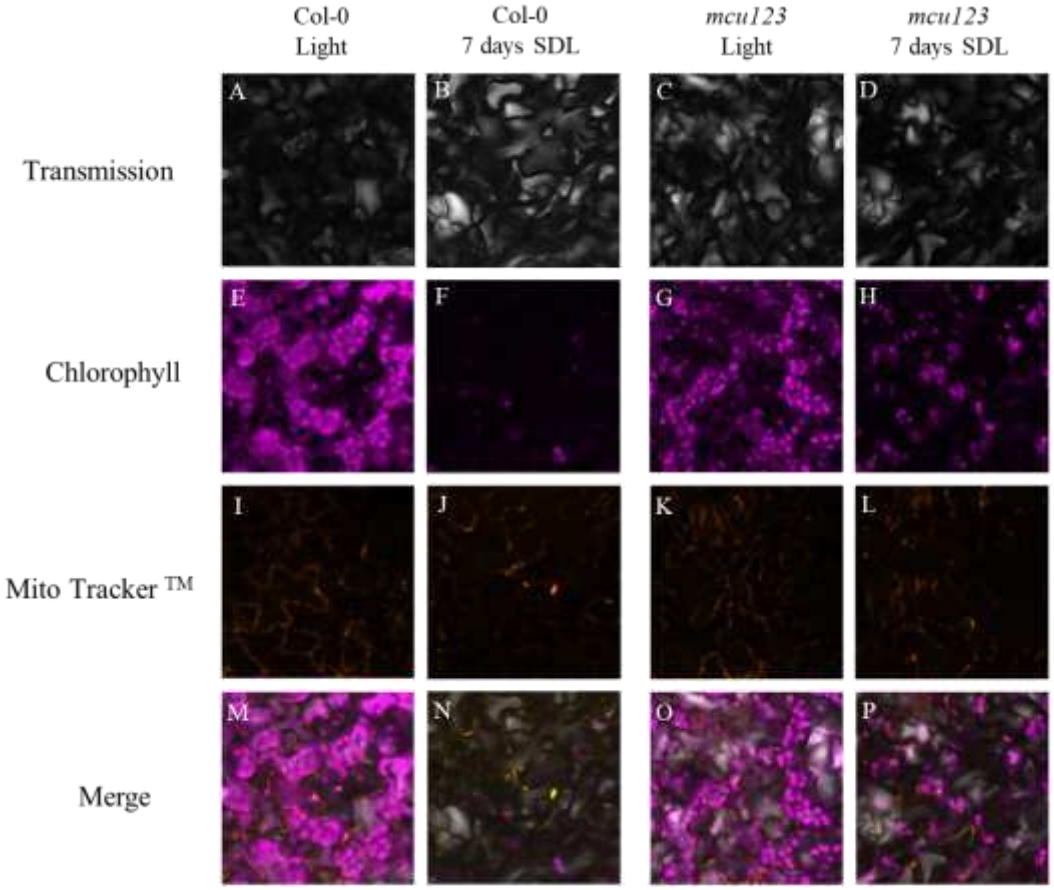

Figure 10: Transmission images of 7-week-old *Arabidopsis thaliana* mesophyll cells after 7 days of single darkened leaf. A leaf disc of 7-week-old *Arabidopsis thaliana* was taken from the wide type (Col-0) in light (A, E, I and M); after 7 days in the dark (B, F, J and N); triple mutant for mitochondrial calcium uniporter (*mcu123)* in light (C, G, K and O) and after 7 days SDL (D, H, L and P). Leaf discs were examined with the ZEISS LSM 980 with Airyscan 2 Confocal Microscope. The scale bar indicates a length of 50 µm. Zoom: 10x. MitoTracker™ Orange CMTMRos (20 min incubation, 1:2000 dilution): Excitation: 551 nm, emission: 560 to 590 nm. Chlorophyll autofluorescence: Excitation: 488 nm, emission above 650 nm.

We further evaluated the expression of senescence related genes, *SAG12* (Fig. 11 A) and *ORE1* (Fig. 11 B). Different from what was expected, even with the delay in chlorophyll degradation, usually a visual senescence marker, the *mcu123* did not show lower expression of

those genes, actually, the expression of both was higher compared to Col-0 after the treatment. It is worth highlighting that *SAG12* expression was higher than *ORE1* for lightened leaves, and for *ORE1*, the expression fold between light and dark treatment was higher.

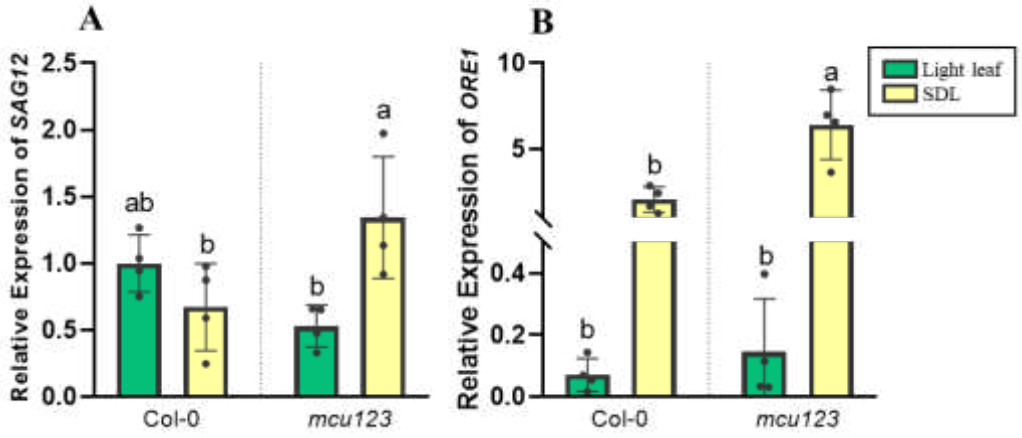

Figure 11: Relative transcript abundance of *SAG12* and *ORE1* in light and single darkened leaves. Reverse transcription–quantitative PCR (RT–qPCR) analysis of **(A)** *SAG12* and **(B)** *ORE1* mRNA abundance in control (light leaf) and SDL leaves of 7-week-old *Arabidopsis thaliana* (Col-0) triple mutant for mitochondrial calcium uniporter (*mcu123)* plants. Relative expression of each gene was normalized by the *SAND* family housekeep gene and for the light leaf in the 0 day. Values represent media ± SD (n= 4). Data were submitted to one-way ANOVA followed by multiple comparisons to Tukey`s test. Letters compare genotypes inside the treatment and different letters indicate significant differences ($P < 0.05$).

DISCUSSION

In the present study, we attempted to unravel the connection between the functional lack of mitochondrial Ca^{2+} uniporter (MCU) and the delay in chlorophyll degradation upon dark-induced senescence. Light is a key player controlling leaf senescence (LIEBSCH & KEECH, 2016); accordingly, in the majority of plants severe shading or darkening, especially if just one part of the plant is affected by it, while the rest of the plant remains in a normal photosynthetic condition, lead to rapid leaf senescence (KEECH et al., 2010). In agreement, our plants had only a single darkened leaf (SDL), and after 7 days of treatment, we could observe a massive chlorophyll degradation for all genotypes, a characteristic symptom of senescence (ONO et al., 2019). Interestingly, two genotypes showed lower chlorophyll degradation when compared to Col-0, namely *mcu123,* and *pif 621*. The *pif 621* has a point mutation in the *PFI5* gene (LIEBSCH et al., 2022), which was previously reported as a crucial gene in dark-induced chlorophyll degradation pathway and senescence (ZHANG et al., 2015). *PIF5* loss function

leads to repression in senescence upon prolonged darkness (SAKURABA et al., 2014), especially for the *pif 621* which was reported to show a delay in dark-induced leaf senescence, based on the gene expression of senescence markers and chlorophyll content (LIEBSCH et al., 2022). Accordingly, *pif 621* showed less chlorophyll degradation, intriguingly also did *mcu123*. The MCU triple mutant line *mcu123* was reported to present a strong impairment in mitochondrial Ca^{2+} uptake, leading it to present less Ca levels in the matrix steady state (RUBERTI et al., 2022). It is important to notice that for the single and double *mcu* mutant lines, we did not observe the same phenotype, suggesting that the MCU has a certain degree of redundancy, as recently suggested (RUBERTI et al., 2022) and the less chlorophyll degradation could be an effect caused by the less Ca^{2+} inside the mitochondrial matrix, only observed in the triple mutant *mcu123*. However, the opposite effect was not observed for *micu* plants, which have more Ca levels in the matrix steady state (WAGNER et al., 2015). *micu* do not have the EF-hand MICU, regulating the MCU channels, therefore it shows higher levels of Ca in the mitochondrial matrix (WAGNER et al., 2015) still presenting the same pattern in chlorophyll degradation as the Col-0.

The *MCU2* overexpression (OE) lines were generated with 35S: *MCU2* (RUBERTI et al., 2022), and the 35S promoter was reported to have a weak expression in dark-grown tissues (SAIDI et al., 2009); therefore we checked the expression of MCU2 after the SDL and even though with a decrease in the expression of *MCU2* over dark, it remains higher than the Col-0 (Supplemental Fig. 2). As observed before, the *MCU2* OE showed a higher matrix Ca level than the *mcu123* and Col-0 (RUBERTI et al., 2022), suggesting that the Ca levels in mitochondria matrix are directly linked to the expression of MCU channels. However, even with higher Ca matrix levels than *micu*, *MCU2* OE lines did not show a more accentuated effect in chlorophyll degradation. That leads us to infer that the impairment in chlorophyll degradation is only present when the plants have lower matrix Ca levels. It is important to notice that the *mcu123* did not present a stay-green phenotype, as presented in some mutants involved in the chlorophyll degradation pathway that stayed green even after 12 days of SDL (LIEBSCH et al., 2022); accordingly, it is possible to observe that after 10 days of SDL, the chlorophyll is being degraded, however, it seems to be in a slower rate in *mcu123* mutant plants. This delay behavior is clear after 7 and 10 days, but not after 3 days. That can be related to the fact that induction of senescence and resource remobilization are tightly controlled to prevent unnecessary metabolic costs under temporarily unfavorable conditions (LIEBSCH & KEECH, 2016; LAW et al., 2018), therefore even though molecular responses can be already happening the visual symptom of SDL can only be quantified after the 3 days.

Since reduced chlorophyll degradation was only observed in the *mcu123* and the higher Ca levels in the mitochondrial matrix presented the same pattern as Col-0, we tested the GDH2 as a possible link between the less matrix Ca and resource remobilization. GDH is the enzyme that connects carbon and nitrogen assimilation pathways, and it is present in all life kingdoms with low variability among plants (GRZECHOWIAK et al., 2020), we were able to separate the phylogenetic tree into two main groups, as revealed by most of monocotyledons and dicotyledons segregation. However, the predicted EF-hand motif of GDH2 (WAGNER et al., 2016) was not well conserved even in species close to *Arabidopsis thaliana*, as observed before by Grzechowiak et al., (2020) which suggests that the EF-hand motif is not essential to the catalytic activity of GDH2. That corroborates with the enzymatic assays, where it was not possible to see an increase in GDH2 activity when applying Ca. It is worth noting that the reaction occurs in all designed cloned constructs, thus the point mutation made to disturb the predicted EF-hand motif and the absence of the mitochondrial transit peptide did not affect the enzymatic capacity of the GDH2. It is important to notice that the reductive amination (2OG → Glu) activity tested here was shown to happen in stress situations, when the carbon is limited (FONTAINE et al., 2012), also when remobilization of nutrients is required (SKOPELITIS et al., 2006), therefore it was the chosen direction of the GDH reaction to be tested. Moreover, it is also the direction of the reaction that was shown to be stimulated by Ca before in other plant species, such as grape and maize (LOULAKAKIS & ROUBELAKISANGELAKIS, 1990; TURANO et al., 1997), however, even with GDH2 being the predominant form in *A. thaliana*, in those studies it was used the isoform 1 (GDH1) and 3 (GDH3), respectively. In this way, even though it presents the predicted EF-hand motif, GDH2 could not be associated with a stimulation by Ca. The same was also verified recently by Grzechowiak et al., (2023) that observed that GDH2 is only slightly affected by Ca. A study by the same group also suggests that the mitochondria target peptide of GDHs is probably not cleaved (GRZECHOWIAK et al., 2020), which goes against what is established that the transient peptides are cleaved off by mitochondrial peptidases and this process is part of protein maturation (BAYSAL et al., 2019). In our assays the presence or absence of the targeting motif did not affect the catalytic reaction when testing the stimulation by Ca addition into the reaction; nevertheless, it showed a different result for the EGTA assay. EGTA is a powerful Ca binding, when added to the reaction it makes any residual Ca unavailable by chelating it (BARR et al., 1980), and it decreases the reaction rate in the constructs baring the mitochondrial target motif. The work that suggested that GDH keeps the mitochondrial targeting motif also suggested that metals bind occur near it (GRZECHOWIAK et al., 2020), which can be the reason why the EGTA affects only the

$_{mt}$GDH2 and $_{mt}$GDH2ΔEF-hand, moreover, recently it was suggested that Ca have only a structural function in GDH2 (GRZECHOWIAK et al., 2023). Hence, the reaction rate is faster in constructs with the target motif, in both assays, once they have the Ca structural site, therefore it was affected by the chelating agent. In summary, our enzymatic tests demonstrated that there is no regulation by Ca in GDH2, despite that the structural Ca, predicted to be close to the target motif, is important to the GDH2 activity but not limiting. As the constructs with and without the EF-hand behaved similarly, we can infer that it is not essential for the catalytic activity of the enzyme. Above all, we corroborate the previously observed results (GRZECHOWIAK et al., 2023), which suggest the EF-hand motif of GDH2 does not have a canonical structure and cannot bind with Ca. In this way, the results of less chlorophyll degradation by *mcu123* could not be directly related to the lower matrix Ca and the regulation of GHD2. Corroborating with the *in vitro* enzymatic assays, the chlorophyll degradation of SDL in *gdh* mutants showed no significant difference. Interestingly, *gdh* mutants presented an increased susceptibility to long dark treatments (MIYASHITA et al., 2008), confirming the importance of GDHs to providing an alternative energy source during carbon starvation, most likely through amino acid degradation, although with only one leaf darkened the *gdh* showed similar results to Col-0. Notably, such results can be explained, at least partially, by the different fates of metabolism under these different conditions, since when the whole plant is in dark treatment, we observe a "standby" of the overall metabolism (LAW et al., 2018) and thus it seems reasonable to assume the alternative fuel of the TCA cycle by GDH activity is likely crucial.

Ca levels are rather stable (DEMIDCHIK et al., 2018). This stability is strongly associated with the tight regulation of Ca levels, especially in the cytosol, which makes Ca a great molecular signal (KUDLA et al., 2018). During the dark treatment, the Ca levels decrease in both cytosol and mitochondria, which is explained, at least in part, by the expression of *MCU*s, which also were downregulated upon dark treatment. It is important to notice that for the *MCU5* almost no expression was found, as previously observed (MERGNER et al., 2020; RUBERTI et al. 2022). The decrease in mitochondrial Ca levels during dark may be correlated with the decrease in the number of mitochondria itself; Keech et al., (2007) observed that after 6 days of SDL, 70% of mitochondria was lost. Intriguing, the Col-0 and *micu* cytosolic Ca levels have an accentuated reduction compared to *mcu123*, which suggests a delay in cell Ca disruptions in this mutant. It seems plausible that this phenotype could be related to mechanisms controlling the survival strategies that lead to the delay in chlorophyll degradation. We

observed the differential pattern in chlorophyll degradation in the confocal microscopy, where we could also observe the mitochondrion upon dark treatment. As previously proposed, the decrease in chlorophyll occurs before the decrease in mitochondrion for SDL (KEECH et al., 2007); this fact aside, we cannot demonstrate, however, that the fate of mitochondria is different between Col-0 and *mcu123*.

The *SENESCENCE-ASSOCIATED GENE* 12 (*SAG12*) was upregulated in *mcu123* after 7 days of SDL, but not in the Col-0. Interestingly, the expression of *SAG12* was higher in the light leaf of Col-0 plants. *SAG12* encodes for the cysteine protease SAG12 which is strongly related to the senescence of leaf tissues (GRBIĆ, 2003). Since SAG12 is an age-dependent gene, strongly related to senescence, and our plants were 8 weeks old, this could explain why the light leaf also presented a considerable expression of SAG12. When comparing darkened leaves between *mcu123* and Col-0, the higher expression in *mcu123* could be explained by the possible degradation of Rubisco that was previously attributed to SAG12 (GRBIĆ, 2003). Accordingly, the *mcu123* would have a higher expression only after 7 days, while Rubisco degradation is already almost over for the Col-0, once the chlorophyll degradation was not delayed. A similar result was found for the NAC transcription factor ORESARA1 (*ORE1*) in *mcu123* darkened leaf as revealed by its upregulation and higher expression compared to the Col-0. *ORE1* positively regulates chlorophyll degradation by promoting the Pheide *a* OXYGENASE (PAO) (QIU et al., 2015). PAO pathway is the main pathway for chlorophyll breakdown (CHRIST & HÖRTENSTEINER, 2014); therefore, it leads us to infer that the upregulation of *ORE1* is only occurring after 7 days of SDL for the *mcu123*, but not for Col-0 since it most likely occurred before. PAO is a 'bottleneck" in the chlorophyll degradation pathway, and it has been shown that jasmonic acid (JA) accumulates in *pao1* mutant plants (AUBRY et al., 2020). Moreover, during dark-induced senescence, the expression of JASMONATE ZIM-domain (JAZ) is increased, whilst JAZ represses JA signaling (YU et al., 2016). It has been also suggested that JA could be a chloroplast retrograde-signaling molecule (SOUZA et al., 2017) and that during senescence, both age-dependent and dark-induced, an increase in JA levels occurs (BREEZE et al., 2011). It has been recently demonstrated that the accumulation of PAO substrate (pheide) can work as a sensor for the chlorophyll degradation rate and the speed of this process, as the senescence speed, is seemingly regulated by JA signaling (AUBRY et al., 2020). Taken together, it seems plausible to suggest that the chlorophyll degradation of *mcu123* mutant plants is at least partially related to JA. In agreement, it has been previously demonstrated that *mcu123* mutant plants are characterized

by a deregulation of JA homeostasis (RUBERTI et al., 2022). Although *mcu123* was characterized by increased JA levels, an increase in enzymes of both biosynthesis and catabolism of JA was observed. It is important to mention that a direct relationship between the lack of the MCU channels and the JA regulation was not unequivocally established and the overall relationship between mitochondria and hormones remains to be better understood (BERKOWITZ et al., 2016). In summary, it seems reasonable to assume that the crosstalk between chloroplast and mitochondria, and the disruption in JA metabolism, as observed in *mcu123* mutant plants, may explain the observed delay in chlorophyll degradation; yet, a comprehensive picture of how and to which extent this mechanism occurs remains to be further elucidated.

CONCLUSIONS

Taken together, our results demonstrated that both Ca levels and the expression of MCU channels decrease during dark-induced senescence. We further confirmed that chloroplast degradation occurs first than mitochondria and that following 7 days under SDL the senescence markers are upregulated. Although the lower chlorophyll degradation phenotype was clearly observed for *mcu123* plants, it was not possible to ascertain whether this is directly related to the channels themselves or due to the less Ca^{2+} in the mitochondria matrix. We further demonstrated that the lower chlorophyll degradation is neither related to the GDH2 regulation itself nor to the putative EF-hand motif that does not play a role in GDH2 responses to Ca. The crosstalk between chloroplasts and mitochondria is seemingly related to this delay in chlorophyll degradation, and our results imply that JA metabolism may be a key to orchestrating physiological, metabolic, and molecular responses to prolonged darkness in plants; however, the points of intersection among chlorophyll degradation, JA signaling pathways and the interactions between MCU and key regulators of cellular Ca homeostasis remain largely uncharacterized.

SUPPLEMENTAL DATA

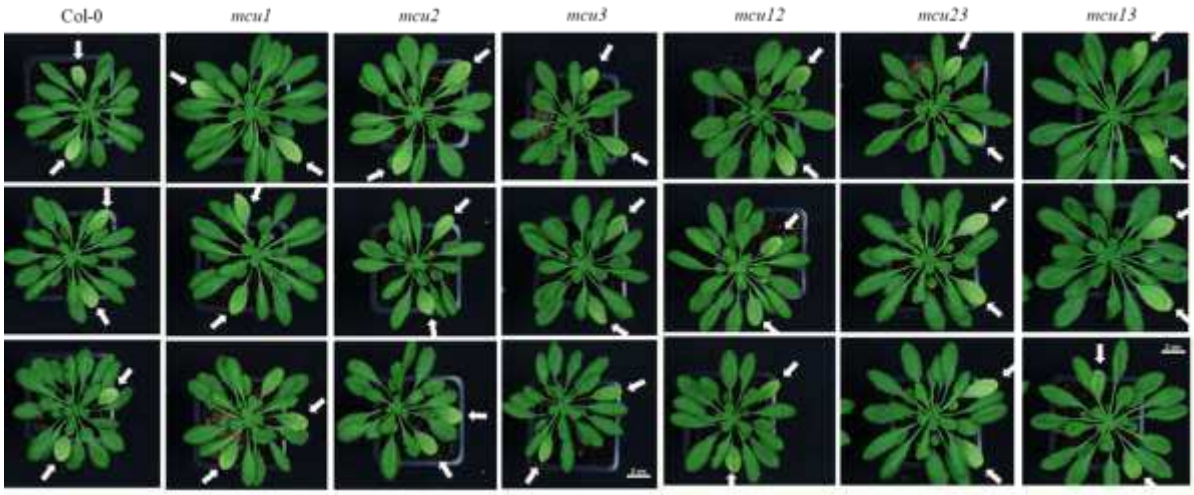

Supplemental Figure 1: Phenotypic characterization of *Arabidopsis thaliana* lines during single-leaf dark-induced senescence. Representative images of 7-week-old plants of wild type (Col-0), single and double mutant lines for mitochondrial calcium uniporter (*mcu1; mcu2; mcu3)* after individually single darkened leaves (SDL) for 7 days. White arrows point to darkened leaves.

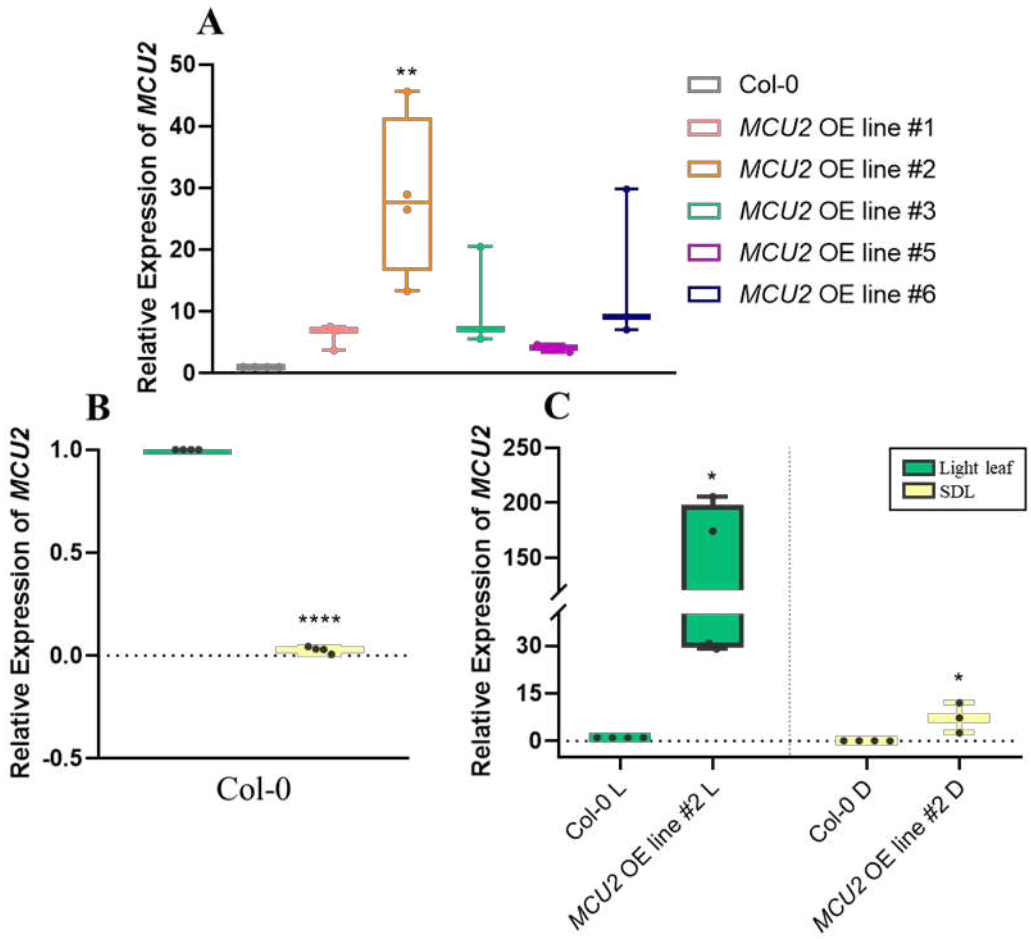

Supplemental Figure 2: Relative transcript abundance of *MCU2* in light and single darkened leaves. **(A)** Reverse transcription–quantitative PCR (RT–qPCR) analysis of *MCU2* mRNA abundance in light leaf of 7-week-old *Arabidopsis thaliana* wide type (Col-0) and mutants overexpressing MCU2 plants (lines #1 – #6) to confirm the over-expression. **(B)** Light leaf and SDL leaves of 7-week-old *Arabidopsis thaliana* wide type (Col-0) reverse transcription–quantitative PCR (RT–qPCR) analysis of *MCU2* mRNA abundance. **(C)** Light leaf and SDL leaves of 7-week-old *Arabidopsis thaliana* wide type (Col-0) and mutants overexpressing MCU2 plants (lines #2). Relative expression of each gene was normalized to the *SAND* family housekeep gene. N = 4 ± SD. An asterisk (*) indicates a significant difference in relation to control as determined by Dunnett's test *$P < 0.05$; **$P < 0.01$; *** $P < 0.005$ ****$P < 0.0001$.

REFERENCES

ALONSO, J.M.; STEPANOVA, A.N.; LEISSE, T.J.; KIM, C.J.; CHEN, H.; SHINN, P.; STEVENSON, D.K.; ZIMMERMAN, J.; BARAJAS, P.; CHEUK, R.; GADRINAB, C. Genome-wide insertional mutagenesis of *Arabidopsis thaliana*. **Science**, v. 301, n. 5633, p. 653-657, 2003.

AUBRY, S.; FANKHAUSER, N.; OVINNIKOV, S.; PRUŽINSKÁ, A.; STIRNEMANN, M.; ZIENKIEWICZ, K.; HERRFURTH, C.; FEUSSNER, I.; HÖRTENSTEINER, S. Pheophorbide a may regulate jasmonate signaling during dark-induced senescence. **Plant Physiology**, v. 182, n. 2, p.776-791, 2020.

BARR, R.; TROXEL, K.S.; CRANE, F.L. EGTA, a calcium chelator, inhibits electron transport in photosystem II of spinach chloroplasts at two different sites. **Biochemical and Biophysical Research Communications**, v. 92, n. 1, p.206-212, 1980.

BAYSAL, C.; PÉREZ-GONZÁLEZ, A.; ESEVERRI, Á.; JIANG, X.; MEDINA, V.; CARO, E.; RUBIO, L.; CHRISTOU, P.; ZHU, C. Recognition motifs rather than phylogenetic origin influence the ability of targeting peptides to import nuclear-encoded recombinant proteins into rice mitochondria. **Transgenic Research**, v. 29, pp.37-52, 2020.

BERKOWITZ, O.; DE CLERCQ, I.; VAN BREUSEGEM, F.; WHELAN, J. Interaction between hormonal and mitochondrial signalling during growth, development and in plant defense responses. **Plant, Cell & Environment**, v. 39, n. 5, p.1127-1139, 2016.

BREEZE, E.; HARRISON, E.; MCHATTIE, S.; HUGHES, L.; HICKMAN, R.; HILL, C.; KIDDLE, S.; KIM, Y.S.; PENFOLD, C.A.; JENKINS, D.; ZHANG, C. High-resolution temporal profiling of transcripts during Arabidopsis leaf senescence reveals a distinct chronology of processes and regulation. **The Plant Cell**, v. 23, n. 3, p.873-894, 2011.

BUCHANAN-WOLLASTON, V.; EARL, S.; HARRISON, E.; MATHAS, E.; NAVABPOUR, S.; PAGE, T.; PINK, D. The molecular analysis of leaf senescence a genomics approach. **Plant Biotechnology Journal**, v. 1, n. 1, p.3-22, 2003.

CHARPENTIER, M.; SUN, J.; VAZ MARTINS, T.; RADHAKRISHNAN, GV.; FINDLAY, K.; SOUMPOUROU, E.; THOUIN, J.; VÉRY, A-A.; SANDERS, D.; MORRIS, RJ.; et al. Nuclear-localized cyclic nucleotide-gated channels mediate symbiotic calcium oscillations. **Science**, v. 352, p.1102–1105, 2016.

CHRIST, B.; HÖRTENSTEINER, S. Mechanism and significance of chlorophyll breakdown. **Journal of Plant Growth Regulation**, v. 33, pp.4-20, 2014.

CZECHOWSKI, T.; STITT, M.; ALTMANN, T.; UDVARDI, M.K.; SCHEIBLE, W.R. Genome-wide identification and testing of superior reference genes for transcript normalization in *Arabidopsis*. **Plant Physiology**, v. 139, n. 1, p. 5-17, 2005.

DE STEFANI, D.; RAFFAELLO, A.; TEARDO, E.; SZABÒ, I.; RIZZUTO, R. A forty-kilodalton protein of the inner membrane is the mitochondrial calcium uniporter. **Nature**, v. 476, p. 336–340, 2011.

DIAZ, C.; LEMAÎTRE, T.; CHRIST, A.; AZZOPARDI, M.; KATO, Y.; SATO, F.; MOROT-GAUDRY, J.F.; LE DILY, F.; MASCLAUX-DAUBRESSE, C. Nitrogen recycling and

remobilization are differentially controlled by leaf senescence and development stage in *Arabidopsis* under low nitrogen nutrition. **Plant Physiology**, v. 147, n. 3, p.1437-1449, 2008.

DRAGO, I.; DE STEFANI, D.; RIZZUTO, R.; POZZAN, T. Mitochondrial Ca^{2+} uptake contributes to buffering cytoplasmic Ca^{2+} peaks in cardiomyocytes. **Proceedings of the National Academy of Sciences**, v. 109, p. 12986–12991, 2012.

ECKSTEIN, A.; GRZYB, J.; HERMANOWICZ, P.; ZGŁOBICKI, P.; ŁABUZ, J.; STRZAŁKA, W.; DZIGA, D.; BANAŚ, A.K. *Arabidopsis* phototropins participate in the regulation of dark-induced leaf senescence. **International Journal of Molecular Sciences**, v. 22, n. 4, p.1836, 2021.

ELÍES, J.; YÁÑEZ, M.; PEREIRA, TMC.; GIL-LONGO, J.; MACDOUGALL, DA.; CAMPOS-TOIMIL, M. An update to calcium binding proteins. **Calcium Signaling**, v. 1131, p.183–213, 2020.

EMANUELSSON, O.; NIELSEN, H.; BRUNAK, S.; VON HEIJNE, G. Predicting subcellular localization of proteins based on their N-terminal amino acid sequence. **Journal of Molecular Biology**, v. 300, p. 1005–1016, 2000.

FONTAINE, J.X.; TERCÉ-LAFORGUE, T.; ARMENGAUD, P.; CLÉMENT, G.; RENOU, J.P.; PELLETIER, S.; CATTEROU, M.; AZZOPARDI, M.; GIBON, Y.; LEA, P.J.; HIREL, B. Characterization of a NADH-dependent glutamate dehydrogenase mutant of *Arabidopsis* demonstrates the key role of this enzyme in root carbon and nitrogen metabolism. **The Plant Cell**, v. 24, n. 10, p.4044-4065. 2012.

GRBIĆ, V. SAG2 and SAG12 protein expression in senescing Arabidopsis plants. **Physiologia Plantarum**, v. 119, n. 2, p.263-269, 2003.

GRZECHOWIAK, M.; SLIWIAK, J.; JASKOLSKI, M.; RUSZKOWSKI, M. Structural studies of glutamate dehydrogenase (isoform 1) from *Arabidopsis thaliana*, an important enzyme at the branch-point between carbon and nitrogen metabolism. **Frontiers in Plant Science**, v. 11, p.545394, 2020.

GRZECHOWIAK, M.; SLIWIAK, J.; JASKOLSKI, M.; RUSZKOWSKI, M. Structural and functional studies of *Arabidopsis thaliana* glutamate dehydrogenase isoform 2 demonstrate enzyme dynamics and identify its calcium binding site. **Plant Physiology and Biochemistry**, v. 201, p.107895, 2023.

HOU, C.; TIAN, W.; KLEIST, T.; HE, K.; GARCIA, V.; BAI, F.; HAO, Y.; LUAN, S.; LI, L. DUF221 proteins are a family of osmosensitive calcium-permeable cation channels conserved across eukaryotes. **Cell Research**, v. 24, p.632–635, 2014.

KANG, X.; ZHAO, L.; LIU, X. Calcium Signaling and the Response to Heat Shock in Crop Plants. **International Journal of Molecular Sciences**, v. 25, n. 1, p.324, 2023.

KEECH, O.; PESQUET, E.; AHAD, A.; ASKNE, A.; NORDVALL, D.A.G.; VODNALA, S.M.; TUOMINEN, H.; HURRY, V.; DIZENGREMEL, P.; GARDESTRÖM, P. The different fates of mitochondria and chloroplasts during dark-induced senescence in Arabidopsis leaves. **Plant, Cell & Environment**, v. 30, n. 12, pp.1523-1534, 2007.

KEECH, O.; PESQUET, E.; GUTIERREZ, L.; AHAD, A.; BELLINI, C.; SMITH, S.M.; GARDESTRÖM, P. Leaf senescence is accompanied by an early disruption of the microtubule network in Arabidopsis. **Plant Physiology**, v. 154, n. 4, p.1710-1720, 2010.

KINDT, R.; PAHLICH, E.; RASCHED, I. Glutamate dehydrogenase from peas: isolation, quaternary structure, and influence of cations on activity. **European Journal of Biochemistry**, v. 112, n. 3, p.533-540, 1980.

KONG, X.; XU, L.; JAMIESON, P. Plant sense: the rise of calcium channels. **Trends in Plant Science**, v. 25, p. 838–841, 2020.

KOSUTA, S.; HAZLEDINE, S.; SUN, J.; MIWA, H.; MORRIS, R.J.; DOWNIE, J.A.; OLDROYD, G.E. Differential and chaotic calcium signatures in the symbiosis signaling pathway of legumes. **Proceedings of the National Academy of Sciences**, v. 105, n. 28, p.9823-9828, 2008.

KUDLA, J.; BECKER, D.; GRILL, E.; HEDRICH, R.; HIPPLER, M.; KUMMER, U.; PARNISKE, M.; ROMEIS, T.; SCHUMACHER, K. Advances and current challenges in calcium signaling. **New Phytologist**, v. 218, n. 2, p. 414-431, 2018.

LAW, S.R.; CHROBOK, D.; JUVANY, M.; DELHOMME, N.; LINDÉN, P.; BROUWER, B.; AHAD, A.; MORITZ, T.; JANSSON, S.; GARDESTRÖM, P.; KEECH, O. Darkened leaves use different metabolic strategies for senescence and survival. **Plant Physiology**, v. 177, n. 1, p.132-150, 2018.

LEA, P.J.; IRELAND, R.J. Nitrogen metabolism in higher plants. **Plant Amino Acids: Biochemistry and Biotechnology**, v. 1, 1999.

LIEBSCH, D.; KEECH, O. Dark-induced leaf senescence: new insights into a complex light-dependent regulatory pathway. **New Phytologist**, v. 212, n. 3, p.563-570, 2016.

LIEBSCH, D.; JUVANY, M.; LI, Z.; WANG, H.L.; ZIOLKOWSKA, A.; CHROBOK, D.; BOUSSARDON, C.; WEN, X.; LAW, S.R.; JANEČKOVÁ, H.; BROUWER, B. Metabolic control of arginine and ornithine levels paces the progression of leaf senescence. **Plant Physiology**, v. 189, n. 4, p. 1943-1960, 2022.

LOGAN, DC.; KNIGHT, MR. Mitochondrial and cytosolic calcium dynamics are differentially regulated in plants. **Plant Physiology**, v. 133, p. 21–24, 2003.

LORO, G.; DRAGO, I.; POZZAN, T.; SCHIAVO, FL.; ZOTTINI, M.; COSTA, A. Targeting of Cameleons to various subcellular compartments reveals a strict cytoplasmic/mitochondrial Ca^{2+} handling relationship in plant cells. **The Plant Journal**, v. 71, p. 1–13, 2012.

LOULAKAKIS, C.A.; ROUBELAKIS-ANGELAKIS, K.A. Intracellular localization and properties of NADH-glutamate dehydrogenase from Vitis vinifera L. purification and characterization of the major leaf isoenzyme. **Journal of Experimental Botany**, v. 41, n. 10, p.1223-1230, 1990.

MANISHANKAR, P.; WANG, N.; KÖSTER, P.; ALATAR, A.A.; KUDLA, J. Calcium signaling during salt stress and in the regulation of ion homeostasis. **Journal of Experimental Botany**, v. 69, n. 17, p.4215-4226, 2018.

MARCHI, L.; POLVERINI, E.; DEGOLA, F.; BARUFFINI, E.; RESTIVO, F.M. Glutamate dehydrogenase isoenzyme 3 (GDH3) of *Arabidopsis thaliana* is less thermostable than GDH1 and GDH2 isoenzymes. **Plant Physiology and Biochemistry**, v. 83, p.225-231, 2014.

MENG, Q.; CHEN, Y.; ZHANG, M.; CHEN, Y.; YUAN, J.; MURRAY, SC. Molecular characterization and phylogenetic analysis of Zm*MCU*s in maize. **Biologia**, v. 70, p. 599–605, 2015.

MERGNER, J.; FREJNO, M.; LIST, M.; PAPACEK, M.; CHEN, X.; CHAUDHARY, A.; SAMARAS, P.; RICHTER, S.; SHIKATA, H.; MESSERER, M.; LANG, D. Mass-spectrometry-based draft of the *Arabidopsis* proteome. **Nature**, v. 579, p.409–414, 2020.

MIYASHITA, Y.; GOOD, A.G. NAD (H)-dependent glutamate dehydrogenase is essential for the survival of *Arabidopsis thaliana* during dark-induced carbon starvation. **Journal of Experimental Botany**, v. 59, n. 3, p.667-680, 2008.

NAKAGAWA, Y.; KATAGIRI, T.; SHINOZAKI, K.; QI, Z.; TATSUMI, H.; FURUICHI, T.; KISHIGAMI, A.; SOKABE, M.; KOJIMA, I.; SATO, S; KATO, T. *Arabidopsis* plasma membrane protein crucial for Ca^{2+} influx and touch sensing in roots. **Proceedings of the National Academy of Sciences**, v. 104, p. 3639–3644, 2007.

ONO, K.; KIMURA, M.; MATSUURA, H.; TANAKA, A.; ITO, H. Jasmonate production through chlorophyll a degradation by Stay-Green in *Arabidopsis thaliana*. **Journal of Plant Physiology**, v. 238, p.53-62, 2019.

QIU, K.; LI, Z.; YANG, Z.; CHEN, J.; WU, S.; ZHU, X.; GAO, S.; GAO, J.; REN, G.; KUAI, B.; ZHOU, X. *EIN3* and *ORE1* accelerate degreening during ethylene-mediated leaf senescence by directly activating chlorophyll catabolic genes in *Arabidopsis*. **PLoS Genetics**, v. 11, n. 7, p.e1005399, 2015.

RESENTINI, F.; RUBERTI, C.; GRENZI, M.; BONZA, MC.; COSTA, A. The signatures of organellar calcium. **Plant Physiology**, v. 187, p. 1985–2004, 2021.

RUBERTI, C.; FEITOSA-ARAUJO, E.; XU, Z.; WAGNER, S.; GRENZI, M.; DARWISH, E.; LICHTENAUER, S.; FUCHS, P.; PARMAGNANI, A.S.; BALCEROWICZ, D.; SCHOENAERS, S. MCU proteins dominate in vivo mitochondrial Ca^{2+} uptake in *Arabidopsis* roots. **The Plant Cell**, v. 34, n. 11, p. 4428-4452, 2022.

SAIDI, Y.; SCHAEFER, D.G.; GOLOUBINOFF, P.; ZRŸD, J.P.; FINKA, A. The CaMV 35S promoter has a weak expression activity in dark grown tissues of moss *Physcomitrella* patens. **Plant Signaling & Behavior**, v. 4, n. 5, p.457-459, 2009.

SAKURABA, Y.; JEONG, J.; KANG, M.Y.; KIM, J.; PAEK, N.C.; CHOI, G. Phytochrome-interacting transcription factors PIF4 and PIF5 induce leaf senescence in Arabidopsis. **Nature Communications**, v. 5, n. 1, p.4636, 2014.

SARASKETA, A.; VEGA-MAS, I.; MARINO, D. *In vitro* Colorimetric Method to Measure Plant Glutamate Dehydrogenase Enzyme Activity. **Bio-protocol**, v. 5, n. 16, p. e1560, 2015.

SCHMITTGEN, T.D.; LIVAK, K.J. Analyzing real-time PCR data by the comparative CT method. **Nature Protocols**, v. 3, n. 6, p.1101-1108, 2008.

SELLES, B.; MICHAUD, C.; XIONG, T.C.; LEBLANC, O.; INGOUFF, M. *Arabidopsis* pollen tube germination and growth depend on the mitochondrial calcium uniporter complex. **New Phytologist**, v. 219, n. 1, p. 58-65, 2018.

SKOPELITIS, D.S.; PARANYCHIANAKIS, N.V.; PASCHALIDIS, K.A.; PLIAKONIS, E.D.; DELIS, I.D.; YAKOUMAKIS, D.I.; KOUVARAKIS, A.; PAPADAKIS, A.K.; STEPHANOU, E.G.; ROUBELAKIS-ANGELAKIS, K.A. Abiotic stress generates ROS that signal expression of anionic glutamate dehydrogenases to form glutamate for proline synthesis in tobacco and grapevine. **The Plant Cell**, v. 18, n. 10, pp.2767-2781, 2006.

SOUZA, A.; WANG, J.Z.; DEHESH, K. Retrograde signals: integrators of interorganellar communication and orchestrators of plant development. **Annual Review of Plant Biology**, v. 68, p.85-108, 2017.

STAEL, S.; WURZINGER, B.; MAIR, A.; MEHLMER, N.; VOTHKNECHT, UC.; TEIGE, M. Plant organellar calcium signalling: an emerging field. **Journal of Experimental Botany**, v. 63, p. 1525–1542, 2012.

TEARDO, E.; CARRARETTO, L.; WAGNER, S.; FORMENTIN, E.; BEHERA, S.; DE BORTOLI, S.; LAROSA, V.; FUCHS, P.; LO SCHIAVO, F.; RAFFAELLO, A.; RIZZUTO, R. Physiological characterization of a plant mitochondrial calcium uniporter *in vitro* and *in vivo*. **Plant Physiology**, v. 173, n. 2, p. 1355-1370, 2017.

TIAN, W.; HOU, C.; REN, Z.; WANG, C.; ZHAO, F.; DAHLBECK, D.; HU, S.; ZHANG, L.; NIU, Q.I.; LI, L.; STASKAWICZ, B.J. A calmodulin-gated calcium channel links pathogen patterns to plant immunity. **Nature**, v. 572, n. 7767, p.131-135, 2019.

TOYOTA, M.; SPENCER, D.; SAWAI-TOYOTA, S.; JIAQI, W.; ZHANG, T.; KOO, AJ.; HOWE, GA.; GILROY, S. Glutamate triggers long-distance, calcium-based plant defense signaling. **Science**, v. 361, p. 1112–1115, 2018.

TURANO, F.J.; THAKKAR, S.S.; FANG, T.; WEISEMANN, J.M. Characterization and expression of NAD (H)-dependent glutamate dehydrogenase genes in *Arabidopsis*. **Plant Physiology**, v. 113, n. 4, p.1329-1341, 1997.

WAGNER, S.; BEHERA, S.; DE BORTOLI, S.; LOGAN, D.C.; FUCHS, P.; CARRARETTO, L.; TEARDO, E.; CENDRON, L.; NIETZEL, T.; FÜßL, M.; DOCCULA, F.G. The EF-hand Ca^{2+} binding protein MICU choreographs mitochondrial Ca^{2+} dynamics in *Arabidopsis*. **The Plant Cell**, v. 27, n. 11, p. 3190-3212, 2015.

WAGNER, S.; DE BORTOLI, S.; SCHWARZLÄNDER, M.; SZABÒ, I. Regulation of mitochondrial calcium in plants versus animals. **Journal of Experimental Botany**, v. 67, n. 13, p.3809-3829, 2016.

WELLBURN, A.R. The spectral determination of chlorophylls *a* and *b*, as well as total carotenoids, using various solvents with spectrophotometers of different resolution. **Journal of Plant Physiology**, v. 144, n. 3, p. 307-313, 1994.

YAMAYA, T.; OAKS, A.; MATSUMOTO, H. Characteristics of glutamate dehydrogenase in mitochondria prepared from corn shoots. **Plant Physiology**, v. 76, n. 4, p.1009-1013, 1984.

YU, J.; ZHANG, Y.; DI, C.; ZHANG, Q.; ZHANG, K.; WANG, C.; YOU, Q.; YAN, H.; DAI, S.Y.; YUAN, J.S.; XU, W. JAZ7 negatively regulates dark-induced leaf senescence in *Arabidopsis*. **Journal of Experimental Botany**, v. 67, n. 3, p.751-762, 2016.

YUAN, P.; YANG, T.; POOVAIAH, B.W. Calcium signaling-mediated plant response to cold stress. **International Journal of Molecular Sciences**, v. 19, n. 12, p.3896, 2018.

ZANDALINAS, S.I.; BALFAGÓN, D.; GÓMEZ-CADENAS, A.; MITTLER, R. Plant responses to climate change: metabolic changes under combined abiotic stresses**. Journal of Experimental Botany**, v. 73, n. 11, p.3339-3354, 2022.

ZHANG, Y.; LIU, Z.; CHEN, Y.; HE, J.X.; BI, Y. PHYTOCHROME-INTERACTING FACTOR 5 (PIF5) positively regulates dark-induced senescence and chlorophyll degradation in Arabidopsis. **Plant Science**, v. 237, pp.57-68, 2015.

FUTURE PERSPECTIVES

In summary, the work presented here demonstrated the paramount importance of mitochondrial metabolism in response to abiotic stresses. Since mitochondria metabolism plays an essential role in plant growth, development, and communication with other organelles, elucidating how it functions in mitigating environmental stress is extremely important, allowing the exploration of the significance of mitochondrial metabolism for the enhancement of stress tolerance in plants. Furthermore, our understanding of the regulation of the responses of classical and alternative pathways of respiration linked to the TCA cycle during plant development and stress situations remains rather limited. A deep understanding of the biological process associated with mitochondrial metabolism is important for crops' stress responses and therefore enhancing stress tolerance and minimizing the negative impacts of the stress on plant growth and productivity is likely much desired for companies and plant breeding programs. More specifically, in tropical and subtropical regions, soil acidity is an important constraint that hinders the increase of food production, thus, understanding the physiological processes related to stress by Al may provide novel insights for the establishment of successful tolerant plants. Maximizing our understanding of the Al impacts on plant fitness, help us to breed Al-tolerant genotypes with lower to no yield penalty. In addition, it seems reasonable that an in-depth understanding of the mechanisms associated with metabolic strategies used by leaves during darkening conditions may open novel directions to biotechnological approaches aiming at improving postharvest shelf life and reducing food waste. Moreover, by deepening our knowledge in resource remobilization it also provides significant mechanistic insights into the function of genetic effects on gene expression and phenotypic plasticity that ultimately may lead to improving grain filling. Exploiting the gained knowledge in crop plants either via genetic transformation or by TILLING technology might help to improve the tolerance of commercial varieties to stress constraints. An in-depth understanding of the global regulation of Ca homeostasis during plant senescence, focusing on the crosstalk between chloroplasts and mitochondria mediated by the JA signaling pathways, may open novel directions in plant genetic engineering and (a)biotic stress tolerance.